A STUDY OF CAPILLARY RISE AND DRAIN CURVES IN PACKED BEDS OF SPHERICAL PARTICLES

by

Weeramundage James Noel Fernando, B.Sc.(Eng.), Dip.Chem. Eng. (Surrey)

JUNE 1974

A thesis submitted for the degree of Doctor of Philosophy of the University of London and for the Diploma of Imperial College

Department of Chemical Engineering
and Chemical Technology,
Imperial College,
Prince Consort Road,
London SW7 2BY

ABSTRACT

Prediction of rise and drain moisture distributions in packed beds requires a knowledge of pore size distributions of such beds. In order to predict pore size distributions, a model which would satisfactorily describe packed beds is needed.

In this work models of porous bodies developed by previous workers are described. A model for the prediction of pore size distributions of random packings of equal size spheres is developed.

An integral equation is developed to predict capillary pressure curves for a given pore. Solutions of this equation are obtained for spherical and cylindrical pores.

Experiments are carried out to determine the capillary pressure curves of packed beds of ballotini. Studies made by previous workers, of moisture distribution in porous bodies under rise and drain conditions are described.

A basic equation for the determination of a capillary pressure curve is developed. A model for the prediction of rise curves of packed beds is developed. It is shown that the experimental rise curves obtained for each grade of ballotini can be satisfactorily predicted with a knowledge of an average capillary diameter of a particle.

A model is developed for the prediction of drain curves of packed beds. It is shown that moisture distribution under drain conditions in packed beds of equal size spheres can be expressed by a unique dimensionless curve. Validity of this is checked for different grades of ballotini and is found to be in agreement.

A possible method for classification of packed beds of spherical particles according to their size distribution is introduced. Pore size distributions which could result on mixing particles of different sizes are studied. The expected behaviour of capillary pressure curves is compared with the experimental capillary pressure curves of packed beds of ballotini mixed in various proportions and is found to be in agreement.

ACKNOWLEDGEMENTS

It is a great pleasure to be able to express my gratitude to Dr. A.R.H. Cornish, without whose advice and guidance this project could not have been carried out. I must thank him for his critical reading of the manuscript. Dr. P. Eisenklam's help during the final stages of this work is gratefully acknowledged.

I am also very grateful to the Ministry of Education of the Government of Sri Lanka for awarding me a Sri Lanka Government-University Scholarship in order to carry out this project. Release of exchange by the Exchange Control Authorities of Sri Lanka during this project, and the financial assistance provided by the Sir Ernest Cassel Educational Trust in the final production of this thesis are acknowledged with appreciation. I must thank the University of Sri Lanka for allowing me leave to carry out this research.

I am indebted to my parents for their patience and sacrifices. Finally, I wish to thank all those who assisted me in many ways in the course of this project, specially Flora Ahmad for typing this thesis and Nimal and Malini for their help in the final stages of preparation of this thesis.

CONTENTS

		Page
Abstract		1
Acknowledgements		2
Contents		3
Chapter 1.	Introduction	8
Chapter 2.	Imbibition, Drain and Hysteresis of Moisture in Porous Media : Introduction and literature survey	11
2.1	Introduction	11
2.1.1	The Rise and drain curves	11
2.1.2	Classification of Moisture in a porous body	14
2.1.3	The Theory of Capillary potential	15
2.2	The movement, distribution and retention of moisture in a porous body under partially saturated and unsaturated conditions	16
2.2.1	General	16
2.2.2	Imbibition	17
2.2.3	Drain	19
2.2.4	The irreversible nature of moisture movement	23
2.3	Experimental Methods	24
2.3.1	The Measurement of Suction or Capillary pressure in a soil	24
2.3.1.1	Tensio-meters	24
2.3.1.2	Pressure membrane apparatus	24
2.3.2	Measurement of Moisture Content in a Soil	25
2.3.3	The measurement of capillary pressure curves	25
2.3.3.1	Column measurements	26
2.3.3.2	Sample measurements	26
2.4	Theoretical Studies of the Capillary pressure Curves	27
2.5	Hysteresis and Irreducible saturation	39
2.5.1	Hysteresis	39

			Page
	2.5.2	Irreducible saturation	40
	2.6	Discussion	41
Chapter 3.	A literature survey of models for packed beds		43
	3.1	Introduction	43
	3.2	Capillaric Models	44
	3.3	Capillary Network models	45
	3.4	Random models for Packed beds	46
	3.4.1	Experimental developments	47
	3.4.1.1	Geometry of Random packings	47
	3.4.1.2	Void Fraction	47
	3.4.2	Theoretical developments	48
	3.5	Conclusion	52
Chapter 4.	A model for the prediction of pore size in a random packing of equal size spheres		54
	4.1	Introduction	54
	4.1.1	Description of the model	54
	4.1.2	Other considerations	56
	4.2	An equilibrium analysis of a packed bed	57
	4.2.1	Forces on a particle and the internal forces in a bed	57
	4.2.2	Evaluation of the probability factor for stability of a tetrahedral unit in a sphere packing	59
	4.3	Model Structure of the packing	62
	4.4	Relative frequencies of occurence of the canonical units	63
	4.5	The fraction of contact edges in the base triangle of a unit T 1	66
	4.6	Number of stable tetrahedra as a fraction of the total geometrically consistent tetrahedra that can be formed of a given configuration T 1	68
	4.6.1	Equilibrium considerations	68

Page

4.6.2 Stability of a sphere resting on another sphere in a given tetrahedral unit T 1 of a packing and the probability of its occurence 70

4.7 The frequency distribution of the critical reactions and its properties 72

4.8 Probability of formation of stable tetrahedra of a given configuration T 1 75

4.9 Generation of a computer model for a packed bed 76

4.10 Evaluation of factor - x for a gently formed bed 80

4.11 Discussion 83

Chapter 5. The Moisture Distribution Under Imbibition : The Rise Curve 97

5.1 The Movement and Distribution of Moisture Under Imbibition 97

5.1.1 A Qualitative Analysis 97

5.1.2 A Theoretical Analysis 97

5.1.2.1 The Capillary Pressure of Moisture in a partially saturated pore 97

5.1.2.2 Void Space in a porous body 99

5.1.2.3 The equivalent radius and the critical radius 104

5.2 Description of the model and the prediction of the Imbibition Curve 106

5.2.1 Basic equation for the determination of a capillary pressure curve of a porous body 106

5.2.2 Description of the Model 108

5.2.2.1 Packed bed 108

5.2.2.2 Model of the mechanism of Imbibition 108

5.2.2.3 Calculation of V_{pw}/V_p and V_{iw}/V_i in Equation (5.20) 109

		Page
	5.2.2.4 Calculation of Ψ_h	111
	5.2.2.5 Calculation of the Imbibition Curve	
5.3	Experimental	114
	5.3.1 Preliminary	114
	5.3.2 Determination of the Drain Curve	115
	5.3.3 Determination of the Imbibition Curve	117
5.4	A Computer program to calculate the Imbibition Curve	118
5.5	Results and Discussion	120
Chapter 6.	The Moisture Distribution Under Drain Conditions: The Drain Curve	126
6.1	The Movement and distribution of moisture under drain	126
6.2	A Model for drainage : Prediction of drain Curve	127
6.3	Computer program for the prediction of Drain Curves	131
6.4	Discussion	134
Chapter 7.	The Effect of mixing different size spherical particles on the capillary pressure curves in a bed	138
7.1	Introduction	138
7.2	Definitions	139
	7.2.1 A complete mixture; Uniform Mixture or a Homogeneous mixture	139
	7.2.2 A classification of mixtures of hard spheres according to the particle size distribution	139
7.3	The effect of mixing on pore size distribution	
	7.3.1 Void Fraction	144
	7.3.2 Representation of beds of mixtures of approximately equal size spheres by an equivalent uniform sphere packing	146
	7.3.3 Beds consisting of mixtures of spheres of different diameters	147

Page

7.3.3.1 General 147
7.3.3.2 Mixtures of two or more components 148
7.4 Experiments 148
7.4.1 Mixing 148
7.4.2 The determination of the rise and drain curves 149
7.5 Results and discussion 149
7.5.1 The Irreducible Saturation 149
7.5.2 Pore sizes 152
7.5.3 Behaviour of Rise Curve 153
7.5.4 Behaviour of drain curve 154
7.5.5 Other Comments 158

Chapter 8. Conclusion 159

Appendices:

Appendix 1. The Experimental Results of Rise Columns for different Grades of Ballotini 162

Appendix 2. The Experimental Results of Drain Columns for different Grades of Ballotini 166

Appendix 3. Microscopic Analysis of different Grades of Ballotini 170

Appendix 4. Solution of Equation (6.11) 174

Appendix 5. Experimental results for packed beds of mixtures of grade 6 and grade 10 ballotini 176

Appendix 6. Predicted Pore Size distributions 184

List of Symbols 186

References 188

CHAPTER 1

Introduction

Partially or completely saturated porous media have been studied in terms of their physical properties, such as dispersion, permeability, strength, thermal conductivity, capillary pressure etc. by research workers of many disciplines of engineering and science. Because of the complex nature of the pore structure in porous media, the investigations have been mainly experimental and have led to the development of empirical formulae, which describe the characteristics of packed beds. Any approach of this type inevitably neglects the true physical structure of porous media, thus giving rise to a gap of physical identity between theory and real behaviour. Mathematical models have been too simple in nature, inadequate in description, or too complicated, so that the description of real porous media could not be satisfactorily represented by the models developed.

The structure and distribution of pore spaces in porous media vary from one body to another, so that the development of a general model of pore space, covering the whole range of porous media becomes impossible. Therefore, in order to study phenomena involving the properties of pore spaces, the pore properties of the particular porous medium are needed.

Systematic packings of spheres have been the most commonly used media investigated. Recently, however, random packings have been used in place of systematic packings in the study of capillary phenomena in packed beds. The stochastic nature of the formation of packings gives rise to pore size distributions for different packings of the same particles. The distributions vary about a mean distribution, thus enabling capillary phenomena to be studied theoretically based on a knowledge of the mean distribution of pore sizes. The theoretical predictions may be compared with experimental observations of capillary phenomena obtained for a number of different packings based on the same set of particles. The wide distribution of pore sizes and the random nature of the distribution of pores in space makes it possible to interpret the results on a more generalised scale than can be obtained by the use of systematic packings.

Models for random packings of uniform spheres have been developed in the past mainly in the fields of gas and liquid state physics. The applicability of such models to packed beds is ambiguous, because their theoretical basis does not include the effect of gravity on the formation of the packed bed. Computer methods have been developed to simulate the formation of packings. The methods usually include analyses of equilibrium positions of each sphere in a packing which is formed by dropping a collection of spheres, one at a time, into a bin. These methods are cumbersome and require large amounts of computing time, so that an analysis beyond a few layers above the floor of the bin becomes impractical.

An alternative method is to combine the stochastic approach with the statics of a packing. If the effects of walls and the base of the packing are excluded, a model is established for pore size distributions which is applicable far away from the walls and from the base of a packing which has formed under gravity. Since the visible variations of capillary moisture content with height are usually observed at heights relatively far away from the bottom of the packing, pore spaces derived from such a model satisfy one of the requirements needed for the determination of rise and drain curves in packed beds.

As the work herein is mainly centred around the development of models to predict rise and drain curves in packed beds in terms of pore properties, attention has been given mainly to the development of pore size distributions from the pore size model. The development of a general model for packed beds of mixed sizes of spheres necessarily requires a thorough understanding of packings of uniform size spheres. Development of a model which describes random packings of uniform spheres is in itself complex and time consuming, and is a principal topic in the present work. A pore space model for random packings of equal size spheres is developed in chapter 4. This follows a literature survey, given in chapter 3, of the previous models that have been developed to represent porous media.

Models for the evaluation of rise and drain curves in packed beds are dealt with separately in chapters 5 and 6 respectively. Throughout the development of the models, an attempt is made to relate the real behaviour of moisture in the pores of a porous medium to the movement of moisture predicted by the models. Previous work that has been carried out to study the capillary pressure curves is outlined in chapter 2.

Both the models, which are developed in chapters 5 and 6 to determine the rise and drain curves respectively, include an analysis of the possibility of retention of moisture in pores on a microscopic scale. The method of evaluation of the drain curve includes a probability analysis of moisture retention in the pores under a given capillary pressure. The mechanism of imbibition is simulated by using a model in which porous media are approximated to layers of interconnected pores. The probability of a particular layer filling up with moisture, because of the presence of moisture in the lower adjacent layer, is analysed. The variation of the moisture content with height is obtained by evaluating the moisture content with height is obtained by evaluating the moisture content at different layers.

The tetrahedral subdivision system, which regards packed beds of spheres as an assemblage of tetrahedral subunits with four spheres occupying the corners of each tetrahedron, is used in the application of the models of rise and drain curves to packed beds.

Experiments to determine the rise and drain curves, which are described in chapter 5, were carried out using unconsolidated beds of ballotini. Six grades of ballotini were used in these experiments. The models for the rise and drain curves were tested for the six grades of ballotini, each grade of which could be regarded as consisting of approximately similar sizes of particles. The pore size distributions derived in chapter 4 for random packings of equal size spheres were used to construct the theoretical rise and drain curves, for packed beds of uniform spheres. The theoretical rise and drain curves are seen to represent satisfactorily the experimental data for the six grades of ballotini, by a choice of an average particle diameter of the packing in each case for rise and drain and for each grade of ballotini.

Construction of the rise and drain curves for packed beds of mixtures of spheres has not been possible, as a satisfactory pore space model for packed beds of mixtures of spheres does not exist at present. Therefore, a qualitative study on the implications on the pore size distributions on mixing different size spheres is made. The behaviour of the theoretical rise and drain curves based on the new pore size distributions are discussed, and the expected behaviour is compared with the experimental rise and drain curves obtained for mixtures of various compositions of mixing. Chapter 7 deals with the study of capillary rise and drain curves for mixtures of spheres.

CHAPTER 2

Imbibition, Drain and Hysteresis of Moisture in Porous Media: Introduction and Literature Survey.

2.1 Introduction

2.1.1 The Rise and Drain Curves

When a dry capillary porous body is dipped in a pool of a wetting liquid, such that one of its faces is just in contact with the pool, moisture starts rising along the pore channels in the porous body due to capillary suction. When equilibrium is reached, the moisture distribution is usually of the form shown in figure 2.1 (Curve A). The curve showing the variation of equilibrium moisture content with height is known as the rise or imbibition curve for the porous body. Similarly, when moisture in a completely wet porous body is allowed to drain, with the porous body just dipping in a pool of a wetting liquid, moisture starts moving from the pores of the porous medium to the pool along the pore channels of the porous body. This process continues, as long as there is an imbalance in the gravitational and capillary forces. When equilibrium is reached, the curve showing the distribution of moisture with height is known as the drain curve for the porous body.

The phenomena or rise and drain have been defined in general terms by Pickell et al. (179) as the wetting phase displacing the non-wetting phase, and the non-wetting phase displacing the wetting phase, respectively. Fig. 2.1 shows typical moisture distribution curves for a porous body under rise and drain conditions. The two curves are distinct, and the asymptotic moisture content of the drain curve as the capillary pressure approaches large values is known as the irreducible saturation.

Consider the equilibrium of moisture at a particular section $X - X$ (Fig. 2.2) at a height h above the free surface of liquid. The moisture in the continuous phase in an element is subjected to two potential fields, namely; the capillary potential and gravitational potential, respectively. At equilibrium the two fields become equal and opposite.

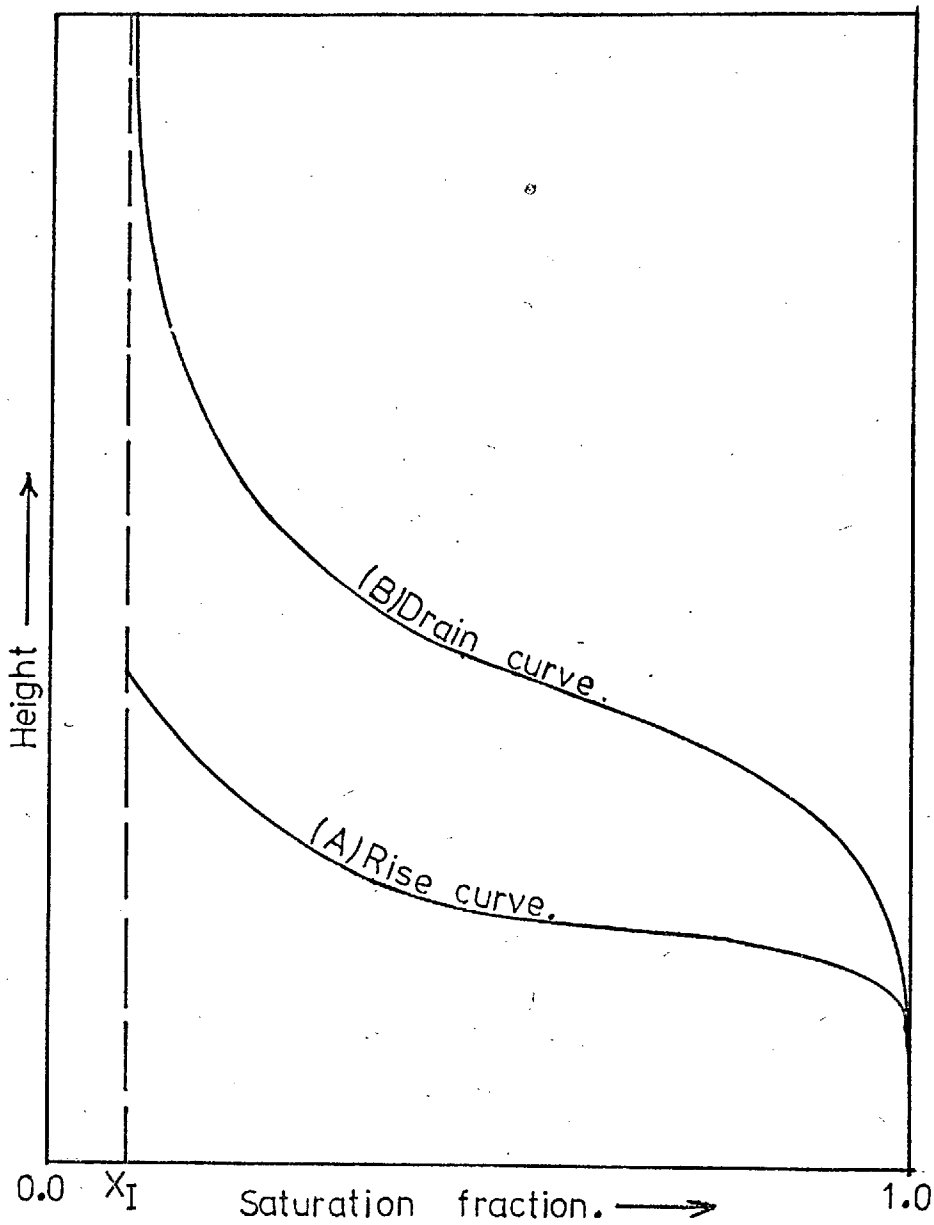


FIGURE 2.1
The rise and drain curves.
(X_I = Irreducible saturation.)

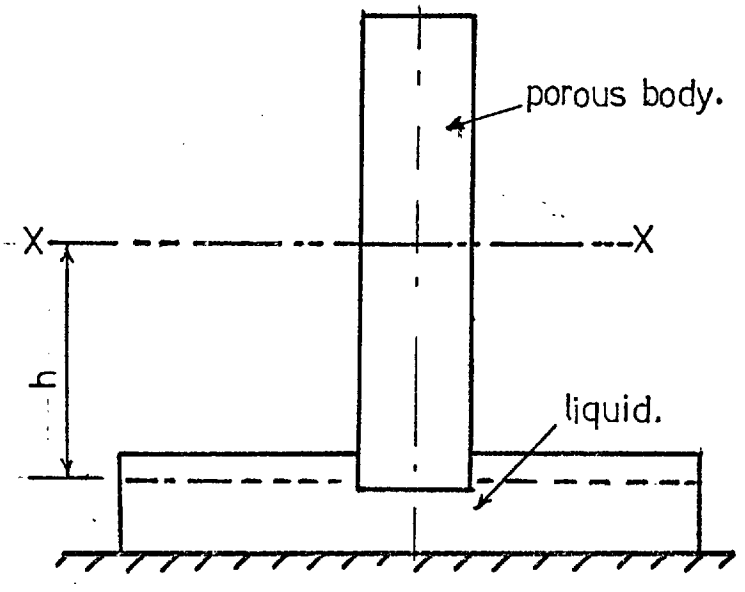


FIGURE 2.2

A porous body dipped in a pool of a liquid.

Hence:

$$p_c = \rho g h \qquad (2.1)$$

where p_c is the capillary pressure of moisture, ρ is the density of liquid, g is the gravitational acceleration, and h is the height above the free surface level of liquid.

If the porous body is homogeneous, or if its properties are independent of position at any height, then over a horizontal cross-section in the body, h remains constant, and hence equation (2. 1) implies that the capillary pressure is only dependent on height.

However, if there is any moisture present as a discontinuous phase, then equation (2. 1) does not hold. Therefore, as long as the moisture distribution in the porous body is continuous and connected with the pool of liquid, the rise and drain curves could be termed the capillary pressure curves under rise and drain conditions, respectively. The two curves generally form a loop which is known as the hysteresis loop of capillary moisture in a porous body. The region enclosed by the rise and drain boundary curves is known as the hysteresis region. Experiments to obtain capillary pressure curves have been carried out by Haines (105), Morrow et al. (167). Poulovassilis (183), Youngs (249, 250) and Topp and Miller (236).

2. 1. 2 Classification of Moisture in a porous body

The moisture in a porous body can be classified into five main groups depending on the nature of the physical effects responsible for its existence in the porous body.

(a) Continuous Capillary Moisture

Under rise and drain conditions, moisture in a porous body can be in the form of a continuous phase which is in communication with the pool of liquid. Capillary forces in the porous body are the primary cause for the presence of this type of moisture, and such moisture in a porous body is termed continuous capillary moisture.

(b) Discontinuous or Trapped Moisture

Apart from the continuous moisture phase, isolated regions of discontinuous or trapped moisture can exist in a porous body. Discontinuous moisture is particularly liable to occur in the case of drainage because of breaking up of the continuous phase.

(c) Adsorbed moisture

A saturated monomolecular layer may be adsorbed on the internal and external surfaces of a porous body. The amount of moisture adsorbed depends on the nature of the surface and can vary from one porous body to another. This type of moisture has been termed moisture bound under adsorption (139).

(d) Osmotically Bound Moisture

When moisture in a porous body contains a solute in the dissolved state, moisture can be transported from one region to another by osmotic effects which arise because of concentration variations. Moisture that is present in a porous body because of osmosis has been termed osmotically bound moisture.

(e) Chemically Bound Moisture

Moisture can be linked with the porous medium by means of a chemical bond, e.g. moisture bound with crystal hydrates etc. This type of moisture is termed chemically bound moisture.

2.1.3 The theory of capillary potential

The concept of capillary potential was first introduced by Buckingham (31). The flow of moisture in a porous body under capillary forces was visualised to be analogous to the flow of heat through a metal bar due to a temperature potential, and to the flow of electricity along a wire due to an electric potential (31, 86-91). It was suggested that the flow of water in the pores of a porous body is caused by the difference between the attraction for water of two regions of the porous body that are not equally moist.

The capillary potential has been defined as the work required to transfer a unit mass of liquid against capillary forces from the point under consideration to the free liquid surface. For a wetting liquid, the capillary forces do mechanical work on the liquid and hence the capillary potential is negative. However, for a non-wetting liquid, the reverse applies, and the capillary potential becomes positive.

If the moisture at the point under consideration is at a pressure p_c, then the work required to transfer a unit mass of liquid from that pressure to atmospheric pressure (p_o) is $(p_c - p_o)/\rho$ units of energy, where ρ is the density

of the liquid. Hence, the capillary potential ψ , can be expressed as

$$\psi = - (p_c - p_o)/\rho \qquad (2.2)$$

Therefore the difference between the pressure of the capillary liquid in a porous body and that of a free surface is a measure of the capillary potential. Later, the quantity pF was introduced by Schofield (206) to represent pF = $\log_{10}\psi$, where ψ is the numerical value of the capillary potential. Several advantages in the use of the quantity pF have been reported (13). The use of the logarithm has made it convenient to transfer the scale to any liquid.

2.2 The movement, distribution and retention of moisture in a porous body under partially saturated and unsaturated conditions

2.2.1 General

The movement of moisture in a porous body nearly all takes place through the pore spaces. The movement is brought about by capillary suction, by gravity or by a combination of both. It has been common to study the rate of movement of moisture in soils in terms of a macroscopic visible wetting front. The movement of the visible wetting front in a column of soil under imbibition has been studied by Moore (162), who concluded that the movement of moisture from wet regions to dry regions is due to capillary action. Capillary movement of moisture in the downward direction has been observed to be slightly faster than in the upper or lateral directions (110).

An investigation into the movement and retention of moisture on a microscopic scale has been carried out by Briggs (28) and later by Haines (104, 105). Briggs (28) suggested that the moisture in a soil could be regarded as a thin continuous film around the surfaces of the soil particles. These films were regarded as convex outwards on the surfaces of the particles and concave outwards at the points of contact. The movement of moisture from one region to another in a soil was attributed to the combined effects of surface tension and gravity.

The filling up of pores in a soil has been classified by Versluys (239) into three different stages. viz.:

(i) Pendular stage: At very low moisture contents, the water in a soil forms discrete rings around the points of contact between the particles. The moisture in this condition is said to be in the pendular stage. The size of the rings increases with moisture content and finally the rings merge with neighbouring rings.

(ii) Funicular stage: Once the pendular rings merge, moisture forms a continuous network throughout the system. Air, too, forms a continuous phase. This stage is known as the funicular stage.

(iii) Capillary stage: A further increase in moisture content leads to complete filling up of the pores. The moisture in this condition is said to be in the capillary stage.

It was due to the work of Haines (103, 104, 105), Fisher (75, 76), and Keen (126) that studies in the movement and distribution of moisture in soils entered a new phase. Idealized beds of either open or close packed structures were used as theoretical models to study the distribution of moisture in soils. The results of these studies are discussed separately for imbibition and drain, in detail below.

2.2.2 Imbibition

Previous studies (75, 76, 103-105, 126) on imbibition have been mainly concerned with the prediction of the behaviour of moisture in theoretical models of regularly packed beds. Studies have been carried out by increasing the saturation fraction from very low values to unity. The predictions have later been compared with the real behaviour of moisture in soils. At very low moisture contents, water is distributed in discrete rings around the points of contact. Keen (126) has shown that the individual pendular rings first make contact with each other, in the planes joining the centres of spheres (Fig. 2.3) enclosing a tetrahedral pore. At this instant, the moisture content has been found to be 22.6 per cent of the pore volume for the closest packing of uniform spheres and

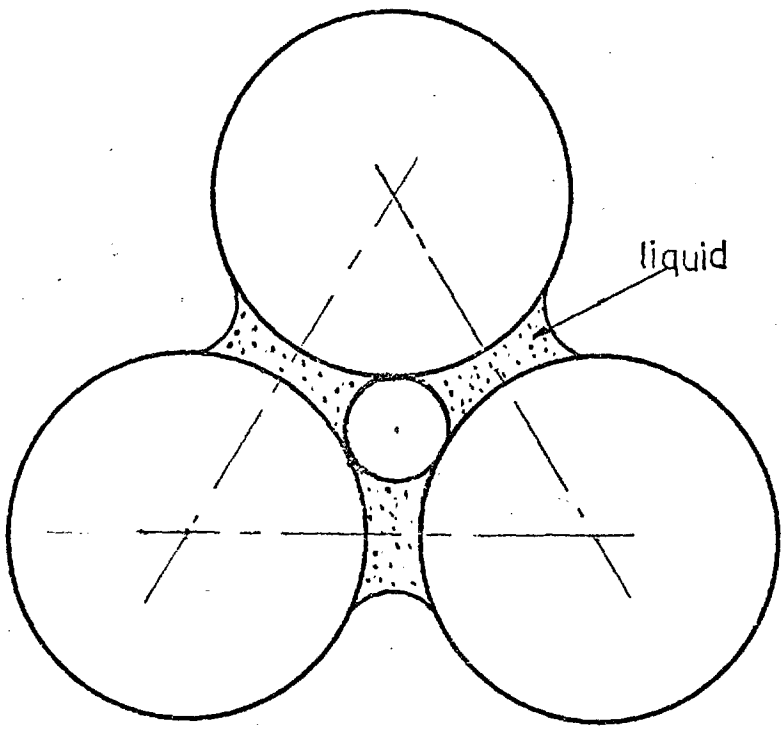


FIGURE 2.3

A section through the centres of three spheres at the end of pendular stage.

18.3 per cent of the pore volume for a cubic packing of uniform spheres. Fig. 2.4 illustrates the pendular stage in a soil.

The capillary pressure p_c, of moisture in a pendular ring formed between two spheres making contact has been expressed as

$$p_c = \frac{\sigma'}{r} \frac{(2 + \tan\Theta - 2\sec\Theta)}{(1 + \tan\Theta - \sec\Theta)} \cdot \frac{1}{(\mathrm{Sec}\Theta - 1)} \qquad (2.3)$$

where σ' is the surface tension and the angle Θ is defined as shown in figure (2.4). Equation (2.3) assumes zero angle of contact between water and the particle. Further, it assumes that the liquid surface makes a part of a circle (see Fig. 2.4).

However, Fisher (75) has shown that the pendular rings have the same total curvature at all points.

At the instant at which the pendular rings make contact with each other, Θ assumes a value of 30° (Fig. 2.5). The pressure deficiency at this instant can be calculated from equation (2.3) as 4.1 σ'/r, for hexagonal packing, where r is the radius of the spheres.

Once the individual pendular rings have merged, the moisture forms a continuous network (Fig. 2.6). Any further increase in moisture content tends to increase the convex surface along the waist of pendular rings, causing the air passage at the waist to decrease. Finally, the surfaces at the waists collapse due to the imbalance caused by the surface forces at the waists. At this instant, the pressure deficiency of moisture in a closest packing can be expressed as 6.9 σ'/r.

As this process continues within the body, more and more cells become completely saturated. This stage is the beginning of the capillary stage (75). The air-water interface area diminishes rapidly with increase in moisture content, thus showing a rapid fall in the pressure deficiency.

2.2.3 Drain

In the reverse process, the pores are initially completely full of moisture and the moisture is in the capillary stage (75).

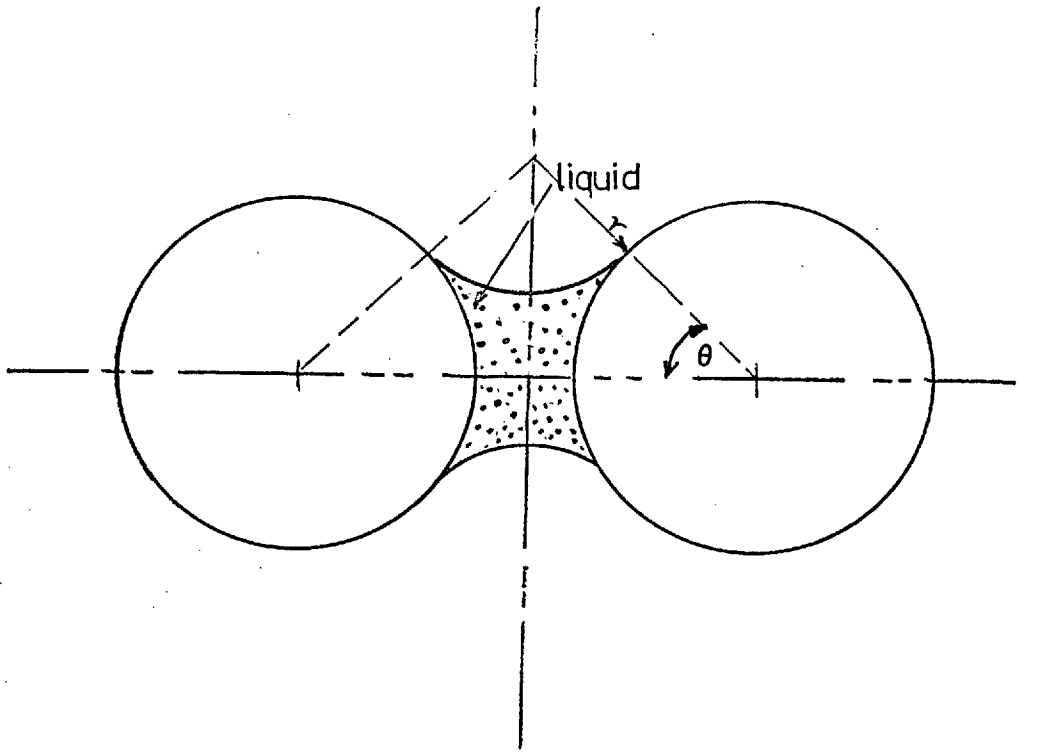


FIGURE 2.4

THE PENDULAR STAGE

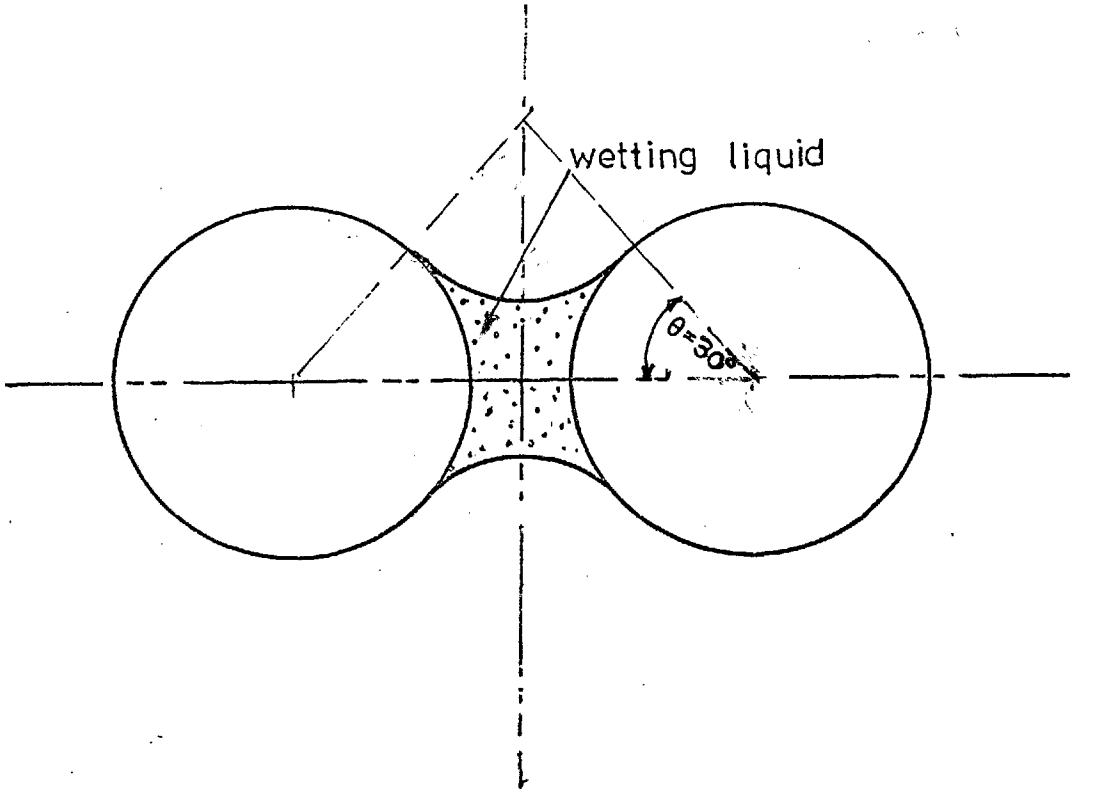


FIGURE 2.5

The pendular stage.

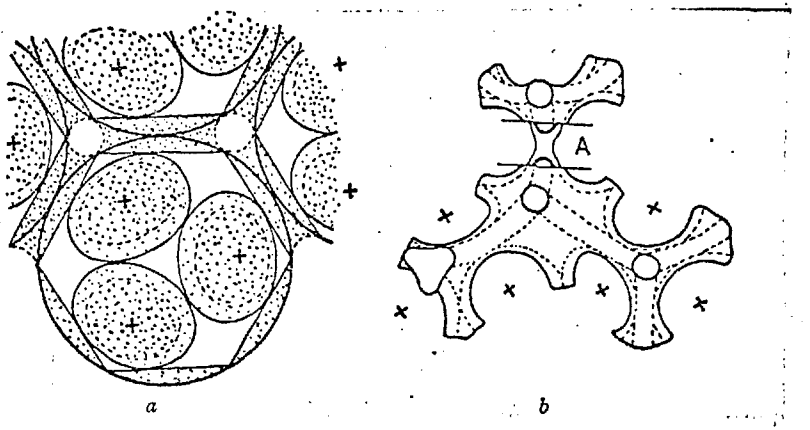


FIGURE 2.6

Distribution and Shape of water films and air spaces in ideal soil. (After Haines(105)).

(a) Distribution of moisture at first stage of coalescence.

(b) Perspective drawing showing shape of continuous air space at first stage of coalescence.

As the moisture is withdrawn from the body, menisci are first formed at the surface pores and these tend to move gradually into the pores of the body. This process increases the surface area of the air-water interface and the capillary pressure increases with the decrease in moisture content. When the meniscus is at the narrowest part of the pore, the capillary pressure was calculated to be 12.9 σ/r for the closest packing. After this, the meniscus enters the neighbouring cell and expands abruptly due to its unstable nature. This abrupt expansion causes redistribution of moisture within the porous body. This is the transition from the capillary stage to the funicular stage. Further removal of moisture yields the pendular stage.

2.2.4 The irreversible nature of moisture movement

Two sets of experiments have been reported by Morrow (165). A heap of slightly tapered capillary tube segments was saturated with a volatile liquid, and the liquid was allowed to evaporate and the system observed under a microscope. It was observed that the air liquid meniscus moved slowly towards the narrower end as the saturation was decreased, causing an increase in the capillary pressure. Occasionally, a meniscus was seen to recede towards the wider end, showing a sudden change in pressure.

A tapered end of a long fine capillary tube was inserted (165) into a pile of spheres heaped on a highly permeable glass membrane. The bed was saturated with a volatile liquid, which was then allowed to evaporate. The pressure was recorded by a sensitive pressure transducer, and it was observed that the pressure rose slowly as evaporation continued, then suddenly fell and slowly rose again. This process was seen to occur several times in the course of a single experiment.

The unstable interfaces have been regarded as the primary cause of these sudden movements of moisture and the sudden changes in pressure. The sudden changes are known as Haines jumps or jerks (156, 159). Heller (113) used the terms rheons and isons to describe the movement of moisture in a soil. Rheon is an alternative name for a Haines jump. Isons are the segments of the pressure-volume displacement curve, between two consecutive rheons. Rheons correspond to smooth reversible displacements.

The movement of moisture in a porous body can therefore be assumed to consist of smooth reversible changes as well as of abrupt changes of the air-water menisci in the pores of the porous body. The sudden changes in the curvature of the menisci, in the capillary pressure and in the distribution of moisture in the pores lead to irreversibility.

2.3 Experimental Methods

2.3.1 The measurement of suction or capillary pressure in a soil

Several types of apparatus have been developed in the past for the measurement of the suction or capillary pressure of moisture in a soil. Of these, tensiometers and pressure membrane apparatuses have been the most widely used by soil scientists. A brief description of each of these two types of apparatus is given below.

2.3.1.1 Tensiometers

The tensiometer consists of cups, the surfaces of which contain pores sufficiently small so that in the presence of moisture, the cups can be regarded as practically impermeable to air. The use of the tensiometer in the laboratory for the measurement of suction in a soil has been discussed by Richards (194). The apparatus was modified by Miller (160) and Croney (47) to enable suction to be measured without significant exchange of moisture between the tensiometer and the soil. The tensiometer is suitable only for suctions less than about 850 cm of water. Beyond this limit, breakdown occurs due to dissolved or entrapped air.

2.3.1.2 Pressure membrane apparatus

The development of this apparatus has been due to Richards (193-195). The apparatus consists of a closed chamber with a membrane fitted at the floor of the chamber. The membrane is capable of withstanding high pressure and is permeable to water. The wet membrane is impermeable to air. Wet soil is placed on the membrane, and compressed air or nitrogen at a known pressure is introduced into the chamber. Transfer of water through the membrane occurs until the soil water is in equilibrium with water outside the membrane. The gas pressure at equilibrium is equivalent to the suction pressure of the moisture in the soil at that particular moisture content.

A modification of this apparatus has been developed by Tanner and Hanks (230), which enables the wetting and drying curves to be obtained. The working range of pressures is usually below 15 atmospheres. However, gas pressures ranging from 0.1 to 170 atmospheres have been used (145). One serious disadvantage of this apparatus has been the reduction of moisture content which takes place under a constant gas pressure when the soil sample has been under test for several weeks (42).

2.3.2 Measurement of moisture content in a soil

The direct method of measurement of moisture content in a sample of a porous medium is to obtain the difference in weights of the wet sample and the completely dry sample.

However, physical properties of porous media, related to the moisture content have been used in the past for the indirect measurement of moisture content (7). The dielectric constant of pure water is appreciably different from that of a dry medium and this has led to the indirect measurement of moisture content by measurement of the dielectric constant of the sample placed between two electrodes. This type of measurement has been reported as being unreliable because of poor contact between the sample and the electrodes (38).

The property of hydrogen in water, of slowing down and scattering fast neutrons has been used (119, 120, 224, 238) in the past to measure the moisture content in soils. Apparatuses have been developed by van Bavel et al. (238), Holmes (119), Stone et al. (224) and Holmes et al. (120). The moisture content obtained in this way represents all forms of moisture, including chemically bound moisture, in the porous medium.

Other methods of measuring moisture content involve the use of electrical conductivity, thermal conductivity, X-ray or Gamma radiation.

2.3.3 The measurement of capillary pressure curves

The experimental techniques in the measurement capillary pressure curves can be classified broadly into two categories.

2.3.3.1 Column measurements

Column experiments usually require a tall column of the porous medium. One end of the porous medium is placed in a pool of liquid. The initial condition of the porous medium is usually that it is either completely dry or completely saturated depending on whether the measurements are for the rise or drain curve, respectively. The system is usually allowed to stand for a few days in order to reach equilibrium. The moisture contents of the porous medium at different heights are obtained either by sectioning the porous medium at different heights and thereafter weighing or by X-ray or Gamma-ray techniques.

A variation of this technique has been used by Morrow (165) who used an epoxy resin as the wetting liquid and allowed it to harden inside the porous medium. The epoxy resin hardened with very little shrinkage. He studied thin sections of the hardened body under a microscope in order to obtain the fractional saturations at different heights.

2.3.2.2 Sample measurements

In general, the measurements involve the use of a small sample of the porous medium to which different suctions are applied. The suctions are measured by a tensiometer, by a pressure membrane apparatus or directly by a manometer. The moisture content at each suction is measured either by noting the movement of a meniscus in the fine tube, which is usually connected to the bulk fluid or by X-ray or Gamma-ray techniques. Techniques similar to these have been employed by Topp and Miller (236), Morrow and Harris (167) and Poulovassilis (183).

Water/air systems have been replaced by air/mercury systems in capillary pressure measurements. Here, the wetting phase is air and mercury acts as the non-wetting phase. Hence, mercury has to be injected under pressure in the process of the experiments. These methods are commonly known as mercury intrusion methods. The method was first developed by Washburn (242) and has been later used by many authors (56, 58, 111, 115, 138, 196).

Pickell et al. (179) describes an alternative method, in which the non-wetting phase is air and the wetting phase is naptha, heptane, octane, or toluene.

If, during sample measurements, the process is reversed from rise to drain or vice versa (e. g. from point A in Fig. 2. 7), the resulting capillary pressure curve has been observed to follow a path which lies in-between the two boundary curves as illustrated by the curve AB in Fig. 2. 7. Such curves are known as scanning curves. The scanning curves cannot easily be obtained from column measurements.

2.4 Theoretical studies of the capillary pressure curves

Several attempts have been made to present theoretical interpretations of the capillary pressure curves. Of these, the simplest treatment is that in which the porous body is considered to contain a bundle of capillary tubes. A hypothetical capillary radii distribution has been defined such that all the tubes of radii (r) less than or equal to $2\sigma/p_c$ will be filled with moisture at a given capillary pressure p_c. Thus the moisture content (χ) at a capillary pressure p_c could be expressed as

$$\chi = \left[\int_0^{2\sigma/p_c} r^2 f(r)dr \right] \Big/ \left[\int_0^{\infty} r^2 f(r)dr \right] \qquad (2.4)$$

But the hysteretic behaviour of capillary moisture in porous bodies cannot be explained by the above model. This difficulty has been overcome by the use of a model consisting of tubes of varying cross-section (134). A tube in which the radius decreases from r_a to r_b at a height h above a free surface (where $2\sigma/r_b > h \geq 2\sigma/r_a$) can be filled to two different heights under conditions of rise and drain (see Fig. 2. 8). Kusakov et al. (134) have shown that several stable heights to which moisture may be filled up can exist in a tube of periodically varying cross section.

However, the models described above do not account for interconnectivity of pores in porous bodies. Therefore a bundle of interconnected capillary tubes of either uniform or varying cross section has been employed in preference to the earlier models to describe various properties of porous media. However, even these models have been inadequate to describe the distribution of moisture in real porous media.

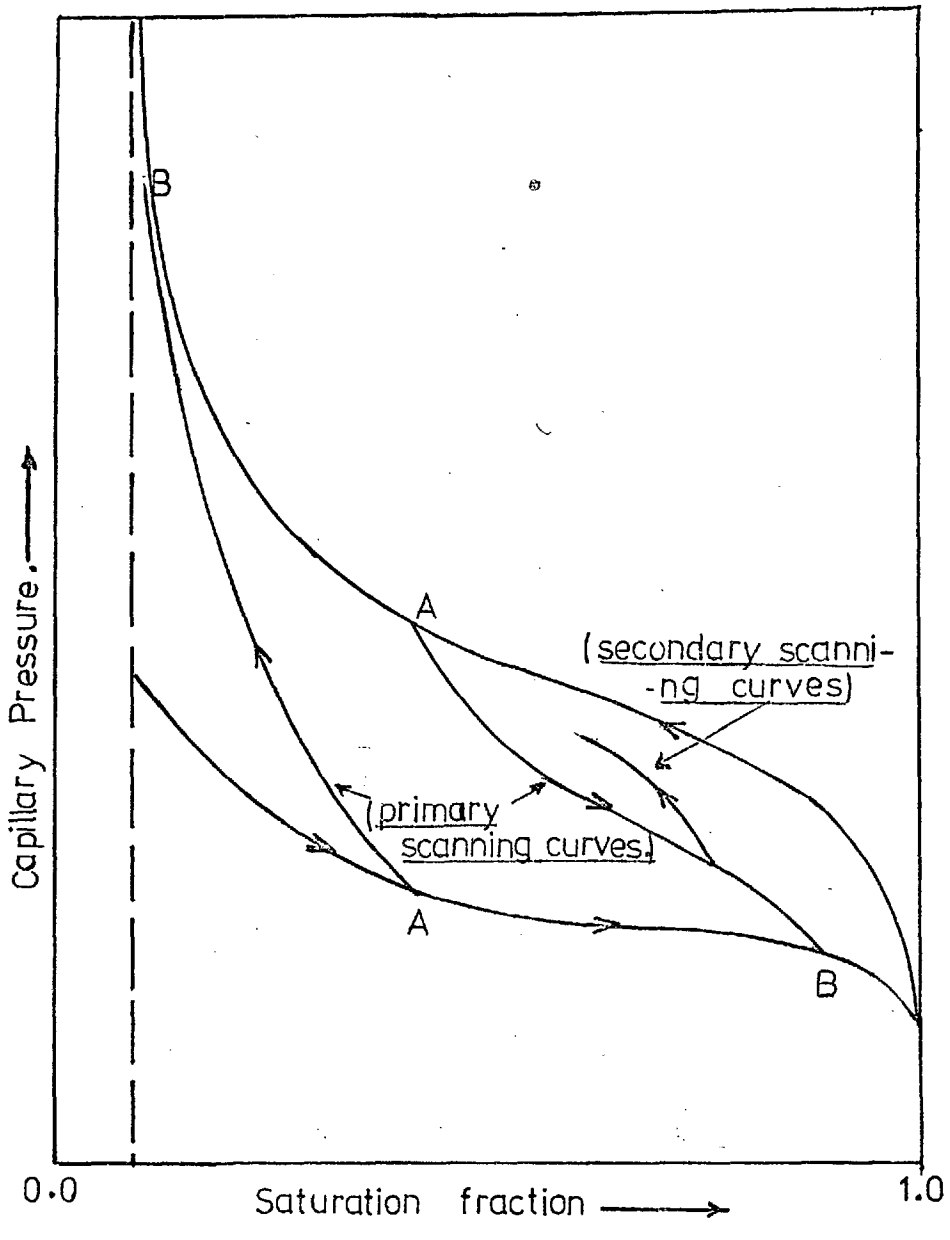
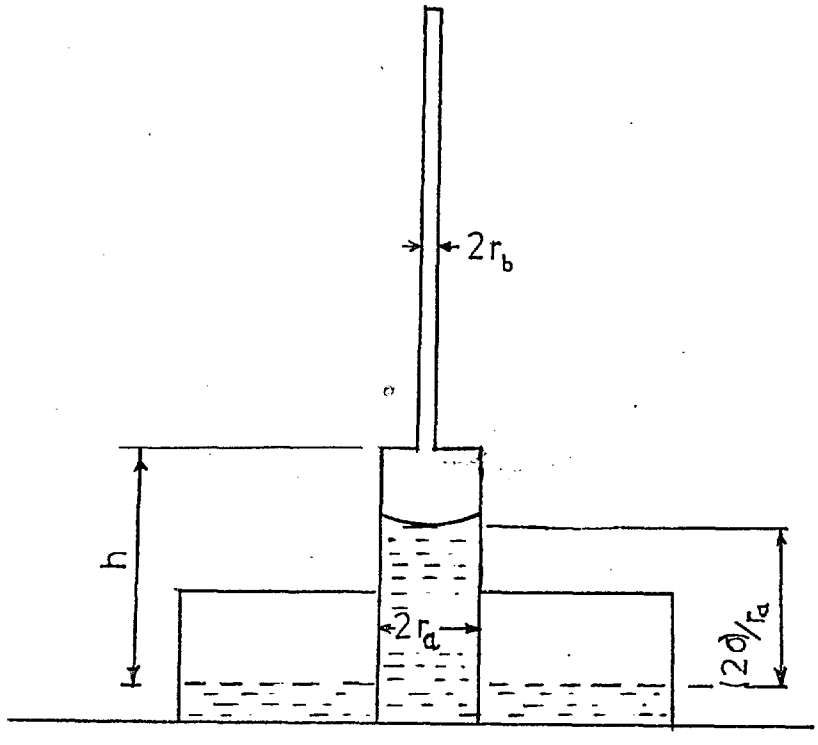
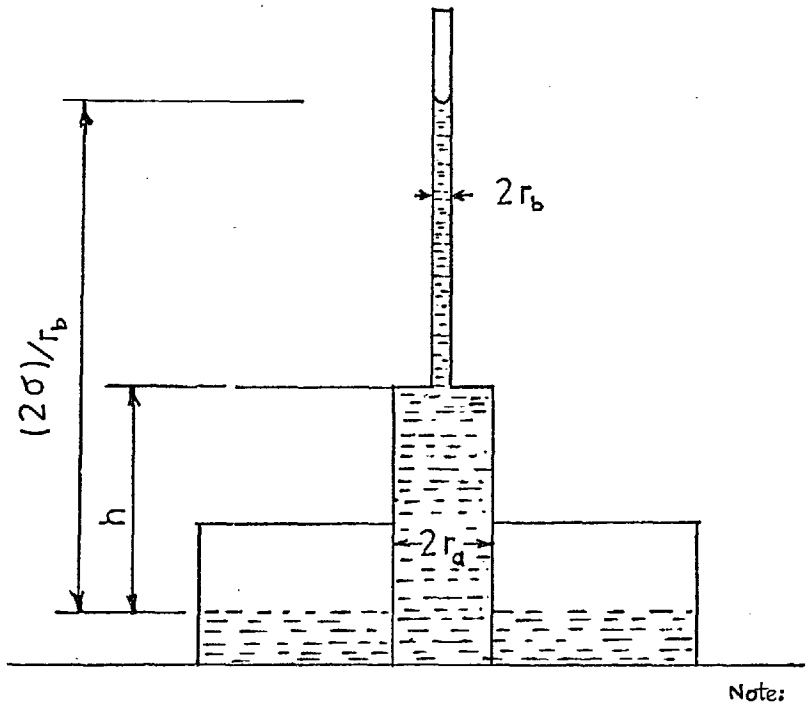


FIGURE 2.7

Scanning curves.



(a) Rise.



(b) Drain.

Note: $\sigma = \sigma'/\rho g$

FIGURE 2.8

Hysteresis effect of moisture in a step tube.

Therefore, empirical methods have been developed to study the capillary moisture distribution curves in porous bodies. Leverett (137) has attempted to study the variation of a dimensionless quantity $\frac{p_c}{\gamma} \left(\frac{k}{p}\right)^{\frac{1}{2}}$ with saturation where p_c is the capillary pressure of a moisture, γ is the surface tension of moisture, k is the permeability of moisture in the porous medium, and p is the fractional porosity. The dimensionless quantity has been commonly known as the Leverett function. Leverett (137) studied the capillary pressure curves for a number of unconsolidated porous media, and showed that the dependence of the Leverett function on saturation can be represented by two distinct curves, one for imbibition and the other for drainage (see fig. 2.9).

Brooks and Corey (30) studied the capillary pressure curves of nine different materials and found that in the case of drainage, the capillary pressure (p_c) can be related to the moisture content (ψ) by the empirical relationship $\log (p_c) = f (\log \psi)$. The curve of $\log (p_c)$ vs $\log \psi$ has been found to be linear over a considerable range of moisture contents.

Poulovassilis (183) used Everett's independent domain theory of hysteresis (62, 63, 65-68) in order to construct the primary drying scanning curves from a knowledge of the primary wetting scanning curves. The independent domain theory of hysteresis, when applied to the behaviour of moisture in porous bodies, suggests that the total volume of water which drains out of a porous body when suction is increased from zero to a certain value, or the quantity of water which enters the porous body when suction is relaxed from a certain value to zero, can be divided into small unique elements which retain their identities. The scanning curves that were constructed by Poulovassilis (183) have been found to be in good agreement with experimental data.

Topp and Miller (236) used Poulovassilis' method to construct scanning curves, but the scanning curves they obtained were not in good agreement with their experimental observations.

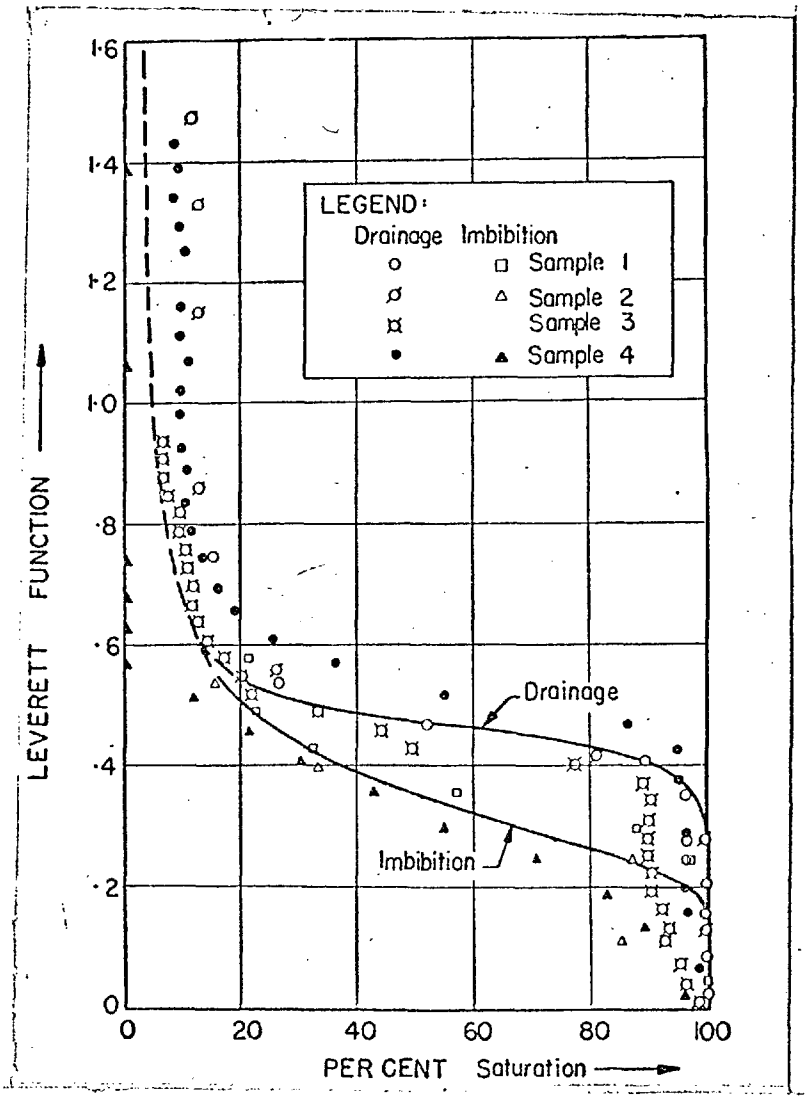


FIGURE 2.9

Typical behaviour of Leverett function with saturation for rise and drain conditions. (After Leverett (137))

A method has been developed (140) to predict the equilibrium moisture distribution in a porous body by evaluating the limiting case (i.e. as time tends to infinity) of the unsteady state moisture distribution. The method employs the solutions of the differential equations which have been developed by Tanaeva (229) to describe the movement of bulk moisture in porous bodies.

A theoretical study has been made on the movement of moisture in the pores of regular packings by Tabuchi (227, 228). The study was extended to construct the drain curve for a regular packing. The model of Tabuchi assumed that a porous body consists of unit pore cells connected regularly and infinitely via nonuniform necks. Both open necks (where the meniscus at the neck is broken and an air passage exists through the neck) and closed necks were assumed to exist in his model. At a given capillary pressure p_c, the probability of air entry through the neck was expressed as $f(p_c)$, where $f(p_c)$ was related to the neck size distribution. The function $f(p_c)$ has been divided into two components $f'(d_n)$ and $p_c(d_n)$. $f'(d_n)$ is the neck size distribution and $p_c(d_n)$ is the relation between the capillary pressure p_c and the diameter of the neck. The function $p_c(d_n)$ has been expressed in the following form.

$$p_c(d_n) = \frac{C'_n}{d_n} = \frac{C'_n}{D_n \phi} \qquad (2.5)$$

where C'_n is the capillary constant of the neck, d_n is the diameter of the neck, ϕ is the diameter of a particle and D_n is the diameter of the neck divided by the particle diameter. The value of C_n depends on the shape of the interface and the surface tension properties of the liquid.

The capillary pressure $p_c(d_n)$ can be related to the height h, to which a liquid column would rise in a capillary of diameter d_n. Hence equation (2.5) has been modified to the form

$$h = C_n/D_n\phi = C_{n/d_n} \qquad (2.6)$$

where C_n is the modified capillary constant of the neck.

Tabuchi approximated the cumulative oversize distribution of neck-sizes to the form

$$f(d_n) = \frac{A_n}{d_n}\phi + C \qquad (2.7)$$

Equation (2. 7) had already been obtained by Tabuchi (227) in his earlier studies of neck sizes. Photographic studies have been made of the neck sizes in a single layer of glass beads. The size distribution of about 190 necks were analysed (227) and approximated to the form given by equation (2. 7).

The value of C in equation (2. 7) has been evaluated in terms of A_n using the fact that the smallest neck diameter that can exist in a packing of uniform spheres is 0. 155ϕ. Hence, when $d_n^* = 0.155\phi$, f = 1. Therefore C has been expressed as

$$C = 1.0 - 6.45\, A_n \qquad (2.8)$$

and hence

$$f(d_n) = \frac{A_n}{d_n}\phi + 1.0 - 6.45\, A_n \qquad (2.9)$$

Equations (2. 6) and (2. 9) have been combined to obtain

$$f'(h) = \frac{A_n}{C_n}\phi h + 1.0 - 6.45\, A_n \qquad (2.10)$$

If H is defined as the product ϕh, equation (2. 7) can be expressed as

$$f'(H) = \frac{A_n}{C_n} H + 1.0 - 6.45\, A_n \qquad (2.11)$$

The value of C_n has been found to be 0. 3 for a spherical interface and 0. 24 for a spheroidal interface (228). A_n has been evaluated to be 0. 2 for a value of C_n of 0. 24.

A function F(f') has been defined as the probability of air entry through a pore cell via the routes within the packing. Alternatively, F(f') has been interpreted as the ratio of the number of cells into which air has been entered, to the toal number of cells. Tabuchi (228) approximated this function to a Weibull distribution of the form

$$F(f') = 1.0 - \exp\left\{ - (f - \gamma)^{\beta} / \alpha \right\} \qquad (2.12)$$

where α, β and γ are the constants of the Weibull distribution function. For the most open packing $\alpha = 0.082$, $\beta = 1.0$ and $\gamma = 0.255$, and for the closest packing $\alpha = 0.095$, $\beta = 1.0$ and $\gamma = 0.305$ (228).

For the most open packing and for the spheroidal meniscus, the equations (2. 11) and (2. 12) have been combined to give

$$F(H) = 1.0 - \exp (-10.2 H + 6.65) \qquad (2.13)$$

The function F(H) has been related to the moisture content $\Theta(H)$ at a height H by

$$\Theta(H) = 1.0 - F(H) \qquad (2.14)$$

$$\text{where } \Theta = (\overline{V}_w - \overline{W}_o)/(\overline{V}_v - \overline{W}_o) \qquad (2.15)$$

and $\overline{V}_v$ is the porosity (percent), $\overline{W}_o$ is the quantity of water retained after drainage, as a per cent of the quantity of water that could be held in the porous body under the condition of complete saturation. $\overline{V}_w$ is the moisture content present in the porous body expressed as a percentage of void space.

Equations (2. 14) and (2. 15) have been used to evaluate the capillary pressure curve in the case of drainage for the most open type of packing.

Because of the absence of knowledge of the pore size distributions in random packings, theoretical studies of the imbibition and drainage of moisture have been limited to models of regular packings.

However, Mason's model (149) for the calculation of pore size distributions in random packings of equal size spheres has made it possible for the imbibition and drainage of moisture in random packings to be predicted. Mason (149) considered packed beds as assemblages of tetrahedral subunits. A tetrahedral subunit has been defined as the tetrahedron formed by joining the centres of four adjacent non coplanar spheres, (see Section 3. 4. 3.). The edges of a tetrahedron so formed do not intersect any other sphere in the packing. Mason calculated the geometrical properties of the pore spaces in these tetrahedral subunits (e. g. tetrahedron insphere radii and face insphere radii etc. - see fig. 2. 10) in order to obtain the distributions of these properties.

Mason (149) considered each tetrahedron to be a domain in a packing. The drainage of the assemblage of tetrahedra was studied in terms of tetrahedral subunits in which the drainage of moisture takes place through one or more of the four faces.

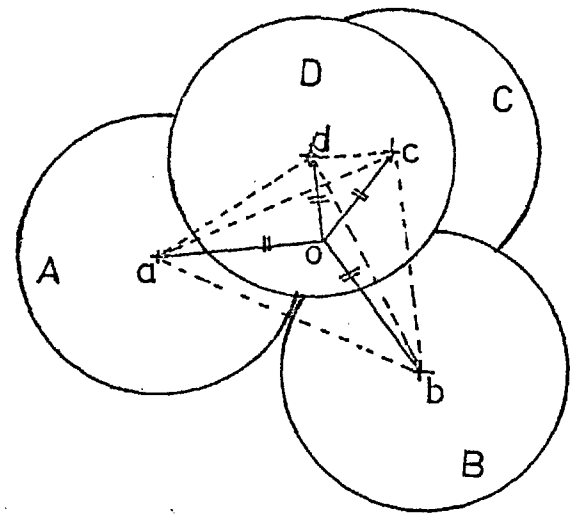


FIGURE 2.10

The tetrahedron insphere radius (R).

a,b,c and d are centres of spheres.

oa = ob = oc = od

R = oa – sphere radius.

Mason assumed that drainage of moisture from a pore always takes place through the face of minimum curvature. This criterion was incorporated into his model in order to enable him to calculate a curve showing the drainage curvature with saturation. However, this method of approach did not take into account the effects of interconnection. Therefore, Mason (149) extended his analysis to provide a limited allowance for inter-connectivity. It was shown that a network of tetrahedra cannot be drained beyond the top layer of tetrahedra in a packing if drainage occurs through only one face of each pore. Hence, it was suggested that, for a drainage front to advance through a pore, it should enter the pore through one face and leave through another. This assumption makes the properties of the two largest faces of each tetrahedron become important in the drainage of the assemblage of tetrahedra. Mason (149) assumed that there is an equal probability of a draining meniscus entering through either of the two largest faces of a tetrahedron. He constructed a curve showing the drainage curvature as a function of saturation for his model. Two similar curves were constructed assuming that (a) the three largest faces are important in the drainage of a pore and (b) all four faces are important in the drainage of a pore, respectively.

The case of imbibition was approached by Mason who assumed that the filling of a tetrahedral pore takes place at a meniscus curvature equal to that of the sphere that would just fit inside a tetrahedral pore. (i. e. the curvature of the tetrahedron insphere). This enabled him to construct a curve showing the imbibition curvature as a function of saturation for his model.

In his later studies on desaturation in porous media, Mason (150) classified the configurations of tetrahedral cells in a packed bed according to the saturation of each cell and according to the saturation of the adjacent cells. The probabilities of a water-water link between two pores becoming a water-air link, and a water-air link becoming an air-air link have been evaluated to obtain the variation of fractional saturation in terms of a parameter p, which has been defined as the probability that, at a given capillary pressure, a meniscus would not pass through a face of a tetrahedral pore.

The parameter p has been defined as

$$p = \left\{ \int_0^{r_i} f(a)\ da \right\} / \left\{ \int_0^{\infty} f(a)\ da \right\} \qquad (2.16)$$

where f(a) is the distribution of radii (a) of drainage menisci in the tetrahedral cells, and r_i is the radius of the meniscus which would just drain at the capillary pressure under consideration.

Mason (150) related the quantity p, to the drainage curvature using the distributions of face radii of his earlier model (149). Mason obtained a curve showing the relation between the saturation fraction and the drainage curvature. The theoretical curve has been compared with the experimental observations of Haines (105) and was reported to be in reasonable agreement.

Palosaari (177) developed a method of predicting a capillary pressure curve from a knowledge of five measured points in a given curve. The development of the method has been based on physical and statistical properties of the phenomenon.

Palosaari (177) assumed that, at a given height h, the moisture content in a porous body can be related to the sizes of the capillaries which are smaller than or equal to the size of the capillary which would just fill up to a height h.

A modified form of the moisture content, Φ_h was defined by Palosaari (177) as follows:

$$\left.\begin{aligned} \Phi_h &= (\Phi - \Phi_r) / (1 - \Phi_r) \text{ for drainage} \\ \Phi_h &= \Phi \text{ if } \Phi \geq \Phi_r \\ \text{and } \Phi_h &= \Phi_r \text{ if } \Phi < \Phi_r \end{aligned}\right\} \text{ for imbibition} \qquad (2.17)$$

where Φ is the saturation fraction and Φ_r is the residual saturation fraction.

Palosaari (177) related the quantity Φ_h to the capillary size distribution function f (r) as follows:

$$\Phi_h = \int_0^{r_{max}(h)} F(f(r))dr \qquad (2.18)$$

where F(f (r)) is a function of the capillary radius distribution and $r_{max}(h)$ is the radius of the largest capillary, which would fill to a height h above a free surface.

The relationship between F and f has been assumed by Palosaari to be of the form,

$$F = C(r)\, n(r)\, f_e(r)\, f(r) \qquad (2.19)$$

where, n(r) denotes the number of capillaries of radius r, $f_e(r)$ is the relationship between the volume of liquid in a capillary and its radius, and c(r) is a coefficient which relates capillary volume to its effective radius. Thus, the quantity Φ_h could be calculated as a function of h. Palosaari (177) preferred to use the distribution of the logarithms of the capillary radii in his calculations. The logarithms of capillary radii can be easily expressed as the logarithms of the capillary rise heights. Therefore Φ_h can be expressed as a function of ln(h) and vice versa, where h is the capillary rise height.

Hence the following relationship between ln(h) and Φ_h was assumed.

$$\ln(h) = \xi(\Phi_h) \qquad (2.20)$$

The capillary radii distribution was assumed to be unimodal and to approximate a Gaussian or normal distribution. This enabled Palosaari to obtain an expression for the capillary pressure curve, in terms of five unknown parameters. The five parameters were evaluated using five measured points in a capillary pressure curve. It was reported (177) that the equation thus obtained is able to describe a capillary pressure curve reasonably satisfactorily.

Palosaari (177) attempted to construct the drain curve from a knowledge of the rise curve, and vice versa. He assumed that a porous material can be considered to consist of volume units of material of different pore sizes, but of the same internal geometry. Further, he assumed that the ratio between the smallest and the largest capillary radii remainsconstant for a given porous body. In such a case, the ratio of the heights of the capillary rise and drain curves is independent of the moisture content. Hence, Palosaari suggested that the ratio of the heights of the capillary rise and drain curves at any given moisture content would be sufficient to predict the drain curve from the rise curve,and vice versa. Palosaari (177) predicted the drain curve for quartz sand from the rise curve which had been obtained for the same sand. The predicted drain curve was reported to be in agreement with the experimental drain curve.

2.5 The Hysteresis and Irreducible saturation

2.5.1 The Hysteresis

The distinct nature of the rise and drain curves in porous bodies shows that hysteresis of moisture content exists in porous bodies. The reason for its existence has been explained (183) in general terms by Everett's theory of independent domains of hysteresis (62, 63, 65-68). However, the general theory of hysteresis, in itself cannot give any useful information about capillary hysteresis unless the factors affecting capillary hysteresis in porous bodies are studied. Pickell et al. (179) have studied the factors which affect the capillary hysteresis of moisture in porous bodies and have classified two types of hysteresis, namely; 'trap' hysteresis and 'drag' hysteresis.

(i) Trap Hysteresis

A pore in a layer of a completely wet porous body is able to retain or trap moisture under drainage conditions, if the narrowest section in the pore is able to retain moisture by capillary forces. However, during imbibition, due to the cellular nature of the pores, the moisture needs to traverse through several layers of varying sectional apertures before reaching a required layer. In this process, the moisture can be prevented from reaching a particular pore if on the path to that pore the moisture encounters an aperture at which gravitational forces predominates over capillary forces. In this way a pore which would have remained filled under drain conditions might not be filled under rise conditions. Hysteresis, that arises as a result of the above behaviour has been termed 'trap' hysteresis.

(ii) Drag Hysteresis

Once trapping has been allowed for, additional hysteresis has been observed (179), for which a physical explanation has not yet been established. However, it has been thought (179) that it may arise as a result of the difference in contact angles exhibited by the advancing and receding interfaces or that it may be because of the change in surface tension that follows a change in the concentration of impurities at a receding interface.

2.5.2 The Irreducible saturation

The irreducible saturation in a porous body is made up of moisture that is retained either by being trapped or as pendular rings. As the moisture at this stage is generally at isolated points, the capillary pressure of moisture cannot be measured in terms of the difference in heights between the position of the point under consideration and the free surface level of the pool. The capillary pressure of pendular rings formed in a random packing of uniform spheres has been studied experimentally by von Engelhardt (241) who found that at irreducible saturation, the different pendular rings are not under the same capillary pressure and that the rings have a distribution of sizes. Further experiments on the capillary pressure of moisture in pendular rings have been carried out by Morrow an Harris (167), who used packed beds of glass beads of 3 mm diameter. When the formation of a pendular ring was observed, a tapered microcapillary probe was taken from the bulk fluid and introduced into the pendular ring, without changing the inclination of the probe to avoid changes in the hydrostatic head. No change in the position of the meniscus was observed, even when suction was increased. However, it was observed that when the probe was re-inserted into the bulk fluid it showed a pressure difference and that liquid flowed from the probe to the bulk fluid until equilibrium was reached. Hence, it has been inferred that moisture in most of the pendular rings was at a pressure equal to that existed within the bulk fluid at that point in the body at the time of the isolation of the pendular rings.

Morrow and Harris (167) extended their experiments in order to study the fractional residual saturation that was due to the existence of pendular rings. They saturated the pore spaces in random packings of equal size chrome steel spheres with dilute acid and then drained the acid from the packing down to the irreducible saturation using a Buchner filter. After about 0.5 hours the spheres were clearly etched over the areas of contact with the retained acid. Spheres were selected at random and the etched surfaces measured as radii or in the case of linked rings, as equivalent radii. Sphere sizes of 3.18 mm, 4.76 mm. and 6.35 mm. were used and the average residual saturations were calculated to be 4.5, 5.0 and 4.6 per cent of the pore volume respectively. However, after air drying, the samples had irreducible saturations of 6-7 per cent. The difference between the two values was explained as being the result of the existence of trapped moisture in isolated pores. The volume of moisture trapped in isolated pores was, therefore, assumed to be about 1 to 2 per cent of the total pore volume.

Morrow (166), in a separate set of experiments has used beds consisting of 3 mm. diameter beads. The beds were saturated with a liquid epoxy resin containing a blue organic dye. The resin, after being allowed to drain hardened without significant shrinkage. The air space was then evacuated and filled with an orange coloured epoxy resin. Six thin sections of the hardened packing were studied and these gave an average irreducible saturation of 7.2 per cent of the pore space.

Mason (150) in a theoretical analysis of the modes of moisture distribution under desaturation, calculated the residual saturation due to trapped moisture to be 2.8 per cent. This value is slightly higher than that obtained by Harris and Morrow (109).

Apart from studies of the fractional residual saturation, studies have been made of the shapes of the individual pendular rings.

The exact solution of the equation for the profile of a pendular ring has been obtained by Fisher (75), Woodrow et al. (247) and Melrose (157). Hackett et al. (102) approximated the curvature of pendular rings with a curvature equivalent to that at which a meniscus would pass through the face of a regular tetrahedral pore. However, some workers have approximated the shape of the pendular liquid surface to that of a toroid. (103,64, 180).

2.6 Discussion

This chapter describes the previous studies that have been made on the distribution of moisture under rise and drain conditions in porous media, with particular reference to packed beds. The various theories that have been used to predict the capillary pressure curves have been linked to various models which describe the porous media. An exception, in which a model has not been used, is that of Poulovassilis (183) who made use of Everett's general theory of hysteresis in order to construct the primary drying scanning curves from a knowledge of the primary wetting scanning curves. In order to study rise and drain phenomena, the assumptions involved in a theoretical analysis should be close to the real behaviour of moisture in the pores of porous media.

For such an investigation, a model which would adequately describe porous media is needed. Many of the models that have been proposed by research workers, have been inadequate in their description of the properties of porous media. Models based on capillary tube bundles, either of uniform or of varying cross-section, and net-work models do not explain the phenomenon of residual saturation. Packed beds of spheres have been used as experimental models in order to study the capillary phenomena. Mason's Model (149) for the determination of the distribution of pore sizesin randomly packed beds of uniform spheres has met some of the shortcomings so far encountered in the description of packed beds. Mason's model has opened up a new line of approach in that it enables porous media to be considered as assemblages of pores and interconnections rather than as capillary tubes.

Mason's (149) analysis of the modes of moisture distribution in pores and the transition from one mode to another as a result of a change in capillary pressure gives a better understanding of the behaviour of moisture under drain conditions in a packed bed. Only a few attempts have been reported, for the prediction of rise curves in porous bodies. The complex nature of the mechanism of imbibition and the simple nature of the models considered have made the prediction of the rise curves difficult. An attempt similar to that made by Tabuchi (227), with the aid of pore size distributions similar to that of Mason's Model could be useful in the prediction of rise curves.

The hysteresis behaviour of capillary moisture in porous bodies under rise and drain conditions implies that the factors involved in the movement and distribution of moisture in the pores of a porous medium are different for each case. Therefore studies aimed at the prediction of rise and drain curves have to be carried out separately, so that the factors governing each phenomenon can be analysed in greater detail.

From this discussion it is seen that realistic models of porous media are needed and that in order to predict rise and drain moisture distributions under a given set of conditions, the phenomena of rise and drain have to be studied in terms of the physical phenomena encountered in the pore spaces of the porous medium.

CHAPTER 3

A literature survey of models for packed beds.

3.1 Introduction

Models for packed beds have been devised and tested in many fields of engineering and science. However, the requirements specified for the models in each of these fields may be different.

Flow through packed beds is often studied by engineers in order to relate the permeability to the void fraction, mean surface area etc., while those engaged in catalysis are involved in the reaction rates on the surfaces of catalyst pellets in a bed. The movement of moisture in packed beds is studied by civil engineers and by soil scientists in order to obtain a better understanding of ground water flow. The structural strength of completely and partially wet soils is studied by civil engineers. The mechanism of moisture movement in packed beds and the distribution of moisture in the pores in packed beds are studied by chemical engineers in order to predict the drying ratesof completely saturated or partially saturated packings. Also, models for packed beds have been studied in physics, where molecules of monatomic liquids are approximated to the spheres in a random packing. Some fields in botany (146) and metallurgy (215) involve the study of randomly packed beds.

These models can, in general be classified into three groups.

(i) Capillaric models in which a porous body is approximated to a bundle of capillary tubes of either uniform or varying cross section.

(ii) Network models in which a porous body is considered to be represented by a bundle of interconnected capillary tubes. The cross sections of the capillary tubes and the interconnecting tubes may be either uniform or varying.

(iii) Random models in which spheres are considered to be packed randomly in three dimensional space according to a specified algorithm. No sphere is allowed to interfere with the other spheres in the packing.

The above models are discussed in greater detail in the following sections.

3.2 Capillaric models

These models have been developed in the study of permeability and its relationship with pore size distribution or with an average pore size (16, 32, 33, 35, 59, 92, 112, 114, 122, 125, 182, 184, 186, 205, 217, 233, 234). The pore size distribution has usually been evaluated from capillary pressure curves.

The simplest model is that of a bundle of uniform capillary tubes of equal cross section. (132, 140, 205). The flow of a fluid through a packed bed or a porous body has been approximated to that of flow through a bundle of uniform parallel capillary tubes. An average pore size of the tubes is evaluated in order to represent the flow through a porous body or packed bed. However, the behaviour of real porous bodies or packed beds differs from the behaviour of a bundle of capillary tubes in many ways. In particular the hysteretic behaviour of moisture in a porous body or in a packed bed cannot be explained by the use of capillary bundle models. This has led to the development of models of porous bodies based on bundles of capillary tubes of varying cross sections.

Many authors (95, 140, 179, 221) have used capillary pressure curves of porous bodies to evaluate hypothetical pore size distributions (See Sect. 2.5). This led to the development of the field of porosimetry. Many commercial porosimeters have been designed (111) to evaluate the pore volume and pore surface area distributions from mercury intrusion data. Dullian et al. (58) used photomiorography and mercury intrusion methods to determine the pore size distributions of sandstone samples. Dullian et al. (58) has observed that the pore size distributions obtained using the two methods described above differ drastically from each other for all samples.

Such pore size distributions are inadequate to describe the hysteretic behaviour of capillary moisture in porous bodies. Also, the transverse dispersion of moisture in porous bodies (i.e. the movement of moisture in a direction orthogonal to the bulk movement of moisture) cannot be explained by the use of capillary tube bundles. The hysteretic behaviour of moisture in a porous body has been explained in terms of a bundle of capillary tubes which have varying cross-sections along their lengths (134). Purcell (184) assumed the capillaries to be parallel to a given direction but with varying cross-section from one face of a porous body to the other face. Kusakov and Nekrasov (134) used a model

based on capillary tubes of varying cross section and showed that the model was consistent with the existence of hysteresis of capillary moisture.

Pore size distribution studies have been made in the field of adsorption of gases or vapours in porous media (27, 51, 69, 100, 169, 188, 212, 223).

3.3 Capillary Network Models

It is to be expected that the complex structural features of porous media influence the characteristics of flow (e.g. dispersion, diffusion, capillary rise, flow etc.) through porous media. Some of the important structural features which may influence such characteristics are as follows.

(i) Channel cross-section and shape

Fluid flow through porous media generally takes place through pore channels. The sizes and shapes of the cross-sections of the channels can vary from one place to another in a porous body. In most of the theoretical work, the circular cylinder has been the commonly used shape because of its simplicity. However, channels of other cross-sectional shapes exist and the actual shapes are dependent on the structural features of the medium.

(ii) Variation of cross-section along its length

The velocity of flow of a liquid in the pore channels of a porous body can, as a result of changing channel cross sections in the flow path, differ from one position to another along a flow path. This results in distortion of flow paths from one section to another section of a porous medium. Analysis of this effect even for idealised models presents considerable difficulties.

(iii) Tortuosity

A particle of fluid moving in a porous body usually takes a tortuous path. Originally tortuosity was defined as the actual length of the path taken by a fluid element in traversing unit distance in the direction of the bulk fluid flow. Tortuosity can be regarded as purely a geometrical property of each porous medium. Attempts have been made to co-relate the electrical conductivity of a saturated porous medium to its tortuosity (9, 82, 222, 248). However, Owen (176) has shown that there is no direct relationship between the geometrical properties of pore spaces and electrical conductivity of a porous medium.

In order to introduce the above structural features of porous media into theoretical studies a number of network models have been proposed. Regular network models have been used by Fatt (70, 71), Dodd and Kiel (55), Ksenzhek (133) and Harris (108) in studies of displacement of fluids through porous media.

Nicholson (170, 171) and Nicholson and Petropoulos (172, 173) have described the use of three dimensional cubic network of interconnected pores to represent porous media. The model has been applied to study sorption and desorption of vapours in porous media (173). Josselin de Jong (123) and Saffman (203) developed random network models of capillary tubes for the prediction of dispersion coefficients in porous media. Fatt (70) has attempted to predict the permeability and capillary pressure curves of porous bodies by the use of network models of non-uniform interconnected tubes. An improvement to the network model has been suggested by Greenkorn (107) who considered the interconnected tubes to be randomly sized and randomly oriented. Calculations based on capillary tube network models have been used by Claridge (39) and Ralf Simon et al. (187) in the field of oil recovery. Drying rates of moist packed beds have been compared with the corresponding drying rates from branched tubes by Oliver (174). It has been observed that drying rates from triple branched tubes were similar to the drying rates of moist packed beds.

3.4 Random models for packed beds

Random packings of equal spheres have been studied by research workers in many disciplines. The rapid development of models of random packings has been due to research in liquid state physics aimed at the prediction of physical properties of monatomic liquids. In such studies, monatomic liquids are approximated to random packings of equal size spheres. (3, 17-20, 24, 83, 118, 190, 191, 202, 209, 232). Studies of heterogeneous porous media (36, 41, 81, 147, 158, 185, 204, 213) and soils and granular beds (48, 52, 97, 129, 155, 163, 214, 218) have been based on the models of packings of spheres. Apart from the practical applications, the study of packings forms a branch of mathematics. (44, 46, 117, 128, 225).

3.4.1 Experimental developments

3.4.1.1 Geometry of random packings

The earliest reported work on packed beds was due to Hales (106) who examined the polyhedral cells (i.e. the polyhedra formed by joining the centres of spheres in a packing) formed by allowing a heap of peas to swell. The regular dodecahedra which he observed have been shown to be erroneous. Instead, polyhedra with five faces have been found to be dominant. (53, 77, 152).

A model which was built by hand, in which spheres were separated by interconnecting spokes, is reported by Fisher (77). The model was constructed to represent the structure of liquid argon and the radial distances between the centres of the spheres were chosen to correspond to liquid argon.

Bernal (20, 24) and Scott (208) constructed random models similar to that described above and measured the co-ordinates of the centres of each sphere in order to obtain the radial distributions of the random packings. Models of hard spheres packed tightly in spherical bladders were used by Bernal and Mason (23) to measure the co-ordination numbers (i.e., the average number of contacts per sphere) of such packings. The measurements were made by studying the marks left after paint had been poured through the array.

Bernal (20) studied his random model in further detail and concluded that his packing could be expressed as an assembly of five canonical types of polyhedra. (viz. tetrahedron, half octahedron, trigonal prism, Archimedean antiprism, dodecadeltahedron in a ratio 73.0:20.3:3.2:0.4:3.1). None of the canonical units were large enough to admit another sphere. These polyhedra were found to fit together in many different ways (more than 197 ways).

Scott (208) constructed a model of a random close packing by embedding ball bearings in wax. The co-ordinates of the centres of 1005 balls were measured by Scott to obtain the radial distribution.

3.4.1.2 Void fraction

The void fraction is another aspect of random packings which has been investigated by many workers. It has been found that the void fraction of a packing can vary from a low value as 0.36 to a value as high as 0.44 depending

on the method of packing. A void fraction of 0.36 has been obtained for vigorously formed packings (141, 181, 207, 209). The void fraction of packings which has been settled gently from dilute suspensions has been observed to be between 0.40 and 0.44 (135, 219, 237).

Packings of equal size spheres have been classified according to their void fractions. Packings with a mean void fraction of approximately 0.36 are known as dense packings and those with void fractions approximately 0.40 and larger are known as loose packings (19, 20, 141, 207, 209, 237). Although void fractions larger than 0.40 have been observed (3, 135, 155, 219, 243) in most cases the void fractions of equal size sphere packings fall within the range of 0.36 (approximately) to 0.40 (approximately) (36, 48, 136, 153, 164, 243).

It has been observed that structures of packings in regions near the walls tend to be ordered or systematic. This has been found to be the case in a layer of thickness of about four to five sphere diameters. Beyond this layer, the packing can be regarded as random. (7, 141, 197).

The effect of vibrations on the void fractions of packed beds have been studied by Debbas and Rumpf (50). The behaviour of void fraction with time of vibration and with the height of bed has been presented in the form of graphs for different frequencies of vibration. It has been observed that with prolonged vibration a bed with an initial void fraction of about 0.40 settles down to a bed with a void fraction of about 0.36. It has also been observed that if an already vibrated dense bed is held in a container and overturned, the void fraction of the resulting bed is the same as that of the original un-vibrated bed. (131).

3.4.2 Theoretical developments

The earliest theoretical study of the modes of packing of spheres and the porosity of packings of spheres is reported to be that of Slitcher (213). Subsequent studies were made by Smith et al. (219), Graton et al. (97), Manegold (142), Manegold et al. (143), Hrubisek (121) Ackerman (1), Foord (80) and Busby (34). Theoretical studies on packings of spheres have been independently developed as a branch of mathematics too. (44, 46, 98).

Recently computers have been used in model studies of packed beds and to simulate phenomena in packed beds (3, 79, 93, 201, 74, 114, 186, 217). Modelling of packed beds using computers has the advantage of the convenience of checking and comparing the results obtained by the use of different algorithms. The earliest models for packed beds usually generated pseudo random numbers, which were later used to obtain co-ordinates of random points in space. The points obtained in this way were regarded as the centres of spheres in a packing. A similar approach has been used by Adams and Matheson (2) to model a random packing. They analysed a packing formed by 5402 spheres, the centres of which were chosen by 5402 random points and obtained a packing density (i. e. the volume of material in a unit volume of packing) of 0. 628. This value is about 0. 8 percent higher than the value obtained by Scott (210).

Bernal (18) modelled a packed bed by generating a series of random Cartesian co-ordinates within a cube. Each point was defined by three Cartesian co-ordinates and was regarded as a centre of a sphere in a packing. Each sphere thus generated was examined to see if it overlapped neighbouring spheres. The properties of the packings generated in 1000 such cubes were analysed using the computer.

The above methods were developed mainly to study the packing densities or void fractions of random packings. However, for a more complete description of a random packing, a knowledge of the distributions of pore sizes are needed. In order to predict the pore size distributions, it is convenient if the packings could be regarded as assemblages of smaller sub-units.

Two methods of subdivision of packings has been established and are given below.

(a) Random packings can be regarded as an assembly of tetrahedral sub-units. A tetrahedral sub-unit in a packing is formed by joining four non-coplanar centres of adjacent spheres.

(b) Random packings can be sub-divided into a set of 'Voronoi Polyhedra'. A Voronoi polyhedron at a point out of a set of points has been defined as the smallest closed polyhedron formed about that point by the planes bisecting the lines joining that point to the neighbouring points, so that

no further planes can be drawn to cut the chosen set of planes. The network of polyhedra formed about the centres of each sphere in a packing has been shown to fill the space completely.

Each method of subdivision has its own advantages and disadvantages. The tetrahedral subdivision system has the advantage of simplicity of analysis (148). More tetrahedral subunits can be formed than Voronoi Polyhedra for a given packing, thus giving statistically more significant results.

On the other hand it has been reported (148) that local variations of void fractions can be easily handled by the use of the Voronoi subdivision system.

Bernal and Finney (74) used the Voronoi subdivision system in their computer calculations in order to model a packed bed and obtained an average packing density of 0.6342. Mason (148) approached the problem of generating a set of random points in three dimensional space. The points thus generated were considered to be centres of small spheres of a given radius. Each sphere was checked with its neighbouring spheres for overlapping. If two spheres were liable to overlap, the two spheres were moved apart until they just touched. Mason (148) used this method to model a packed bed with the aid of a computer.

Finney (74) used the Voronoi subdivision system in a computer aided study of the geometrical properties of a random array of spheres. An average packing density of 0.6366 ($\pm$ 0.0004) was obtained (74). Finney (74) analysed Scott's packing (207) using the Voronoi-polyhedra subdivision system and obtained a packing density of 0.6342 $\pm$ 0.0012, which is slightly smaller than the packing density previously calculated by Finney (74).

Mason (149) developed a computer model for the prediction of pore sizes in a random packing of equal spheres. Mason analysed the geometrical properties of an assembly of tetrahedra by making use of tetrahedral subdivision system. Mason's computer program generated a set of random numbers which were later used to produce edge lengths (i.e. the lengths of edges of tetrahedra) using an approximate radial distribution. He obtained a packing density of 0.635 in his analysis.

Computer models, which analyse the mechanics of formation of random packings, have been developed independently by Visscher et al. (240) and by Tory et al. (237). These methods analyse the stable positions attained by spheres as they are considered to be dropped one at a time into a container. A regular hexagonal close packed structure was obtained by the computer model of Visscher et al. (240) up to 7 or 8 layers of spheres from the base of the packing. The packing densities for different heights of packing from the base of the container were evaluated (240). An average packing density of 0.582 to 0.600 was observed for random packings of monosize spheres.

Tory et al. (237), using a computer, modelled a packed bed formed by very slow settling of rigid equal spheres from a dilute slurry. He calculated the average void fraction of his model to be 0.42.

A model for a packed bed of monosized or approximately monosized spheres has been developed by Alkiviades et al. (4). They assumed that a packed bed consists of statistically identical unit bed elements, each of which consist of a number of unit cells connected in parallel. Each unit cell was assumed to resemble a piece of constricted tube of random dimensions. The constrictions were defined as windows and the cells were defined as pores. The model was used to study flow through porous media.

Apart from random or Monte Carlo models, semi-theoretical approaches have been made in order to study randomly formed beds. Wicksell (244) studied the frequency distribution of the diameters of circles obtained by the intersection of the spheres with a plane section through the bed. He obtained a relationship between the frequency distribution of the diameters of the circles and the frequency distribution of the diameters of the spheres in the packing. Debbas and Rumpf (50) have suggested a method for the determination of the co-ordination number in a bed of spheres, by the analysis of thin sections of hardened packings of spheres.

3.5 Conclusion

The capillary phenomena of moisture in packed beds or porous media cannot be adequately described by the use of capillaric models. This is because the pore structure of a packed bed or of a porous medium differ widely from that of a bundle of capillary tubes. Network models might represent a packed bed or a porous body better than capillaric models. However, a considerable number of unknown parameters (e.g. number of tubes branching from a junction, tube diameters, tube orientations etc.) are required for the use of network models. This makes the usage of network models impractical even for the simplified case of random packing of equal size spheres.

Random or Monte Carlo methods which make use of a computer to model random packings have been developed in order to obtain better representations of the pore sizes in packed beds than those obtained by capillaric models.

The following conclusions can be drawn from studies of the packing densities measured by experiments and from computer calculations based on random models of equal size spheres.

(i) Both experimental and computer models based on sets of random points in space which were regarded to be the centres of spheres in a packing gave an approximate packing density of 0.64. The spheres in these models were usually tested to see that they did not over-lap the space occupied by neighbouring spheres.

(ii) Actual random packings of equal size spheres formed under the gravitational force can have packing densities in the range of 0.58 to 0.64 depending on the way the bed was formed and on its subsequent treatment.

A packing formed free of disturbances has been observed to have a packing density of 0.58 to 0.60. If a random packing is disturbed or vibrated, the packing density of the resulting bed has been found to lie in the range of 0.58 and 0.64. A random bed of equal size spheres of packing density 0.64 has been observed not to settle any further as a result of vibrations or disturbances applied to the bed. Thus the maximum packing density which can be experimentally achieved by a random packing of equal size spheres

has been found to be approximately 0. 64. However, it has been shown mathematically (161) that packing densities upto a maximum of 0. 7797 are theoretically possible.

The experimental maximum packing density is found to be approximately the same as that obtained for models developed to represent monatomic liquids (18, 74, 210).

(iii) It has to be expected that the structure of a random packing of hard spheres formed under gravity will be different from the structure of a mathematical array of non-overlapping spheres distributed randomly in a 3-D space. Calculations which make use of the pore size distributions obtained from such mathematical arrays to predict characteristics of phenomena in real packed beds are questionable. Further the models do not explain the behaviour of settling which can be observed in real packed beds.

(iv) The methods developed by Visscher et al. (240) and Tory et al. (237) provide a better description of packings than that provided by random arrays of spheres. However, these methods consume considerable amounts of computing resources and are complicated in analysis so that calculations beyond a few layers from the bottom of the packings become impractical.

An alternative approach is to combine the common features of the two basic types of computer methods. The next chapter deals with the development of such a model in order to predict the pore size distributions of random packings of equal size spheres.

CHAPTER 4

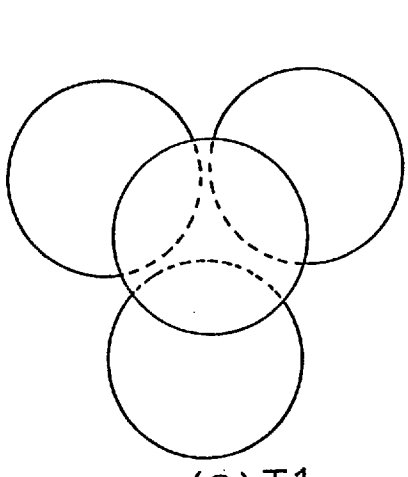
A model for the prediction of pore sizes in a random packing of equal size spheres.

4.1 Introduction

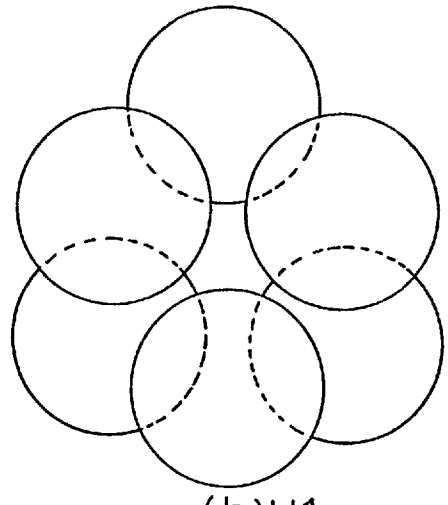
4.1.1 Description of the model

When a collection of spheres is allowed to fall into a container, in the absence of wind effects electrostatic effects or buoyancy effects, each ball falls under gravitational force till it hits the wall, the base or another sphere. If it hits the wall or the base of the container it might rest or roll along the surface till it meets the base or a side of the container or another sphere. In the presence of restitution, each sphere which hits a side of the container or the base or another sphere tends to rebounce. When a sphere is rebounced, it moves freely under gravity till it once again hits a side of the container, the base or another sphere.

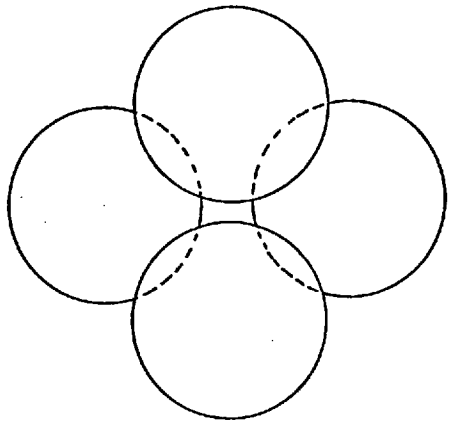
In the absence of restitution or spinning, a sphere which falls on another sphere will roll along the surface of the second sphere till it meets a third sphere. If the position is unstable, which is usually the case for two point contact equilibrium, it will roll along both these surfaces until another sphere is met. If the position is stable, it will rest giving a tetrahedral configuration of type T 1 (Fig. 4.1(a)). If not, it will loose contact with one of the spheres and roll along the other two. If the present position is stable it will rest giving a tetrahedral configuration T 1. Otherwise it will once again loose contact with one of the spheres and roll along the surface of the other two. The series of movements will be repeated until a stable position is reached. In certain cases a sphere can loose its contact with two of the supporting spheres and then can roll along the surface of the remaining sphere. A sphere at an unstable position of resting on three other spheres even can loose all its contacts with the three supporting spheres and make a fresh start towards a stable configuration.



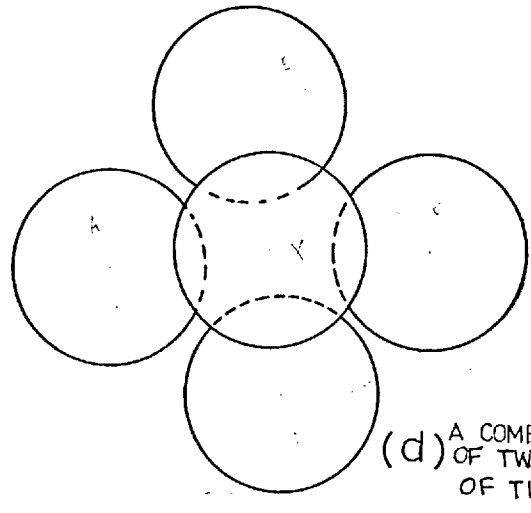
(a) T1



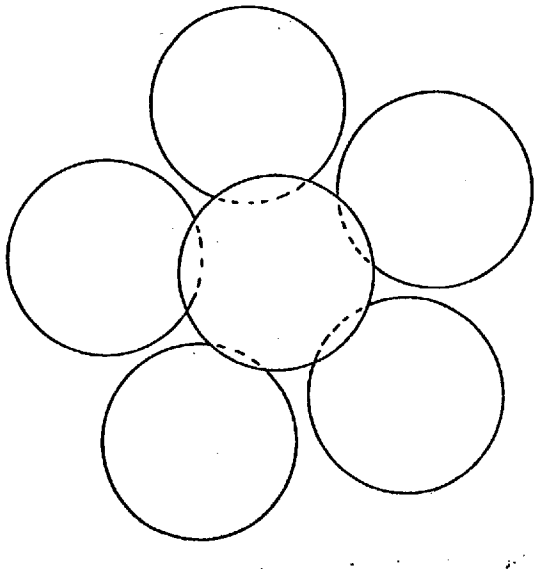
(b) U1



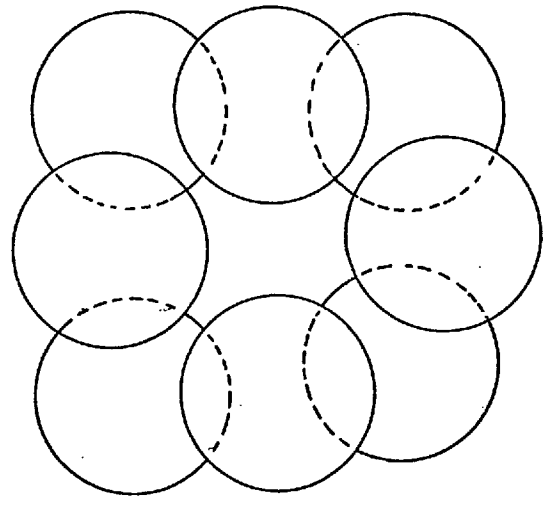
(c) T2



(d) A COMBINATION OF TWO UNITS OF T1



(e) T1 AND T2 COMBINATIONS.



(f) U3

FIGURE 4.1
Some possible arrangements of spheres in a packing.

However, it should be noted that finally each sphere will rest on at least three other spheres for a stable packing. The degree to which a tetrahedral unit is stable is partly determined by the coefficient of friction between the surfaces of the two spheres. Therefore the packing can be considered to consist of a large number of tetrahedra of type T 1 and of separating spaces in-between these tetrahedra. This arrangement can be regarded to be similar to the arrangement of tetrahedral cells and rhombohedral cells in a hexagonal packing. The geometry and the position of each tetrahedral unit T 1 determines the stability of its configuration. Fig. 4. 1 gives diagrams of a tetrahedral unit T 1 and of a separating space U 1 (see Fig.4.1(b)) that can exist between tetrahedra T 1 in a packing.

Addition of further spheres on top of a set of stable spheres in a packing, increases the load on each sphere in the lower layers of the packing, and occasionally some spheres are liable to get dislocated from their previously stable configuration and move on to a neighbouring U 1 unit. This gives rise to another subunit similar to U 2 shown in fig. 4.4. This subunit will be surrounded by high density tetrahedral units and hence can significantly restrict its further movement. A sphere which undergoes a similar dislocation can therefore be considered to reach a more sta ble position in U 2 than in the previous T 1 position. However, further dislocations of U 2 are possible and will be assumed to be of insignificant nature. Hence a random packed bed formed under gravity can be assumed to consist of three main subunits T 1, U 1 and U 2. A few of other types of subunits can be formed as a result of dislocated U 2, but can be regarded to be insignificant. The subunits T 1, U 1 and U 2 can be assumed to form randomly in a random packing of spheres.

4. 1. 2 Other considerations

If a model for the prediction of pore sizes in a random packing is required in order to explain rise and drain curves in packed beds, a study of pore sizes in the regions where there is an appreciable variation of moisture content with height is required. This usually appears to occur at heights more than a few layers above the free surface and hence far away from the base of the packing. Hence, the following analysis will be concerned only on the pore size distributions of a random packing of spheres in regions far away from the bottom of the bed. The wall effects of the container too will be neglected in the following analysis.

An equilibrium analysis of the spheres in a packing will be given in the next Section. A computer model for analysis of the probability distribution of pore space properties of an ensemble and hence evaluation of the representative void space properties of a randomly packed bed of equal spheres is given in Section 4. 9.

4. 2 An Equilibrium analysis of a packed bed.

4. 2. 1 Forces on a particle and the internal forces in a bed.

Consider a single particle (j) in a packed bed. Let the forces acting on it be $\underset{\sim}{F}_{ij}$ which make angles $\underset{\sim}{\Theta}_{ij}$ and $\underset{\sim}{\alpha}_{ij}$ to the horizontal from a horizontal datum and to the vertical respectively (Fig. 4. 2). The forces F_{ij} are transmitted to the particle by its neighbouring particles (i) which make contact with the particle (j).

For equilibrium of each particle, the resolved components of the forces in three perpendicular directions should be zero.

Hence
$$\sum_{\text{all j}} F_{ij} \cdot \text{Cos}\ \alpha_{ij} = 0 \quad \ldots\ldots\ldots\ldots\ldots\ldots \quad (4.1)$$

$$\sum_{\text{all j}} F_{ij} \cdot \text{Sin}\ \alpha_{ij} \cdot \text{Cos}\,\Theta_{ij} = 0 \quad \ldots\ldots\ldots\ldots\ldots\ldots \quad (4.2)$$

and
$$\sum_{\text{all j}} F_{ij} \cdot \text{Sin}\ \alpha_{ij} \cdot \text{Sin}\,\Theta_{ij} = 0 \quad \ldots\ldots\ldots\ldots\ldots\ldots \quad (4.3)$$

Hence the equilibrium condition of the complete packing can be expressed as:

$$\sum_{\text{all i}} \sum_{\text{all j}} F_{ij} \cdot \text{Cos}\ \alpha_{ij} = 0 \quad \ldots\ldots\ldots\ldots\ldots\ldots \quad (4.4)$$

$$\sum_{\text{all i}} \sum_{\text{all j}} F_{ij} \cdot \text{Sin}\ \alpha_{ij} \cdot \text{Cos}\,\Theta_{ij} = 0 \quad \ldots\ldots\ldots\ldots\ldots\ldots \quad (4.5)$$

and
$$\sum_{\text{all i}} \sum_{\text{all j}} F_{ij} \cdot \text{Sin}\ \alpha_{ij} \cdot \text{Sin}\,\Theta_{ij} = 0 \quad \ldots\ldots\ldots\ldots\ldots\ldots \quad (4.6)$$

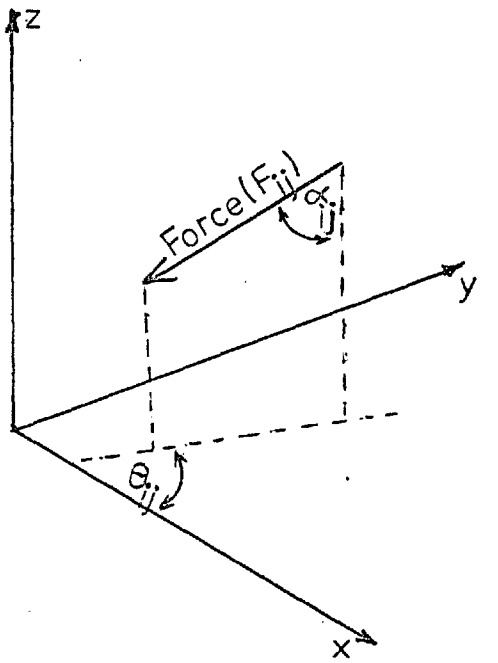


FIGURE 4.2

Force diagram at a point of contact.

A necessary condition for a packing to be stable is that each particle should at least bridge on three other particles, except for those in the bottom layer or in the wall layer.

However, conditions given by equations (4. 1) to (4. 3) together with the above condition are not sufficient for a sphere (i) to be stable in a given packing. An additional and an important criterion for equilibrium is that the reactions imposed by the sphere (i) on each neighbouring sphere (j) should not exceed the maximum force (say $F_{ji_{max}}$) which the sphere (j) could withstand in the direction ij. This condition can be expressed mathematically as:

$$F_{ij} \leqslant F_{ji_{max}} \quad \ldots\ldots\ldots\ldots\ldots\ldots\ldots\ldots \quad (4.7)$$

The importance of the inequality (4. 7) on the stability of a tetrahedral unit will be discussed in more detail in the next section.

4. 2. 2 Evaluation of the probability factor for stability of a tetrahedral unit in a sphere packing.

Consider the tetrahedral unit of type T 1 (fig. 4. 3) composed of spheres A, B, C and D with the sphere D bridging on the three spheres A, B and C. Let F_D be the force experienced by D due to the neighbouring spheres other than the spheres A, B and C. Let α be the inclination of this force to the perpendicular drawn to the plane joining the centres of A, B and C and let Θ be the angle the projection of this force makes on the plane joining the centres of A, B and C with a chosen datum on this plane.

Let the reaction between the sphere D and any of the spheres A, B or C (say k) be denoted by F_k. The reaction F_k will be a function of F_D, Θ, α, the geometry of the tetrahedral unit (denote by a factor Γ), and on the coefficients of friction $\underset{\sim}{\mu}$ between the sphere D and the other three spheres.

Therefore F_k can be expressed as:

$$F_k = f_k(F_D, \Theta, \alpha, \Gamma, \underset{\sim}{\mu}) \quad \ldots\ldots\ldots\ldots\ldots\ldots\ldots \quad (4.8)$$

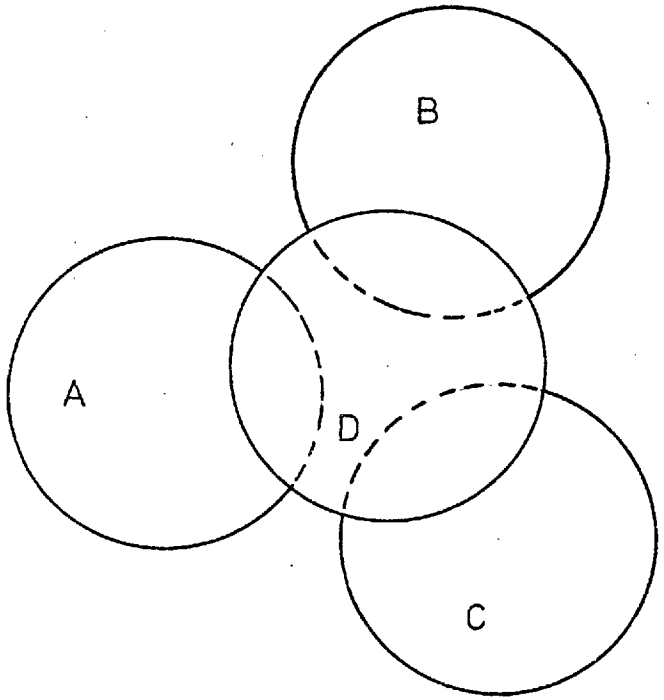


FIGURE 4.3

Plan of a tetrahedral unit T 1.
(sphere D resting on spheres A, B and C)

Now, let us increase F_D till k dislocates, where k is now chosen to be the sphere out of A, B and C, which is liable to undergo a dislocation first. Let the values of F_D and F_k when dislocation just occurs be denoted by F* and F_k^* respectively.

Then,

$$F_k^* = f_k\,(F^*,\ \Theta,\ \alpha,\ \Gamma,\ \underset{\sim}{\mu}) \qquad \ldots\ldots\ldots\ldots\ldots\ldots \quad (4.9)$$

From equation (4.9), it can be seen that for a given value of $F_k = F_k^*$ a set of values for F* can be obtained by varying the values of Θ and α. Several values of F* are possible to dislocate a tetrahedral unit U 1 depending on the values of Θ and α. Each value of F* in the above set also depends on the geometry of the tetrahedral unit. Therefore the values of F* which would dislocate tetrahedra T 1 chosen randomly from a packing can be assumed to be expressed by a distribution function f (F*). The function f(F*) can therefore be considered to represent the number of tetrahedra chosen randomly from a packing, which would be just dislocated by transmission of a load of F* on the sphere D by the neighbouring spheres other than A, B and C. A lower limit (F^*_{min}) and an upper limit (F^*_{max}) of F* can be expected. f can be expressed as:

$$f = f(F^*) \qquad \ldots\ldots\ldots\ldots\ldots\ldots\ldots\ldots\ldots\ldots \quad (4.10)$$

For a given value of F*, the fraction ζ of tetrahedral subunits T 1 which would be stable out of a random set of tetrahedral subunits chosen from a packing can be expressed as:

$$\zeta = \left[\int_0^{F^*} f(F^*)dF^*\right] \Big/ \left[\int_0^{F^*_{max}} f(F^*)dF^*\right] \qquad \ldots\ldots\ldots \quad (4.11)$$

Or

$$\zeta = \left[\int_{F^*_{min}}^{F^*} f(F^*)\,dF^*\right] \Big/ \left[\int_{F^*_{min}}^{F^*_{max}} f(F^*)\,dF^*\right] \qquad \ldots \quad (4.12)$$

ζ is a function of F* and f. Both F* and f are functions of the coefficients of friction ($\underset{\sim}{\mu}$) between the surfaces of spheres. For a packing consisting of approximately smooth particles, $\underset{\sim}{\mu}$ can be considered to be negligible. Therefore, for a packing of smooth particles, ζ can be regarded to be independent of the friction between the surfaces of the particles.

4.3 Model Structure of the Packing

A packing can be considered to be completely consolidated, if its void fraction cannot be diminished by any further disturbances applied to the packing. A packing formed by allowing a collection of spheres to fall under gravity cannot be regarded as completely consolidated. Therefore, each sphere in such a packing can be displaced even slightly, when a load is applied on the packing. However, when the spheres in a packing have undergone changes in position by application of a load on the packing, each sphere in the packing finally reaches an equilibrium position once again.

A sphere in a packing which makes contact with another sphere in the same packing can be said to be

(a) Resting on the second sphere, if the first sphere dislocates from its present position in the packing when the second sphere is removed from the packing without interfering the rest of the packing.

(b) Supporting the second sphere, if the second sphere dislocates from its present position in the packing when the first sphere is removed from the packing without interfering the rest of the packing.

Each sphere in a packing can be supported by three or more other spheres in the packing. A sphere resting on three other spheres forms a statically determinate structure. Therefore a given sphere resting on three other spheres in a packing can settle to a stable configuration without a real necessity of an additional supporting sphere. Therefore, the possibility that each sphere in a packing resting on more than three other spheres in the same packing can be regarded to be negligible. The tetrahedral unit T 1 can therefore be regarded as the primary equilibrium determining structure of the packing. Further, it is clear that occurence of two adjacent tetrahedral units T 1 can not be common in a random packing.

The possible configurations of sphere combinations in a packing are many and some of them are shown in fig 4. 1. Many of the configurations can be regarded as combinationsof simpler configurations as shown in the figure.

In figure 4. 1, U 1 is a rhombohedral unit similar to the space that exist between tetrahedral units in a hexagonal packing.

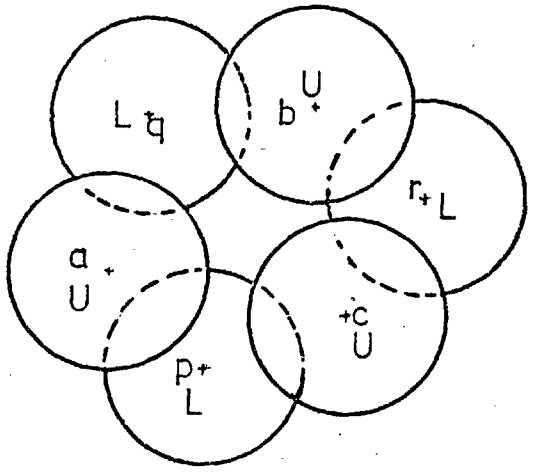
A random loose packing can thus be assumed to consist of discrete equilibrium determining tetrahedral units T 1 and spaces in-between these tetrahedral units. The spaces in-between neighbouring tetrahedral units can be of the form U 1 (Fig.4.4) or even larger units. However, large spaces can easily be occupied by incoming spheres during the formation of the packing. Therefore, it can be assumed that the possibility of the existence of large spaces to be remote. A similar assumption has been made by Tory et al. (237) in his computer calculations of simulation of random packings of equal spheres.

Therefore, the packing can be assumed to be primarily made up of tetrahedral units T 1 and rhombohedral units U 1. However, the disturbances while and after the formation of the packing, or the external loads applied on the packing might dislocate some of the spheres from tetrahedral unit configuration. This could make the dislocated spheres to move into the neighbouring rhombohedral spaces, thus giving a configuration of the type U 2 shown in Figure 4. 4. (b) (see Section 4. 1. 1).

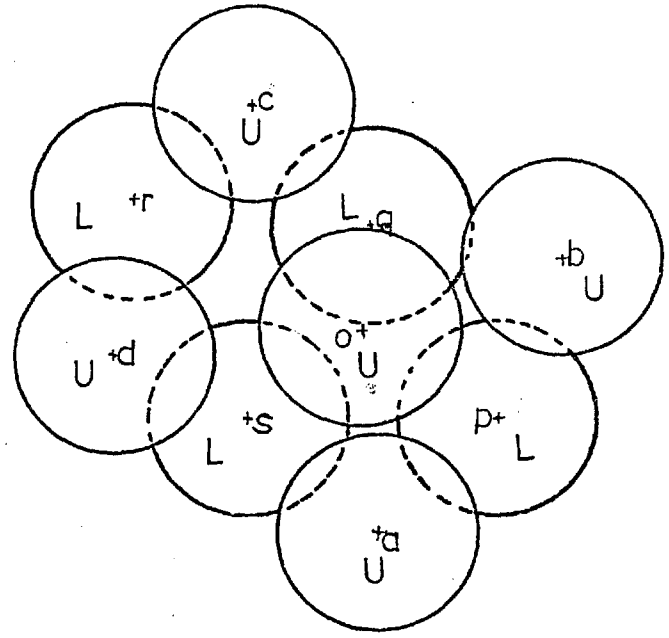
4.4 Relative frequencies of occurence of the canonical units.

A randomly formed packed bed under unidirectional gravitational force can be assumed to consist mainly of tetrahedra of type T 1 and units U 1 and U 2. A few details of units U 1 and U 2 are given below.

Unit U 1: The polyhedron formed by joining the centres of spheres in a unit U 1 has 8 outside faces with 6 distinct contact edges (a contact edge is defined as an edge of a polyhedron, of length equal to the diameter of a sphere in the packing). All these six contact edges are common to the adjacent tetrahedra of type T 1.



(a) Subunit U1



(b) Subunit U2

FIGURE 4.4
Subunits U1 and U2.
(U — spheres in upper layer)
(L — spheres in lower layer)

Unit U 2: The polyhedron formed by joining the centres of spheres in a unit U 2 has 14 outside faces with 11 contact edges. The contact edges are common to the adjacent tetrahedra of type T 1. Altogether there are 21 edges per unit of U 2. Apart from the 11 contact edges, 5 of the remaining 10 edges can become contact edges. If p is defined as the probability of two spheres out of the spheres separated by the above 5 edges making a contact, then the probability that the above five edges becoming a contact edge is 5p and for becoming non contact edges is 5(1-p). Therefore, as an average 11 + 5p contact edges and 10 - 5p non contact edges can be expected in a unit U 2. If equal probability is assumed for making a contact and a non contact, then p = 0. 5 and hence an average of 13. 5 contact edges and 7. 5 non contact edges can be expected in a unit U 2.

Let y units of U 1 and ν units of U 2 exist in a packing. The outside faces of these are usually common with the faces of tetrahedra T 1. Therefore, average No. of tetrahedra T 1 associated with U 1 = 8y/4 = 2y. Average No. of tetrahedra T 1 associated with U 2 = $14\nu/4 = 3.5\nu$.

$\therefore$ Total no. of tetrahedra of type T 1 = $(2y + 3.5\nu)$.

Let x denote the fraction of tetrahedra T 1 dislocated to the neighbouring rhombohedra U 1 to yield ν units of U 2.

Hence, the total no. of dislocations of T 1 undergone while and after the formation of the packing can be expressed as $\frac{x_o(2y + 3.5\nu)}{(1-x)}$

But the total number of dislocations is equal to the total number of U 2 units formed.

Therefore,

$$\nu = \frac{x}{(1-x)} \cdot (2y + 3.5\nu) \quad \ldots\ldots\ldots\ldots\ldots\ldots \quad (4.13)$$

hence,

$$\frac{y}{\nu} = \frac{2 - 9x}{4x} \quad \ldots\ldots\ldots\ldots\ldots\ldots \quad (4.14)$$

Using equation (4. 14), the ratio between the number of tetrahedra T 1, rhombohedra U 1 and units U 2 can be evaluated as $4(1 - x) : (2 - 9x) : 4x$.

In order to make computations easier, each unit of U 2 can be subdivided into smaller units. It can be easily seen that units U 2 can be subdivided into simpler units of U 1, T 1 and T 2. Each unit U 2 can be subdivided into a single unit of U 1, a single unit of T 1 and two units of T 2 (see Fig. 4. 1(c)).

i.e., $U2 = U1 + T1 + 2T2$ ..... (4. 15)

The overall bed can be subdivided into y units of U 1, ν of U 2 and $2y + 3.5\nu$ units of T 1.

Hence, we can write

$$\text{Bed} = y\,U1 + \nu\,U2 + (2y + 3.5\nu)\,T1 \quad \text{..... (4. 16)}$$

$$= y\,U1 + \nu\,(U1 + T1 + 2T2) + (2y + 3.5\nu)\,T1 \quad \text{..(4. 17)}$$

$$= (2y + 4.5\nu)\,T1 + (y + \nu)\,U1 + 2\nu\,T2 \quad \text{..... (4. 18)}$$

Using equations (4. 14) and (4. 18) the ratio of the number of units T 1, U 1 and T 2 that exist in the bed can be expressed as $4 : 2 - 5x : 8x$.

4. 5 The fraction of contact edges in the base triangle of a unit T 1.

If a sphere D rests on the three spheres A, B and C, then the lines joining the centres of A, B and C can be defined as the sides of the base triangle of the tetrahedral unit formed by the spheres A, B, C and D.

Triangles abc and pqr of unit U 1 (see fig. 4. 4. (a)) and triangles (oad, obc, prs, prq) or (oab, ocd, pqs and rqs) of unit U 2 (see fig. 4. 4(b)) can become base triangles of tetrahedra T 1 in a packing. In a unit U 2, the spheres of which the centres are o, a, b, c and d can be positioned so that the spheres touch each other. Let p be the probability of two of the above spheres

making a contact. Then, p is also the probability of the edges bc, oa, ob, oc and od becoming contact edges. Therefore, an average value of 5p contact edges which belong to base triangles of tetrahedra T 1 can be expected to be present in a unit U 2.

The following table gives the expected average of the number of contact edges and non-contact edges in units U 1 and U 2 which can constitute bases of tetrahedra T 1.

Table 4-1

	TYPE	
	U 1	U 2
Contact edges	0	5p
Non-Contact edges	6	11 - 5p
Total	6	11

Since the ratio between the number of U 1 units and U 2 units is $y : \nu$, the ratio of the number of contact edges to the number of non contact edges in base triangles of tetrahedra T 1 can be evaluated to be $5p\nu / (6y + (11 - 5p)\nu)$.

If the probability of the spheres o, a, b, c, and d (Fig. 4.4(b)) making a contact is assumed to be the same as their probability of not making a contact, p can be assumed to be 0.5. Therefore the ratio of the number of contact edges to the number of non contact edges in base triangles of tetrahedra of type T 1 in a packing can be simplified to the form $2.5/(6y/\nu + 8.5)$.

But $$y/\nu = (2 - 9x)/4x \quad \ldots\ldots\ldots\ldots\ldots\ldots \quad (4.19)$$

$$\therefore \quad \frac{\text{No. of Contact edges}}{\text{No. of Non Contact edges}} = 5x/(6 - 10x) \quad \ldots\ldots\ldots\ldots \quad (4.20)$$

hence, $$\frac{\text{No. of Contact edges}}{\text{Total No. of sides}} = 5x/(6 - 5x) \quad \ldots\ldots\ldots\ldots \quad (4.21)$$

Equations (4.20) and (4.21) are derived for the base triangles of tetrahedra T 1.

Hence, if the fraction (x) of dislocated tetrahedra of type T 1 is known, the number of contact edges as a fraction of the total number of sides of the base triangles of tetrahedra T 1 in a packing can be determined.

4. 6 Number of stable tetrahedra as a fraction of the total geometrically consistent tetrahedra that can be formed of a given configuration T 1.

4. 6. 1 Equilibrium considerations.

Let us consider a tetrahedral unit T 1 in which a sphere D rests on three other spheres A, B and C. Let F_A, F_B and F_C be the reactions between the sphere D and the spheres A, B and C respectively. Let each of these forces has angular co-ordinates (Θ_A, α_A), (Θ_B, α_B) and (Θ_C, α_C) respectively, where Θ is the angle which a given force makes with the perpendicular to the plane joining the centres of spheres A, B and C and α is the angle which the projection of the force on the plane joining the centres of A, B and C makes with a datum on that plane.

Let F_D be the total force exerted on D by all the other spheres which are in contact with D, other than the spheres A, B and C.

Let the angular co-ordinates of F_D be (Θ_D, α_D).

Equations (4. 1), (4. 2) and (4. 3) can be applied to the above force system as:

$$F_A \cos\Theta_A + F_B \cos\Theta_B + F_C \cos\Theta_C = F_D \cos\Theta_D \quad \ldots\ldots\ldots \quad (4.22)$$

$$F_A \sin\Theta_A \cos\alpha_A + F_B \sin\Theta_B \cos\alpha_B + F_C \sin\Theta_C \cos\alpha_C = F_D \sin\Theta_D \cos\alpha_D \quad \ldots\ldots\ldots\ldots \quad (4.23)$$

and

$$F_A \sin\Theta_A \sin\alpha_A + F_B \sin\Theta_B \sin\alpha_B + F_C \sin\Theta_C \sin\alpha_C = F_D \sin\Theta_D \sin\alpha_D \quad \ldots\ldots\ldots\ldots \quad (4.24)$$

Expressing these equations in Matrix form:

$$\begin{bmatrix} \mathrm{Cos}\Theta_A & \mathrm{Cos}\Theta_B & \mathrm{Cos}\Theta_C \\ \mathrm{Sin}\Theta_A\mathrm{Cos}\,\alpha_A & \mathrm{Sin}\Theta_B\mathrm{Cos}\,\alpha_B & \mathrm{Sin}\Theta_C\mathrm{Cos}\,\alpha_C \\ \mathrm{Sin}\Theta_A\mathrm{Sin}\,\alpha_A & \mathrm{Sin}\Theta_B\mathrm{Sin}\,\alpha_B & \mathrm{Sin}\Theta_C\mathrm{Sin}\,\alpha_C \end{bmatrix} \begin{bmatrix} F_A \\ F_B \\ F_C \end{bmatrix} = F_D \begin{bmatrix} \mathrm{Cos}\Theta_D \\ \mathrm{Sin}\Theta_D\mathrm{Cos}\,\alpha_D \\ \mathrm{Sin}\Theta_D\mathrm{Sin}\,\alpha_D \end{bmatrix} \quad \ldots\ldots\ldots\ldots\ldots \quad (4.25)$$

or $\underset{\sim}{M} \cdot \underset{\sim}{F} = F_D \cdot \underset{\sim}{u}$ ..... (4.26)

Where $\underset{\sim}{M} = \begin{bmatrix} \mathrm{Cos}\Theta_A & \mathrm{Cos}\Theta_B & \mathrm{Cos}\Theta_C \\ \mathrm{Sin}\Theta_A\mathrm{Cos}\,\alpha_A & \mathrm{Sin}\Theta_B\mathrm{Cos}\,\alpha_B & \mathrm{Sin}\Theta_C\mathrm{Cos}\,\alpha_C \\ \mathrm{Sin}\Theta_A\mathrm{Sin}\,\alpha_A & \mathrm{Sin}\Theta_B\mathrm{Sin}\,\alpha_B & \mathrm{Sin}\Theta\,\mathrm{Sin}\,\alpha_C \end{bmatrix}$ ... (4.27)

$$\underset{\sim}{F} = \begin{bmatrix} F_A \\ F_B \\ F_C \end{bmatrix} \quad \ldots\ldots\ldots\ldots\ldots\ldots\ldots\ldots \quad (4.28)$$

and

$$\underset{\sim}{u} = \begin{bmatrix} \mathrm{Cos}\Theta_D \\ \mathrm{Sin}\Theta_D\mathrm{Cos}\,\alpha_D \\ \mathrm{Sin}\Theta_D\mathrm{Sin}\,\alpha_D \end{bmatrix} \quad \ldots\ldots\ldots\ldots\ldots\ldots \quad (4.29)$$

If the matrices $\underset{\sim}{M}$ and $\underset{\sim}{u}$ are known, $\underset{\sim}{F}$ can be evaluated as a function of F_D. $\underset{\sim}{M}$ is known for a tetrahedral unit of a given configuration. F_D can assume any value between the limits F_{min} and F^*_{max} (see Section 4.2.2).

If any of the forces F_A, F_B or F_C exceeds the respective critical reactions F^*_A, F^*_B or F^*_C, then the tetrahedron can be assumed to dislocate.

Let $f = f(F^*)$ be the frequency distribution of the critical reactions F^* of the particles of the bed. By denoting the critical force F^* as a fraction of the maximum of the critical forces, the frequency distribution f can be expressed as: $f = f(\eta)$ ..... (4.30)

where $\eta = F^*/F^*_{max}$ ..... (4.31)

Equation (4.26) can therefore be modified as:

$$\underset{\sim}{M}\ \underset{\sim}{F'} = F'_D\ \underset{\sim}{u} \quad \ldots\ldots\ldots\ldots\ldots\ldots\ldots\ldots\ldots\ldots \quad (4.32)$$

Where

$$\underset{\sim}{F'} = \begin{bmatrix} F_{A/F^*_{max}} \\ F_{B/F^*_{max}} \\ F_{C/F^*_{max}} \end{bmatrix} \quad \ldots\ldots\ldots\ldots\ldots\ldots\ldots\ldots\ldots\ldots \quad (4.33)$$

i.e., $$\underset{\sim}{F'} = \begin{bmatrix} \eta_A \\ \eta_B \\ \eta_C \end{bmatrix} \quad \ldots\ldots\ldots\ldots\ldots\ldots\ldots\ldots\ldots\ldots \quad (4.34)$$

and $$F'_D = F_{D/F^*_{max}} = \eta_D \quad \ldots\ldots\ldots\ldots\ldots\ldots \quad (4.35)$$

η_D can assume values between $F_{min/F^*_{max}}$ and unity. Any of η_A, η_B, or η_D can not exceed η^*_A, η^*_B and η^*_C respectively.

4.6.2 Stability of a sphere resting on another sphere in a given tetrahedral unit T 1 of a packing and the probability of its occurence.

Consider a tetrahedral unit T 1 in which a sphere D rests on three other spheres A, B and C in a packing. Let F_D be the load transmitted to the sphere D by all the spheres which are in contact with the sphere D other than by A, B and C.

Equation (4.32) can be applied to the force system acting on sphere D in order to obtain the reaction between the spheres A and D in dimensionless form η_A ($= F_A/F^*_{max}$). η_A is a function of η_D which can vary from a minimum value of η_{min} (ie. F_{min}/F^*_{max}; see Section 4.2.2 and Section 4.6.1) to a maximum value of unity. If it assumed that η_D can have values between zero and 1.0, independent of the configuration of the tetrahedral unit T 1, then

it can be shown (using equation 4.32) that η_A can lie between a minimum value ($\eta_{Amin} = 0$) and a maximum value (say η_{Amax}). η_{Amax} is the value of η_A when $\eta_D = 1.0$. In these calculations η_{Amax} can exceed 1.0 which is contradictory to the definition of η. Stability analysis of such cases will be dealt separately in the following.

Case 1. $\eta_{Amax} \leq 1.0$

Let $\zeta'(\eta_A)$ be the probability of a sphere A in a packing remaining stable under the influence of a dimensionless force η_A exerted by the spheres in the packing other than by those on which the sphere A is resting. Then equation (4.12) can be applied as:

$$\zeta'(\eta_A) = \left\{ \int_{\eta_A}^{1.0} f(\eta)d\eta \right\} / \left\{ \int_{\eta^*_{min}}^{1.0} f(\eta)d\eta \right\} \quad \ldots\ldots (4.36)$$

Where $f(\eta)$ is the frequency distribution of the dimensionless critical reactions.

Equation (4.36) can be written in the form:

$$\zeta'(\eta_A) = \left\{ \int_{\eta_A}^{1.0} f(\eta)d\eta \right\} / \left\{ \int_{0}^{1.0} f(\eta)d\eta \right\} \quad \ldots\ldots (4.37)$$

If several ensembles of packings are considered, it can be assumed that several tetrahedra of a given configuration can exist in the ensembles. In such tetrahedra, spheres similar to the sphere D under consideration can be exerted by loads (dimensionless) η_D within the range zero to 1.0. If equal probability is assumed for the occurence of a value of η_D within the above range, then the probability $\zeta(\eta_{Amax})$ of existence of a combination of two spheres D and A in a tetrahedral unit of a given configuration can be expressed as:

$$\zeta(\eta_{Amax}) = \left\{ \int_{0}^{\eta_{Amax}} \zeta'(\eta)d\eta \right\} / \left\{ \int_{0}^{1.0} \zeta'(\eta)d\eta \right\} \quad \ldots\ldots (4.38)$$

Case 2. $\eta_{A\max} \geq 1.0$

In this case η_D cannot take values upto 1.0, because η_A becomes 1.0 at a value of η_D less than 1.0. The value of η_D at which η_A becomes 1.0 can be easily shown to be $1.0/\eta_{A\max}$.

Therefore, it can be seen that η_D can take values only between zero and $1.0/\eta_{A\max}$. Therefore the probability $\zeta(\eta_{A\max})$ can be expressed as:

$$\zeta(\eta_{A\max}) = 1.0/\eta_{A\max} \quad \ldots\ldots\ldots\ldots \quad (4.39)$$

or

$$\zeta(\eta_{A\max}) = \eta^{-1}_{A\max} \quad \ldots\ldots\ldots\ldots \quad (4.40)$$

4.7 The frequency distribution of the critical reactions and its properties.

A method is developed in this work, to evaluate the minimum dimensionless critical reaction in a packing and will be described below:

Consider a tetrahedral unit T 1 in which a sphere D rests on three other spheres A, B and C in a packing. Let the dimensionless reactions on the spheres A, B, C and D be denoted by the usual notation η_A, η_B, η_C and η_D respectively. Then for a given η_D, values of η_A, η_B and η_C can be calculated using equation (4.32). Suppose for $\eta_D = 1.0$, values of η_A, η_B and η_C are calculated for a large set of random tetrahedral units of type T 1, then a maximum (say η^{**}) of the values of η_A, η_B and η_C can be obtained. One thousand random tetrahedra were generated in a similar manner to that described in Section 4.9. For each tetrahedron equation (4.32) was solved using computer and the maximum value of the reactions i.e., η^{**} was evaluated to be 1.31. However, a dimensionless critical reaction can not exceed 1.0 by definition. Therefore, the value of η_D for which the particular reaction becomes unity is the maximum value of η_D that the particular tetrahedral unit would withstand. However, this value of η_D is the minimum dislocating value of η_D for the whole set of tetrahedra.

If the random tetrahedra generated in the computer is assumed to represent the tetrahedral units of type T 1 in a packing, the above value of η_D can be shown to be the minimum dimensionless critical reaction of the packing. The minimum critical reaction (say η^*_{min}) can easily be shown to be $1.0/\eta^{**}$.

$$\therefore \quad \eta^*_{min} = 1.0/\eta^{**} \qquad \ldots\ldots\ldots\ldots\ldots (4.41)$$

It is reasonable to assume that the number of cumulative dislocations is proportional to the force applied.

Therefore, we could write

$$\int_0^{\eta} f(\eta)d\eta \propto \eta \qquad \ldots\ldots\ldots\ldots\ldots (4.42)$$

or $$f(\eta) = K \qquad \ldots\ldots\ldots\ldots\ldots (4.43)$$

where K is a constant.

The type of the distribution is shown in fig (4. 5).

For this distribution

$$\left.\begin{aligned} \zeta'(\eta_A) &= (1 - \eta_A)/(1 - \eta^*_{min}) \\ &\qquad \text{if } 1 \geqslant \eta_A \geqslant \eta^*_{min} \\ \text{and } \zeta'(\eta_A) &= 1.0, \text{ if } \eta_A < \eta^*_{min} \end{aligned}\right\} \ldots\ldots\ldots (4.44)$$

and

$$\left.\begin{aligned} \zeta(\eta_A) = \frac{\left[\int_{\eta^*_{min}}^{\eta_A} (1.0 - \eta)d\eta + \int_0^{\eta^*_{min}} (1 - \eta^*_{min})d\eta\right]}{\left[\int_{\eta^*_{min}}^{1.0} (1 - \eta)d\eta + \int_0^{\eta^*_{min}} (1 - \eta^*_{min})d\eta\right]} \\ \text{if} \quad 1 \geqslant \eta_A \geqslant \eta^*_{min} \\ \text{and } \zeta(\eta_A) = 1.0 \text{ if} \quad \eta_A < \eta^*_{min} \end{aligned}\right\} (4.45)$$

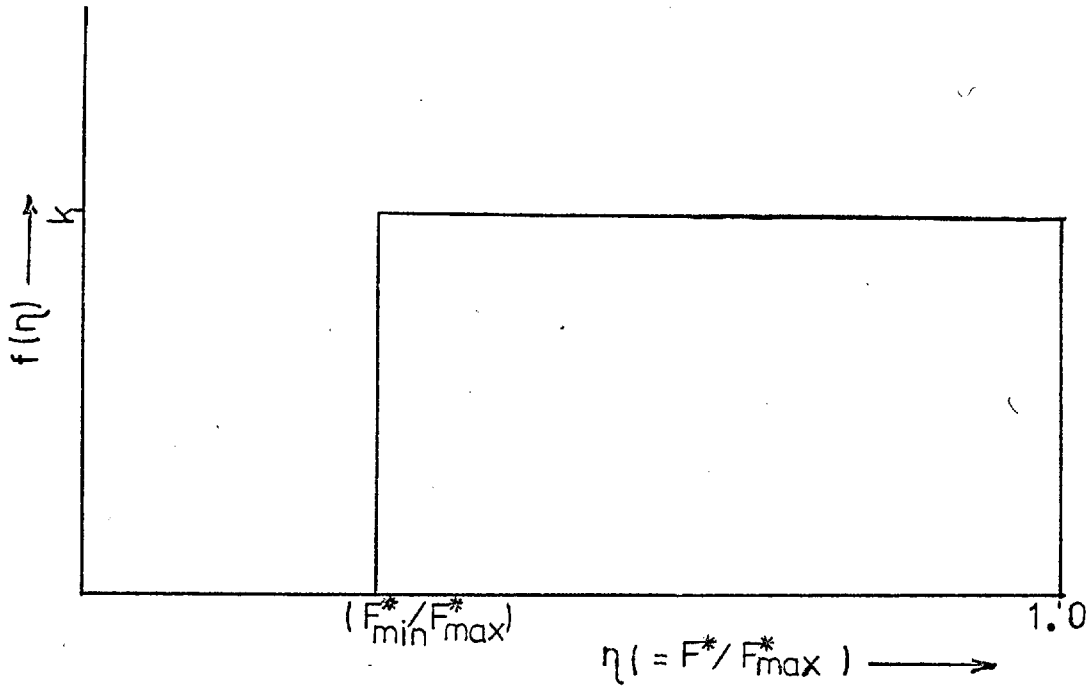


FIGURE 4.5

Rectangular distribution of critical reactions (dimensionless).

4.8 Probability of formation of stable tetrahedra of a given configuration T 1.

This is evaluated in a subroutine of the main computer program which will be described in Section (4.9). The subprogram was called, for each tetrahedron of a set of random tetrahedra of type T 1 generated in the main program. The subprogram generates 1000 sets of random values of (Θ_D, a_D). Assuming $\eta_D = 1.0$ and with the use of equation (4.32), η_A, η_B and η_C were evaluated for each set. For a single set (i), the largest of the three η_A, η_B and η_C is evaluated. Let this be $\eta_{i\,max}$. Now two cases arise in the evaluation of the probability value.

Case 1. $\eta_{i\,max} \leqslant 1.0$

In this case the probability (ζ'') that all the three supporting spheres A, B and C are stable simultaneously is given by

$$\zeta_i'' = \zeta(\eta_A) \times \zeta(\eta_B) \times \zeta(\eta_C) \quad \ldots\ldots \quad (4.46)$$

$$\zeta_i'' = \prod_{j=A,B,C} \{\zeta(\eta_j)\} \quad \ldots\ldots\ldots\ldots\ldots\ldots \quad (4.47)$$

Case 2. $\eta_{i\,max} > 1.0$

In this case η_D can not vary upto 1.0. Instead it can have a value only upto $1.0/\eta_{i\,max}$. When η_D assumes a value of $1.0/\eta_{i\,max}$, the corresponding dimensionless reactions on spheres A, B and C can be shown to be $\eta_A/\eta_{i\,max}$, $\eta_B/\eta_{i\,max}$ and $\eta_C/\eta_{i\,max}$ where η_A, η_B and η_C are the dimensionless reactions on spheres A, B and C respectively as calculated from equation (4.32) corresponding to a value of η_D equal to unity.

Hence, the probability could be expressed as:

$$\zeta_i'' = \frac{1.0}{\eta_{i\,max}} \zeta\left[\eta_A/\eta_{i\,max}\right] \times \zeta\left[\eta_B/\eta_{i\,max}\right] \times \zeta\left[\eta_C/\eta_{i\,max}\right] \quad \ldots\ldots\ldots\ldots\ldots\ldots \quad (4.48)$$

In both the above cases if a set of n values of (Θ_D, α_D) are considered, tetrahedron of a given configuration T 1 becoming stable can be given by

$$\zeta'' = \left\{ \sum_{i=1}^{n} \zeta_i'' \right\} / n \qquad \ldots\ldots\ldots\ldots\ldots \quad (4.49)$$

4.9 Generation of a computer model for a packed bed

Stage 1 Tetrahedral Unit T 1

The computer program started by assuming a value for x (eq., 4.21). The number of contact edges as a fraction of the total number of sides in the bases of the tetrahedra of type T 1 was then evaluated with the use of equation (4.21). The total number (N) of contact edges in 1000 bases was evaluated.

A pseudo-random number generator produced (3000 - N) random numbers between 0.0 and 1.0. These random numbers were converted into random edge lengths, by taking the lower limit of the edge length as the sphere diameter and the upper limit as twice the sphere diameter. However, it was observed that the program could be made more efficient (8) without affecting the results appreciably by taking the upper limit of the edge length as $\sqrt{3}$ times the diameter. This particular edge length can be regarded as corresponding to the extreme case shown in fig. 4.6. Therefore, 3000 edge lengths were produced between the diameter and 1.74 (a convenient value $> \sqrt{3}$) times the diameter by taking the above (3000 - N) random edge lengths and N contact edges to form 1000 base triangles of 1000 tetrahedra.

Three edge lengths at a time were chosen at random from the collection of 3000 edge lengths and used to construct the base of a tetrahedron T 1. The probability factor for stability of the tetrahedron was evaluated as described in Section (4.8). The properties of the tetrahedron T 1, e.g., face radii, tetrahedron insphere radii etc. were evaluated using the corresponding probability factor for each property.

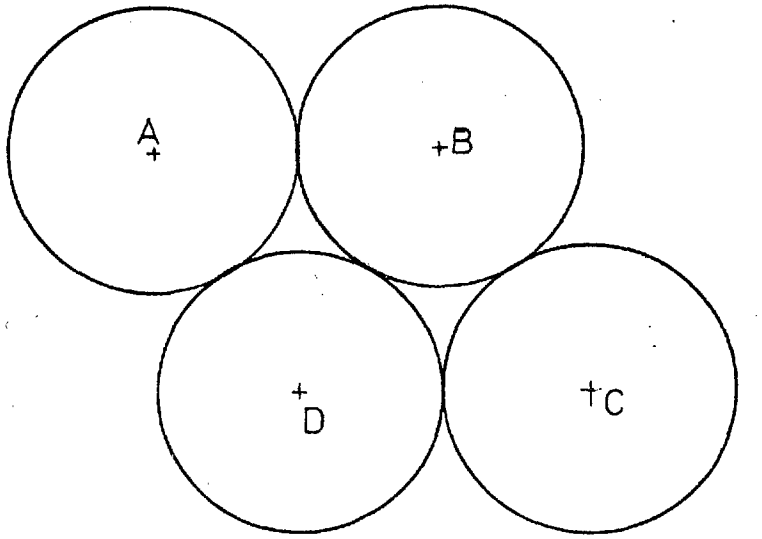


FIGURE 4.6

An extreme case of a tetrahedral subunit.
(AC = $\sqrt{3}$ × sphere diameter.)

The properties of approximately 1000 tetrahedra were evaluated in this way as were the distributions of the properties of the tetrahedra.

Stage 2. Rhombohedral Unit U 1.

In a random packing subunitsof type U 1 can be assumed to form randomly. A set of random edge lengths were generated as described in the previous section, and in each case three edge lengths were taken to form the base abc (fig. 4. 7) of a unit U 1. Then three spheres were placed randomly each touching two different pairs of spheres A, B and C in each case. This was done by generating randomly the angle formed between the plane obtained by joining the centre of the resting sphere (say d) and the centres of the supporting spheres (a and c), and the plane joining the centres of the spheres of the base abc. The upper limit of this angle was taken as π radians and the lower limit as the angle formed when the resting sphere touched all the three base spheres. The technique of random angle generation was similar to the technique employed for the random edge length generation between two limits, described in stage 1. In this process, if any two spheres are overlapped so they did not satisfy the separation restrictions, that particular unit was eliminated and the next unit was taken. Otherwise the pore space was divided into four tetrahedral units (not T 1) e.g., abcd, afbd, bced, and edfb and the pore space properties of each tetrahedral unit evaluated. In this way the distributions of the pore space properties for a random collection of U 1 units are obtained.

The probability of the formation of each unit was determined from the probability of the occurence of the six lengths ab, bc, ca, ed, df and fe. This was deduced from the edge length frequency distribution of the bases of the tetrahedra T 1 presented in stage 1.

Stage 3. Tetrahedral Unit T 2.

In a manner similar to that already described,the tetrahedral unit T 2 can be assumed to have been formed randomly. Two thousand random edge lengths are generated and two of these at a time are chosen to construct a

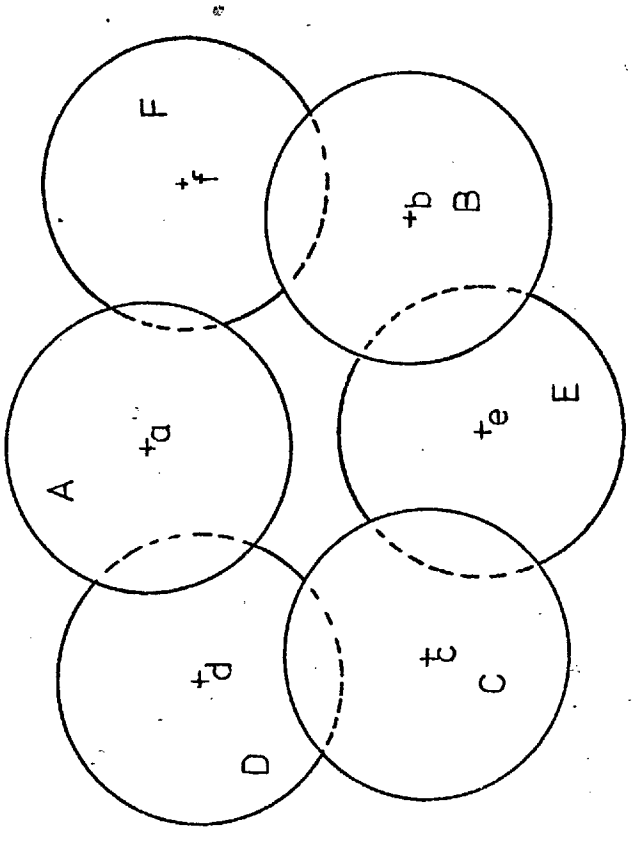


FIGURE 4.7
Subunit U1

tetrahedral unit T 2. The pore space properties of each unit and hence the distributions of the pore space properties of a collection of T 2 units are evaluated.

The probability of the formation of each unit was determined as in the earlier case, by the probability of the occurence of the two edges, (Fig. 4.8) ab and cd. This value was deduced from the edge length frequency distribution of the bases of the tetrahedra T 1.

Stage 4. The Bed

The bed was assumed to consist of units T 1, U 1 and T 2. (Section 4.4), and their relative frequencies of occurence were known in terms of x (Section 4.4). Hence, the overall pore space properties were evaluated from the knowledge of the pore space properties of each type of unit.

A flowsheet for the computer model is given in fig. (4.9).

4.10 Evaluation of factor - x for a gently formed bed.

A gently formed bed could be defined as a bed in which every sphere in the bed which has been dislocated from a once formed tetrahedral configuration, has been dislocated for no other reason than that of load action from top layers. This is an ideal case, as a bed formed by dropping a collection of spheres into a bin is always associated with disturbances such as jerks, impulses, vibrations, etc.

However, for this special case x could be evaluated as follows. The computer program assumes a value of x and generates 3000 edge lengths similar to that for the tetrahedral unit T 1 in Section 4.9. For each tetrahedron configuration (j) of type T 1, the probability factor for stability (ζ_j'') is evaluated. If it is assumed that the probability of formation of each configuration is initially given by

$$1 - x = \left\{ \sum_{j=1}^{M} \zeta_j'' \right\} / M \qquad \ldots\ldots\ldots\ldots\ldots \quad (4.50)$$

Where M is the total number of geometrically consistent tetrahedra considered.

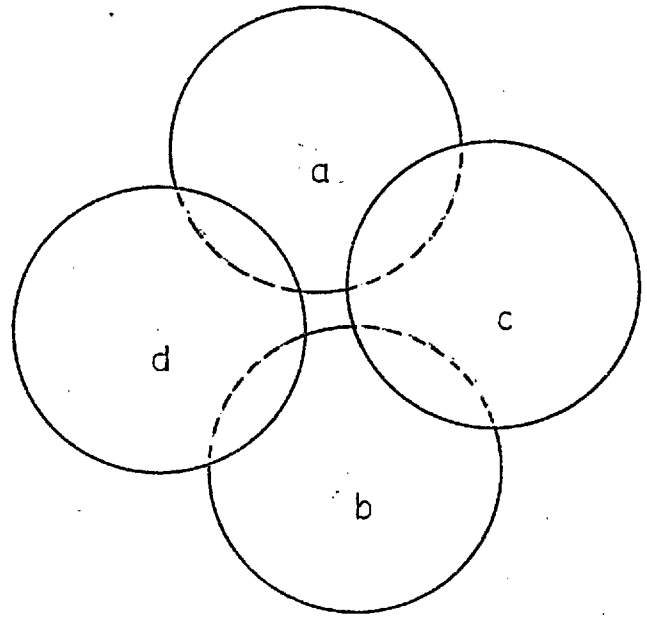


FIGURE 4.8
Subunit T 2

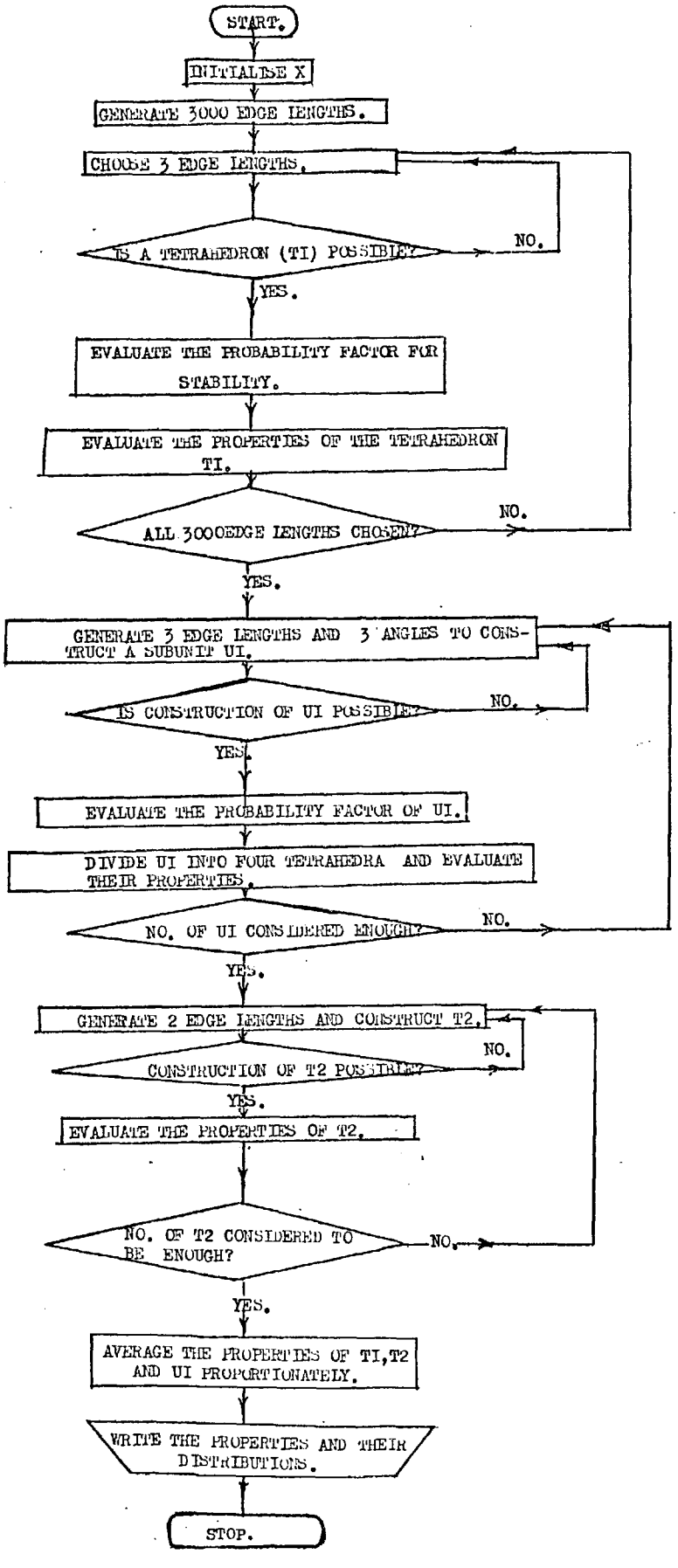


FIGURE 4.9

Flow-chart of the computer program which determines pore size distributions in a random packing.

The value of x evaluated from eq. (4. 50) was compared with the previously assumed value and if the difference was large and not acceptable a new value of x was assumed and the process repeated until the difference was small. The flow diagram of the computer program is given in fig. (4. 10). A value of x = 0. 04 was obtained for the distribution discussed in Section (4. 7). The term x could be regarded as representative of the amount of disturbance imposed on the bed and could be termed the disturbance factor.

4. 11 Discussion

Several Monte Carlo runs were made for different values of the disturbance factor (x) and it was found that a x-factor of 0. 13 gave a void fraction approximately equal to the void fractions obtained for packed beds used in experiments described in later chapters. An experimental mean void fraction of 0. 4044 was obtained with a variance of 0. 0037. These values were compared with a mean of 0. 4045 and variance of 0. 0003 obtained from five Monte Carlo runs. The difference between the means was 0. 02 percent on the theoretical void fraction. This difference can be regarded as negligible.

The normalised distributions of face radii, tetrahedron insphere radii, tetrahedron volumes, cell volumes and edge lengths, for five Monte Carlo runs and their mean distributions for a disturbance factor (x) of 0. 13 are shown in Figs. 4. 11 to 4. 15 respectively. Fig. 4. 16 to 4. 20 shows the distributions for six degrees of disturbances. The variation of the void fraction of a packed bed with the disturbance factor x is shown in Fig. 4. 21. The values were obtained from five computer runs for different values of x. Variation of void fraction with disturbance was studied by Kolbuszewski (131) who performed experiments, in which the influence of the rate of pouring and vibration on the porosity of sand beds was obtained. It was observed that a high rate of fall of sand gave a low porosity and a low rate led to a higher porosity. It could be expected that a high rate of fall would give rise to a higher disturbance factor x and hence give rise to a low void fraction.

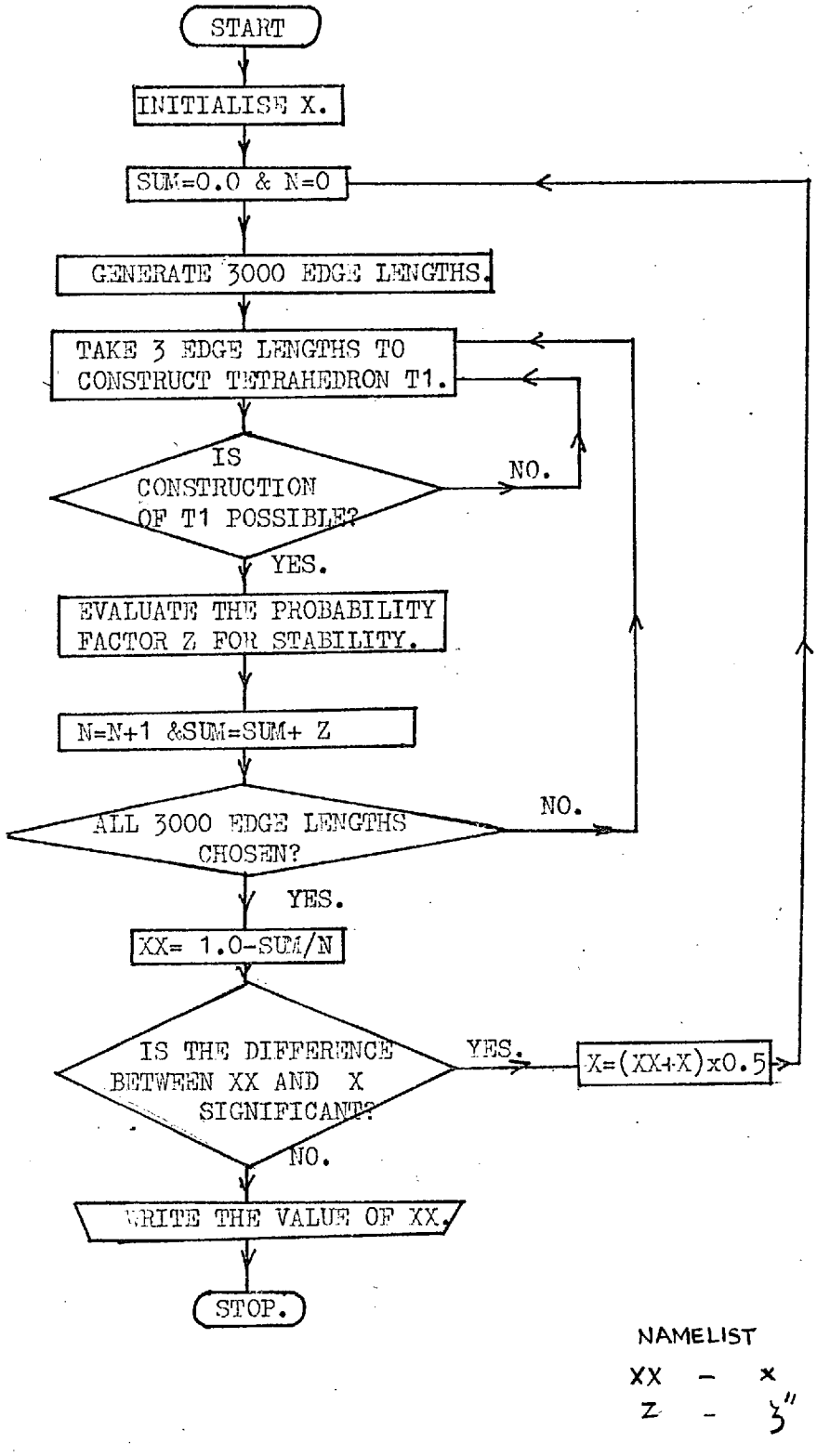
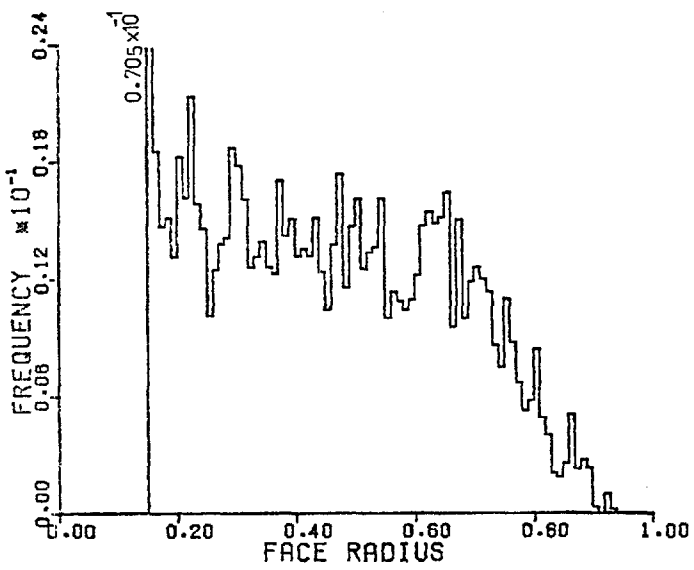
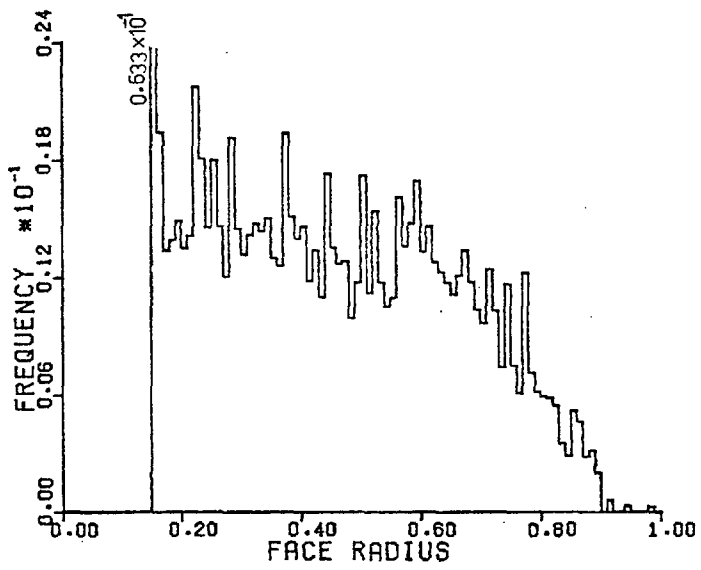


FIGURE 4. 10

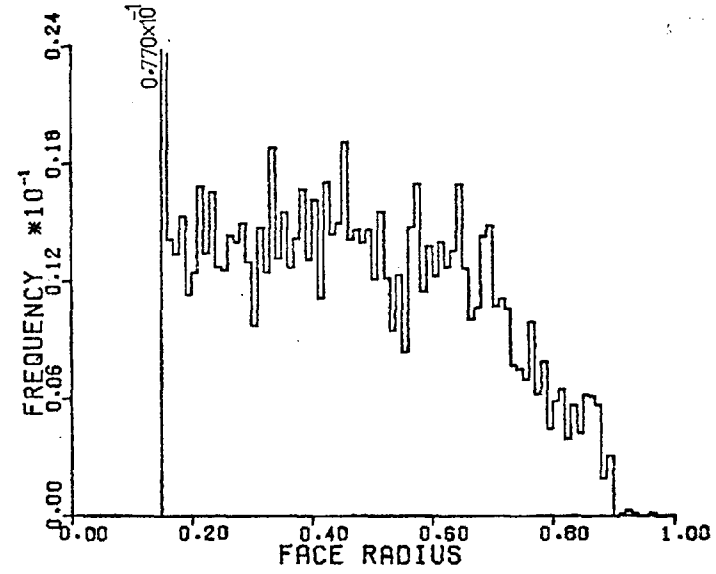
FLOW-CHART OF THE COMPUTER PROGRAM WHICH EVALUATES FACTOR X.



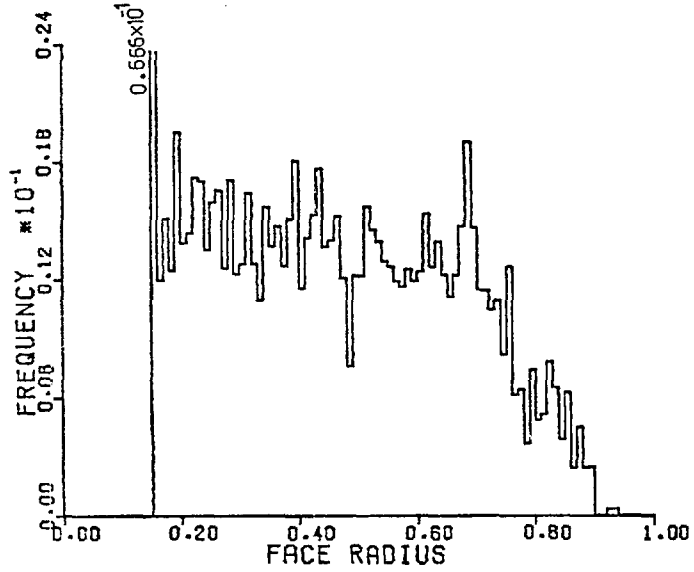
(a) Run 1.



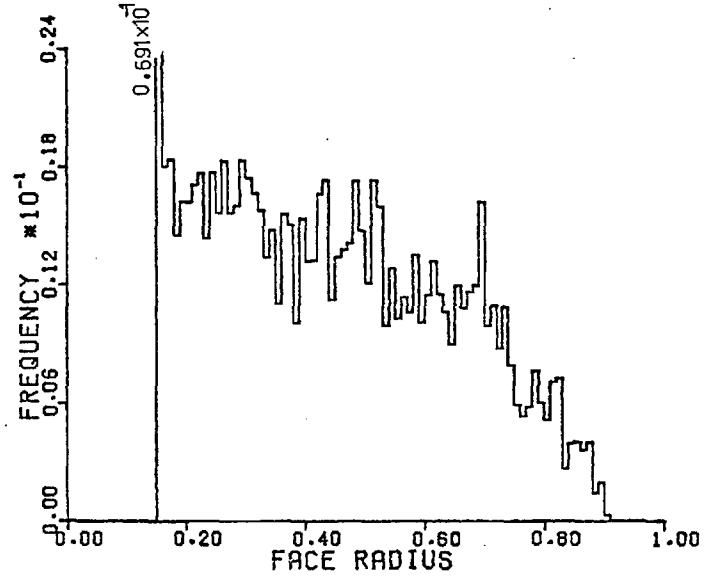
(b) Run 2.



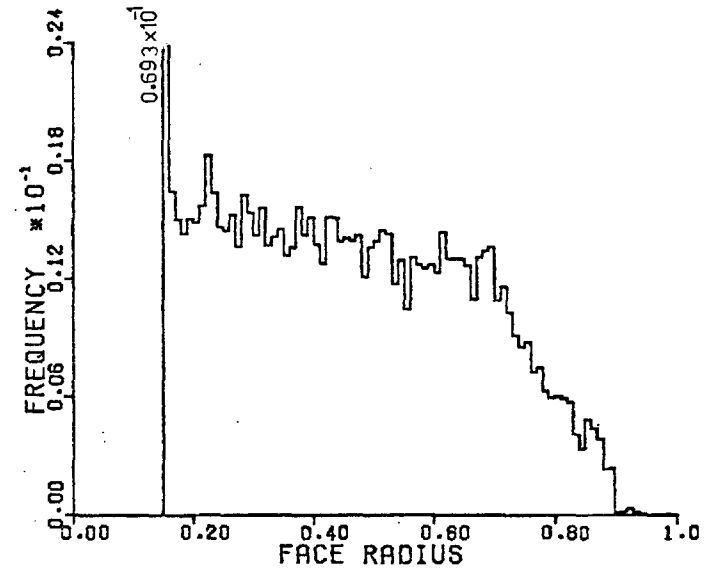
(c) Run 3.



(d) Run 4.

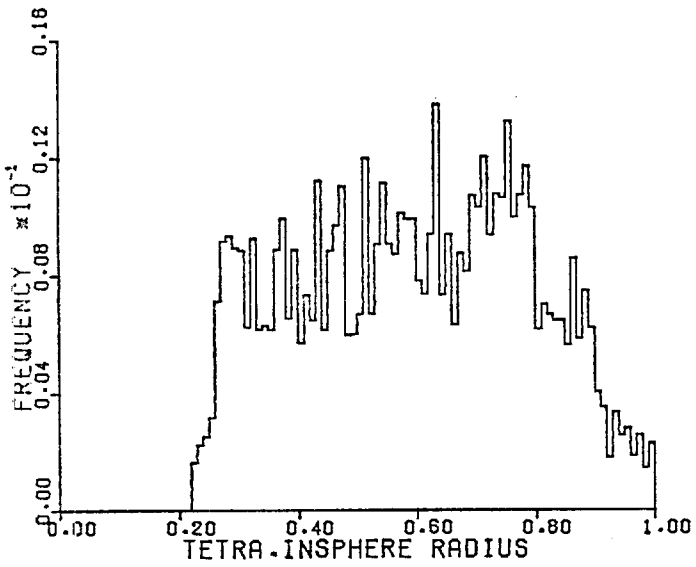


(e) Run 5.

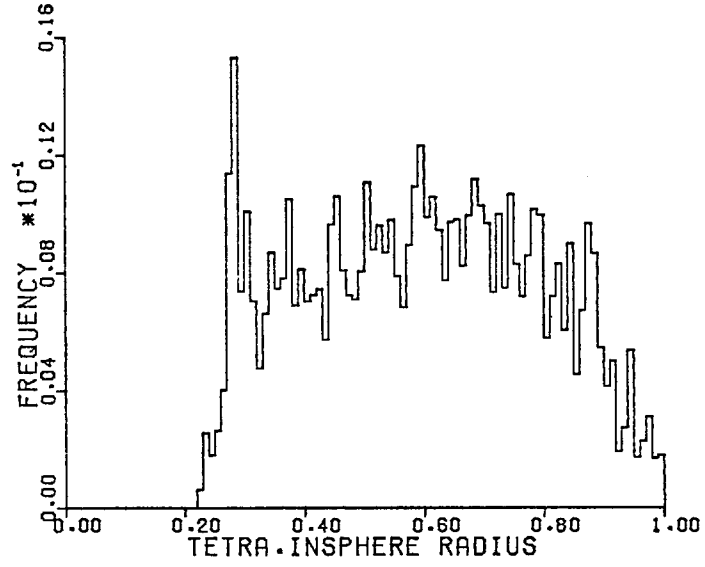


(f) Mean distribution.

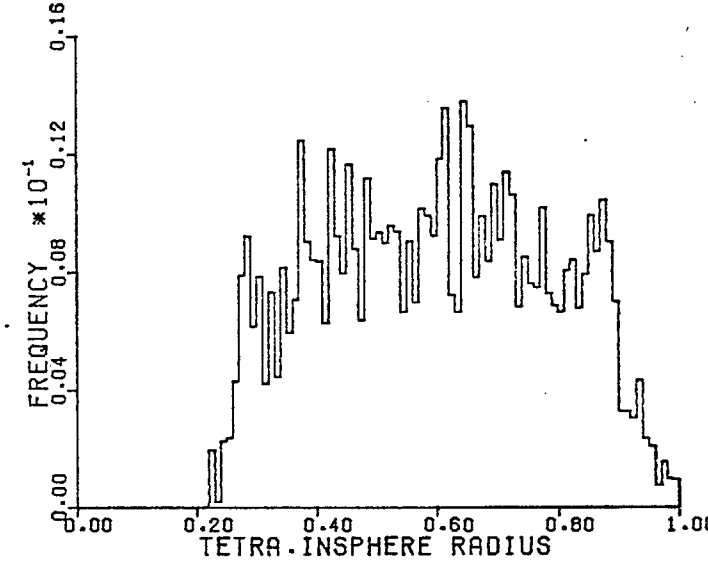
FIG.4.11 THE NORMALISED FACE RADII DISTRIBUTIONS FOR FIVE MONTE CARLO RUNS AND THE MEAN DISTRIBUTION.



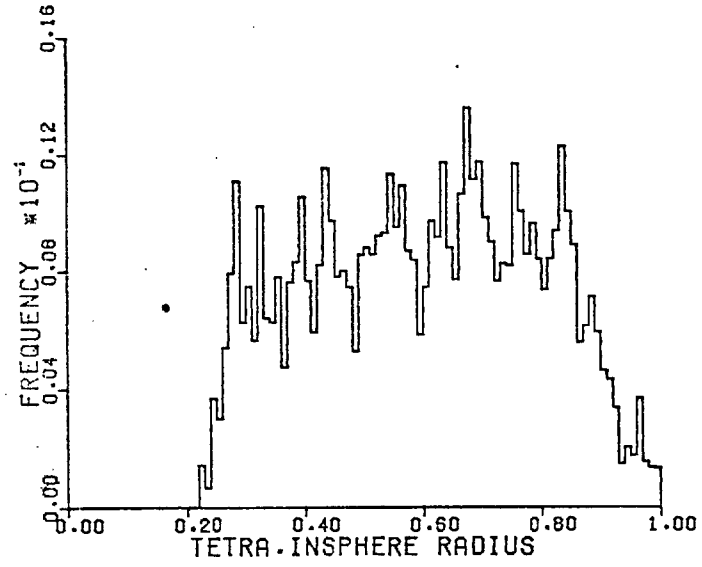
(a) Run 1.



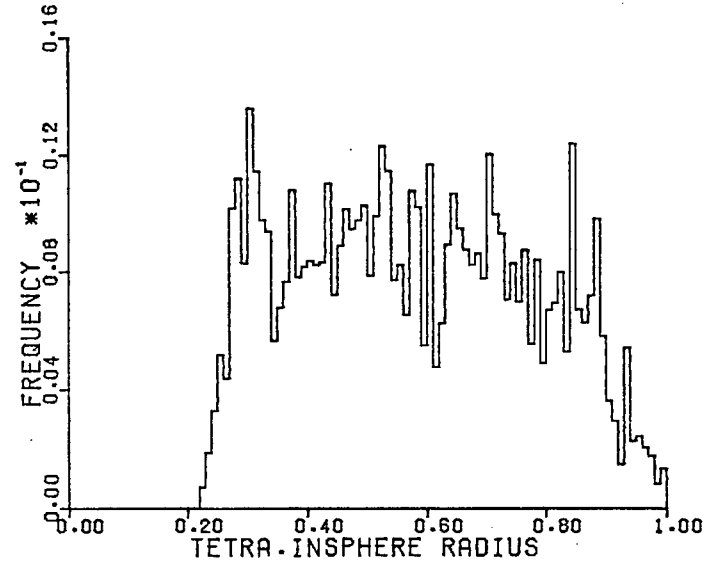
(b) Run 2.



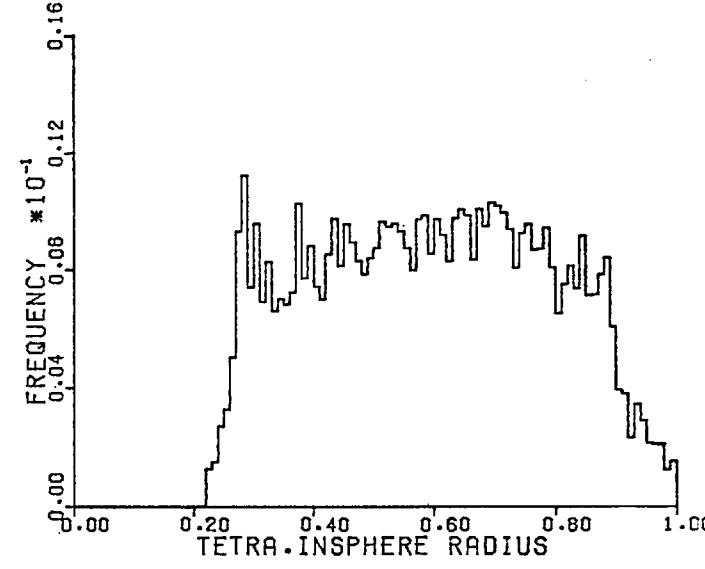
(c) Run 3.



(d) Run 4.

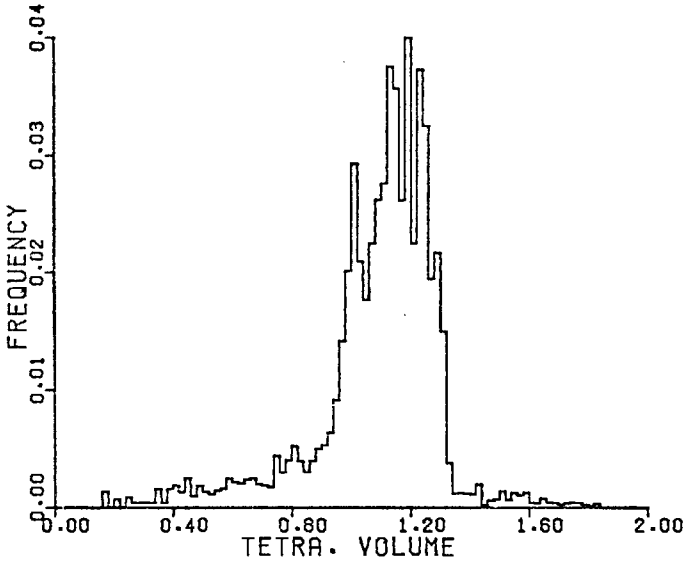


(e) Run 5.

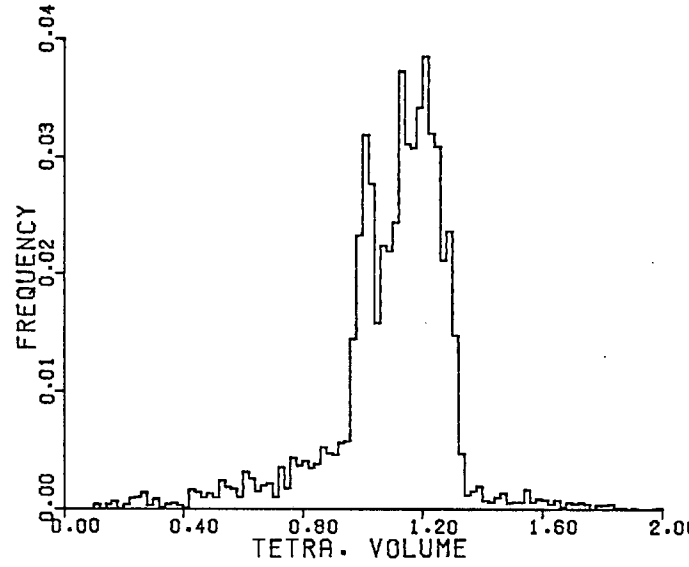


(f) Mean distribution.

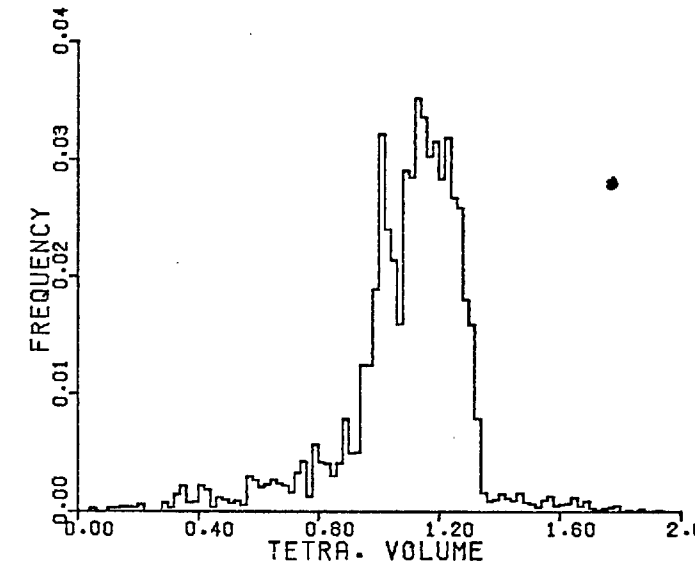
FIG. 4.12 THE NORMALISED TETRA.INSPHERE RADII DISTRIBUTIONS FOR FIVE MONTE CARLO RUNS AND THE MEAN DISTRIBUTION.



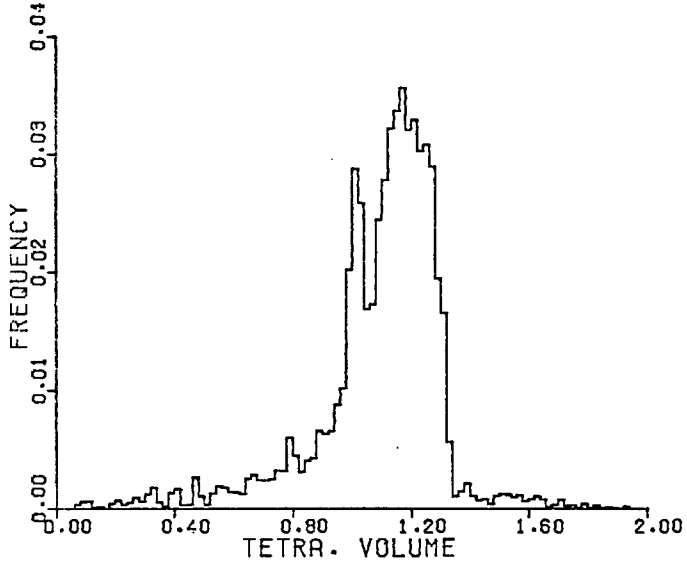
(a) Run 1.



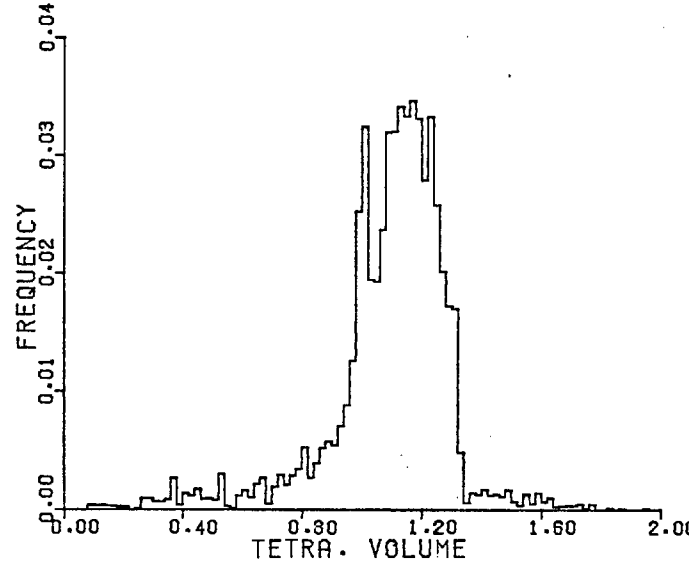
(b) Run 2.



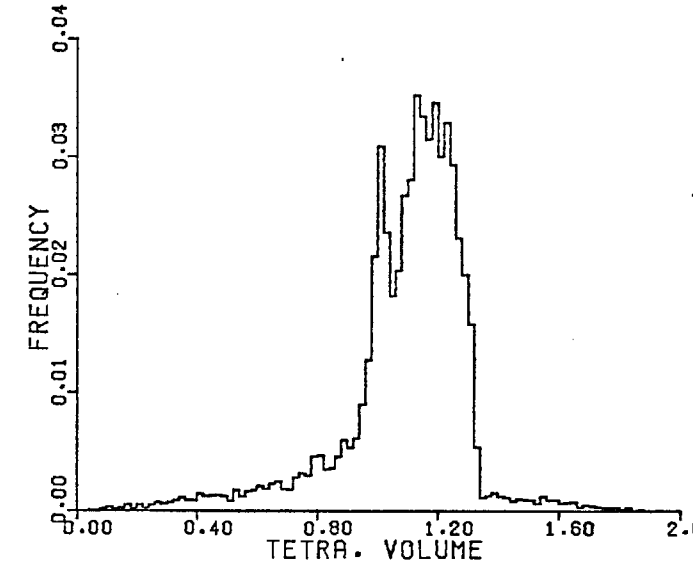
(c) Run 3.



(d) Run 4.

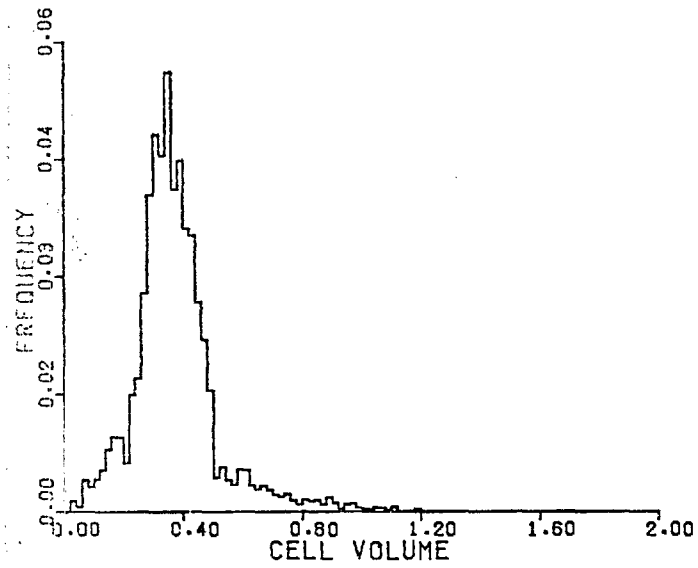


(e) Run 5.

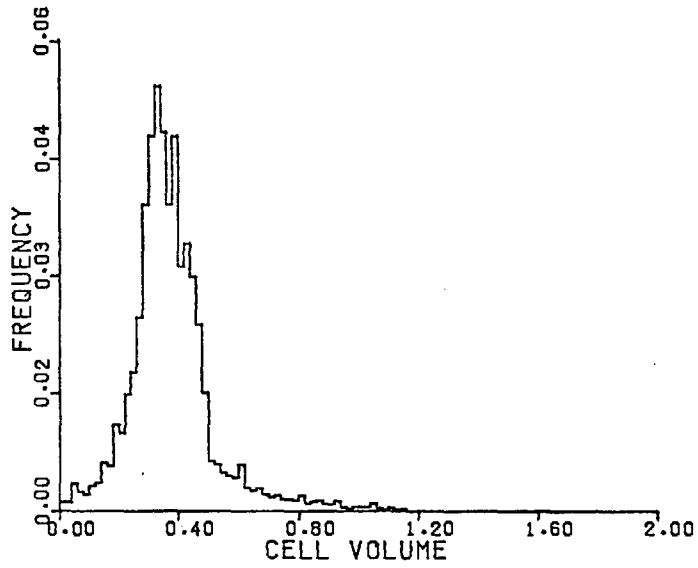


(f) Mean distribution.

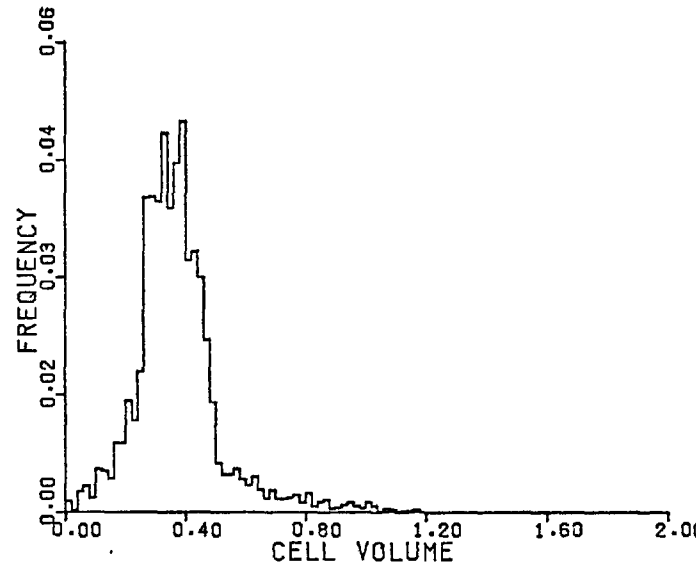
FIG.4.13 THE NORMALISED TETRA. VOLUME DISTRIBUTIONS FOR FIVE MONTE CARLO RUNS AND THE MEAN DISTRIBUTION.



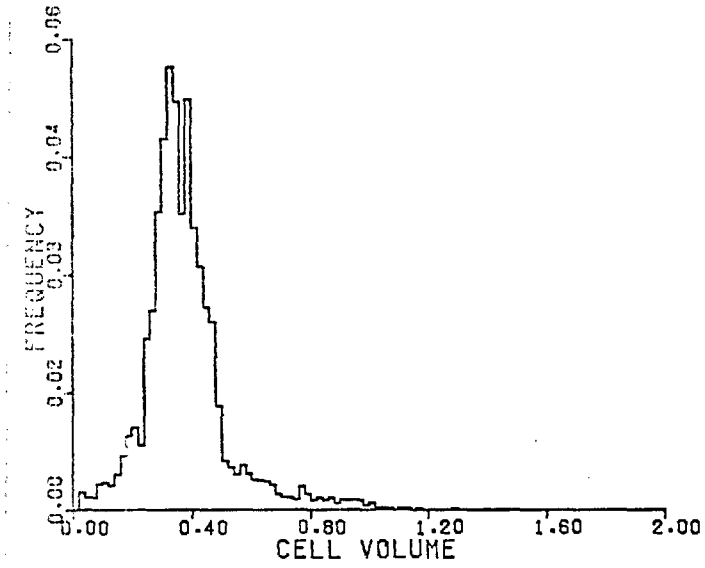
(a) Run 1.



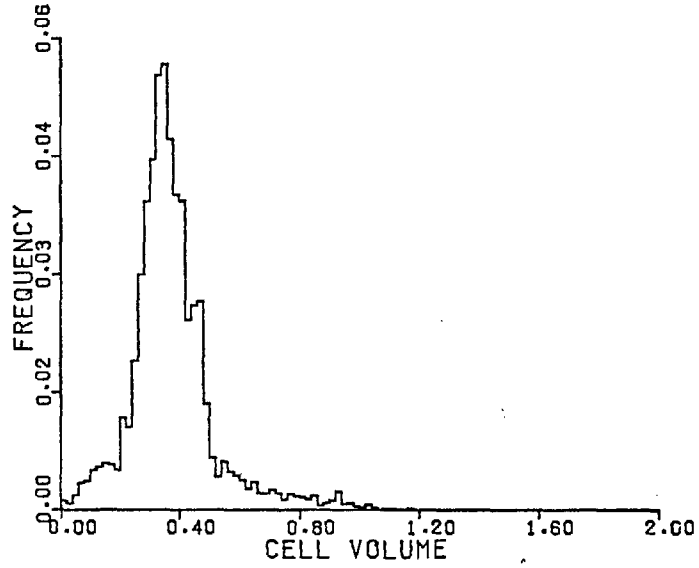
(b) Run 2.



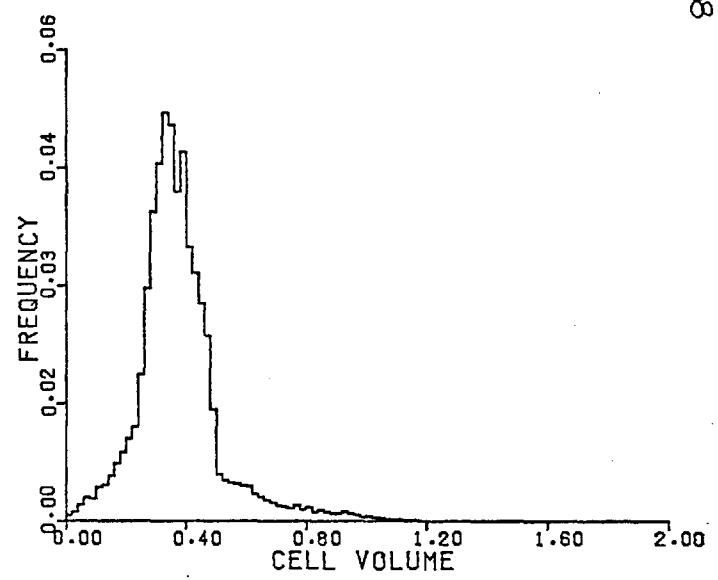
(c) Run 3.



(d) Run 4.

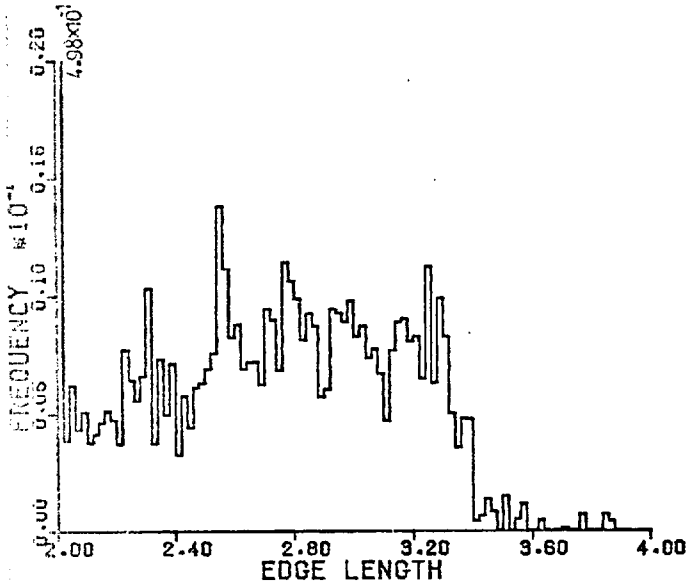


(e) Run 5.

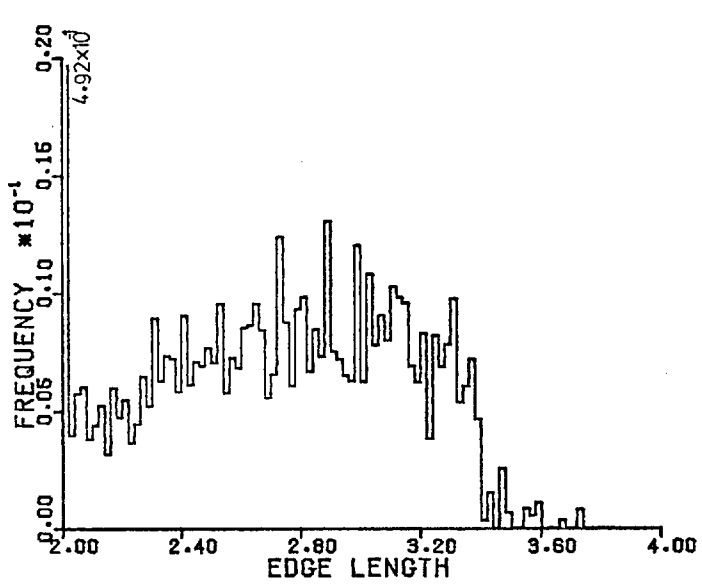


(f) Mean distribution.

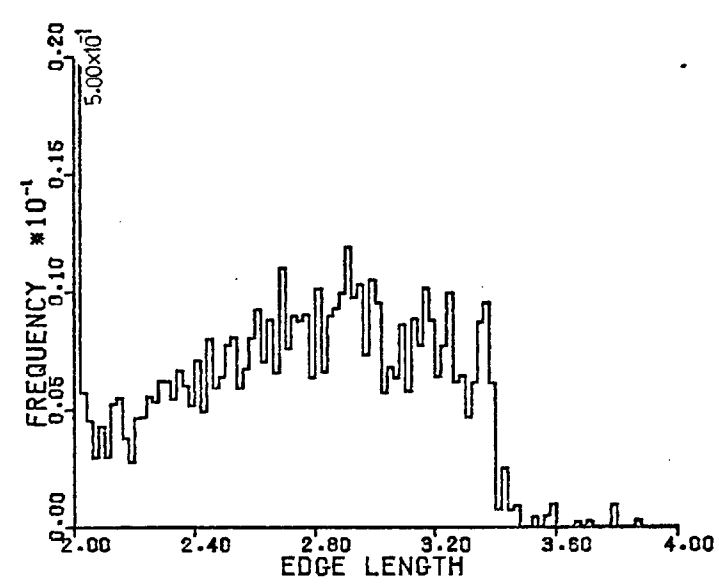
FIG. 4.14 THE NORMALISED CELL VOLUME DISTRIBUTIONS FOR FIVE MONTE CARLO RUNS AND THE MEAN DISTRIBUTION.



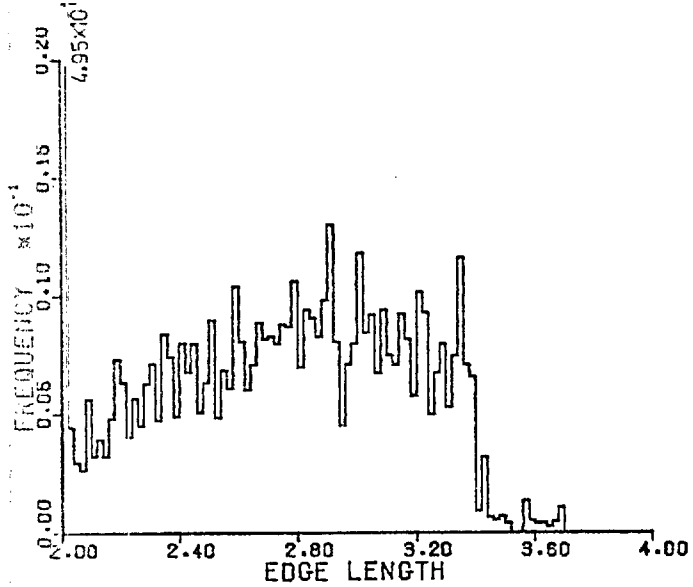
(a) Run 1.



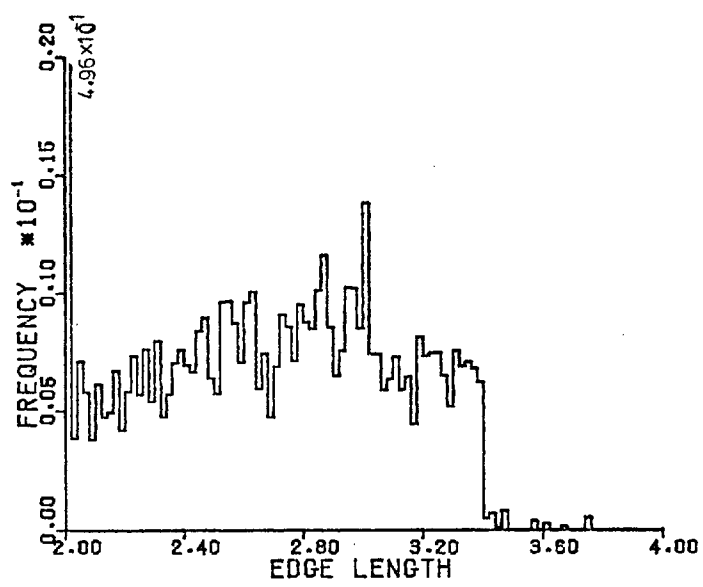
(b) Run 2.



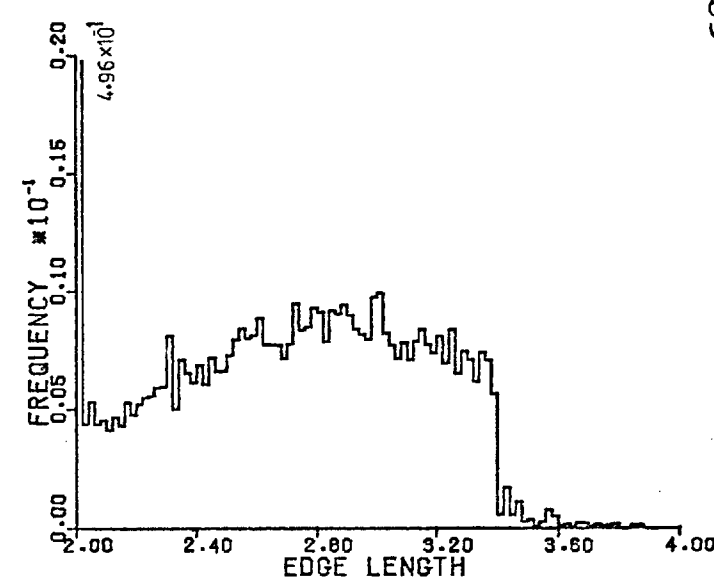
(c) Run 3.



(d) Run 4.

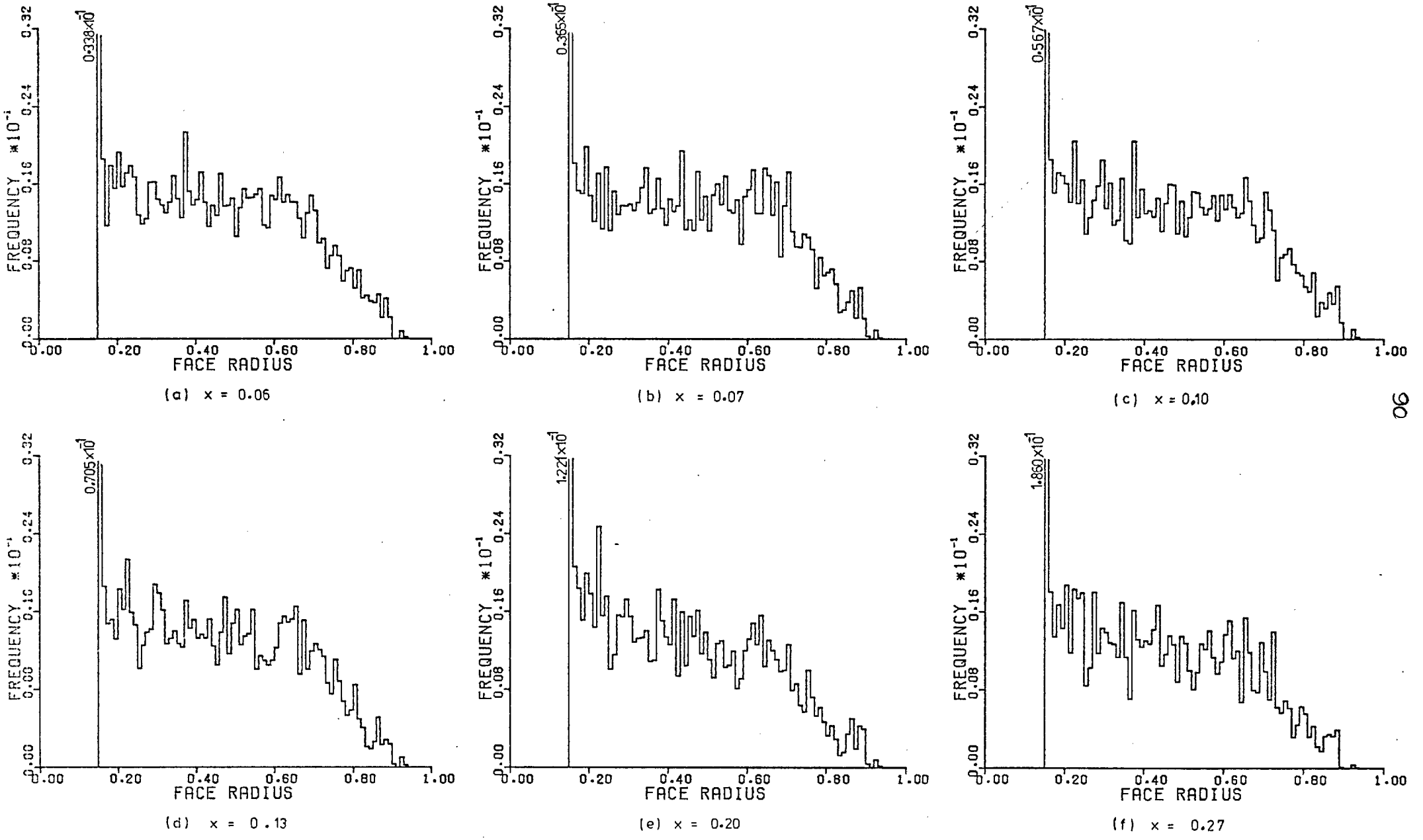


(e) Run 5.



(f) Mean distribution.

FIG. 4.15 THE NORMALISED EDGE LENGTH DISTRIBUTIONS FOR FIVE MONTE CARLO RUNS AND THE MEAN DISTRIBUTION.



(a) x = 0.06 (b) x = 0.07 (c) x = 0.10

(d) x = 0.13 (e) x = 0.20 (f) x = 0.27

FIG. 4.16 THE NORMALISED FACE RADII DISTRIBUTIONS FOR SIX DEGREES OF DISTURBANCE

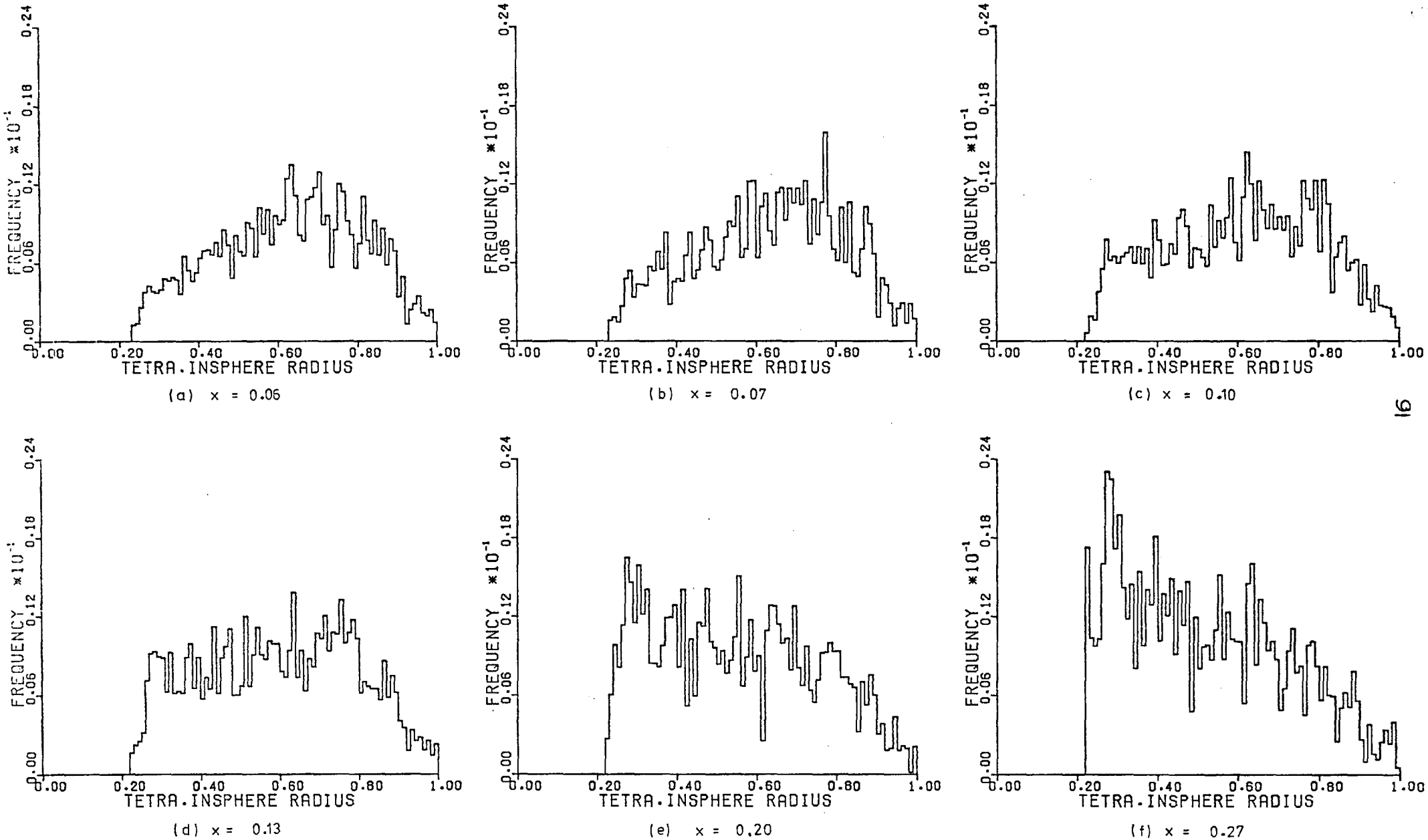


FIG.4.17 THE NORMALISED TETRA. INSPHERE RADII DISTRIBUTIONS FOR SIX DEGREES OF DISTURBANCE

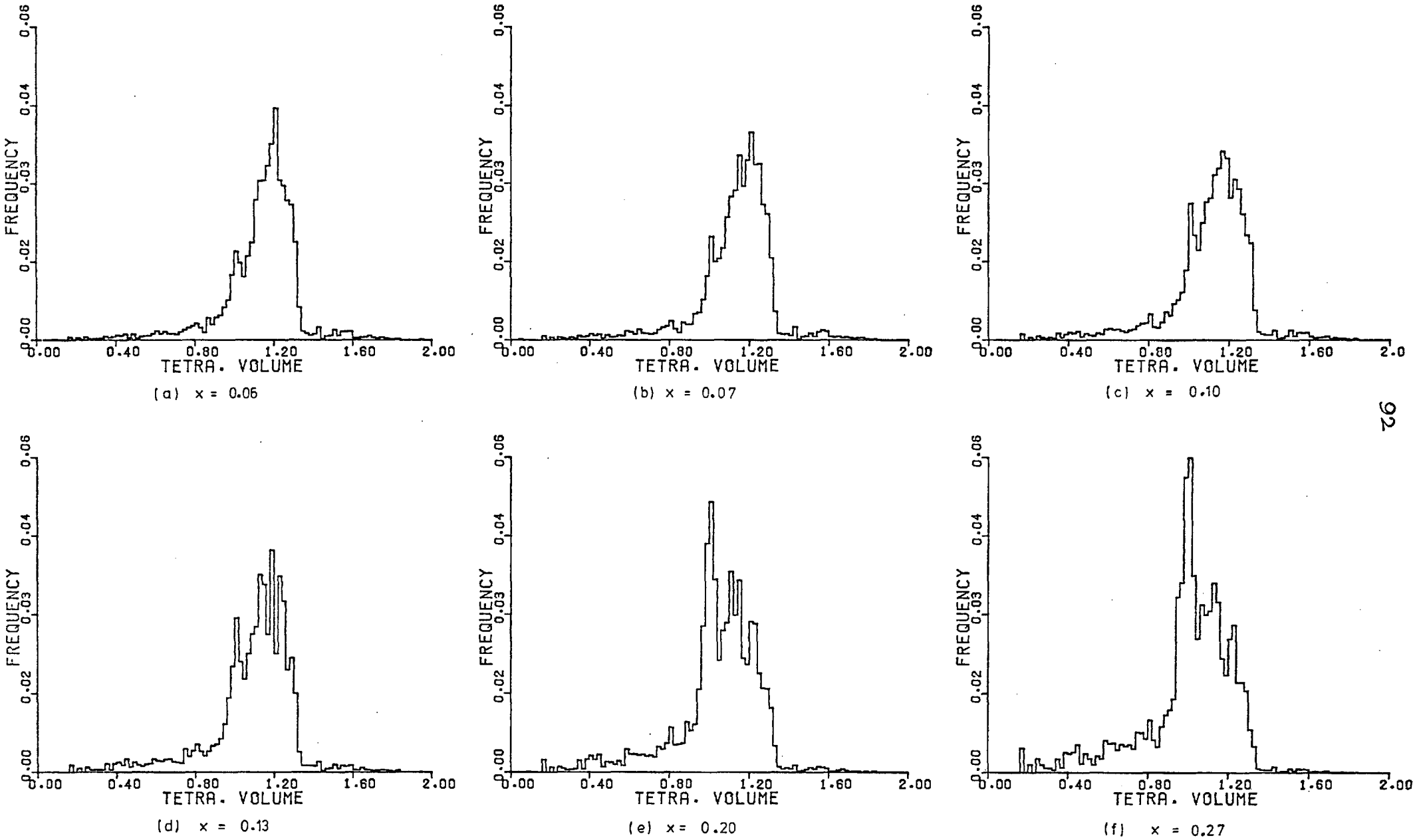


FIG. 4.18 THE NORMALISED TETRA. VOLUME DISTRIBUTIONS FOR SIX DEGREES OF DISTURBANCE

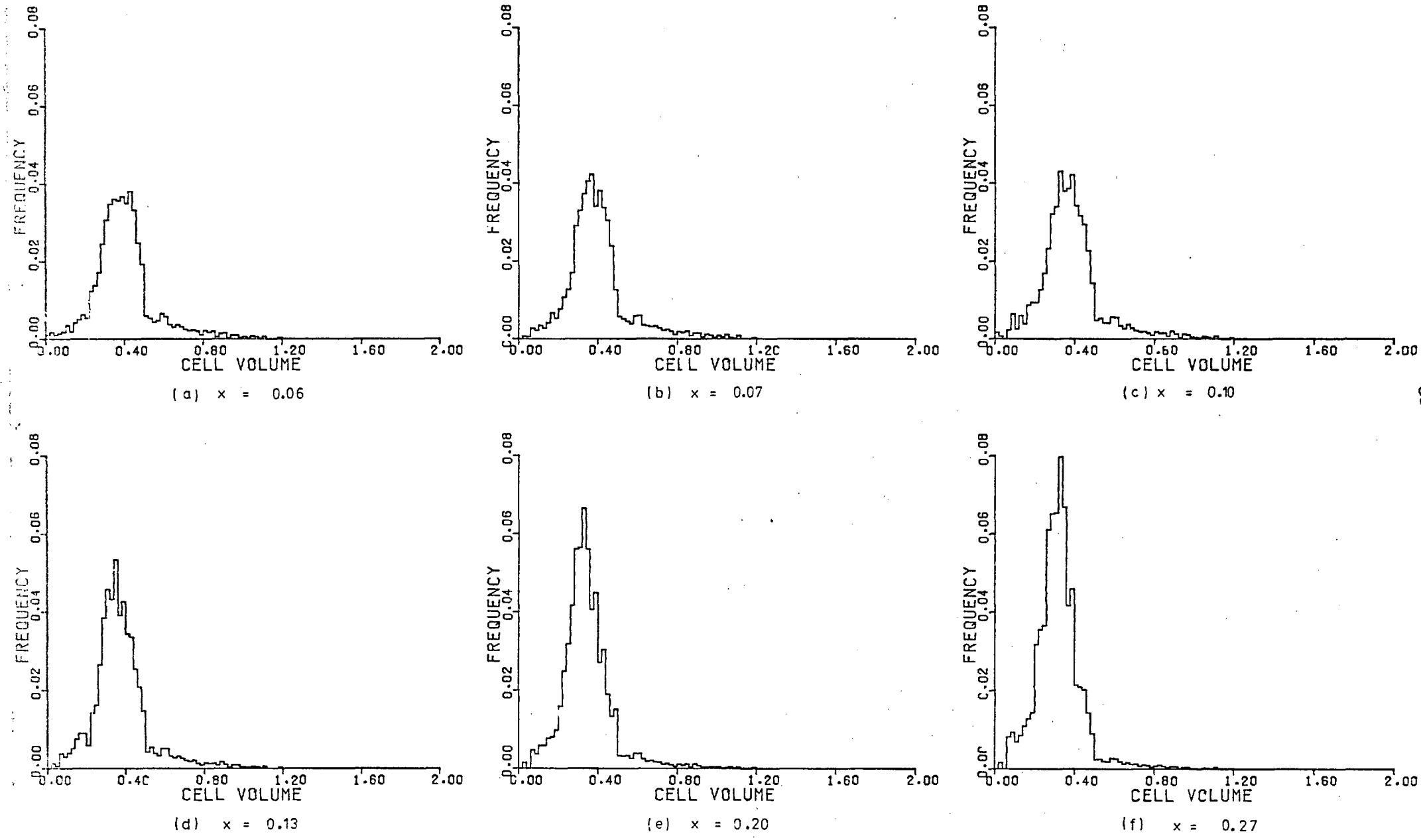
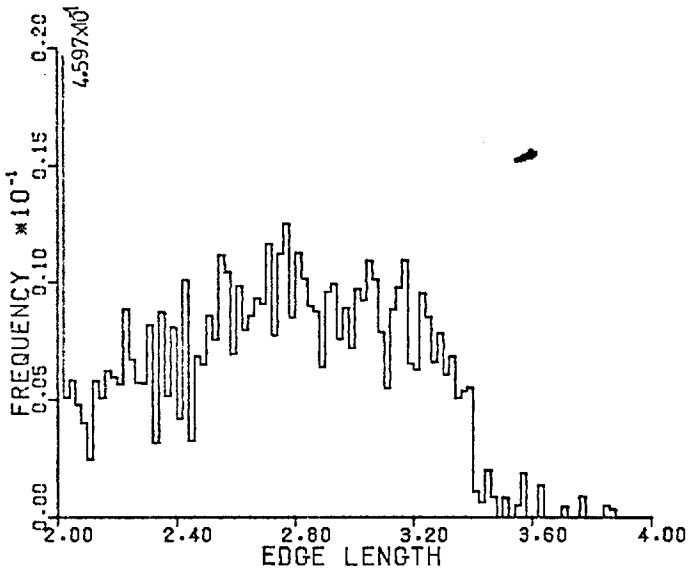
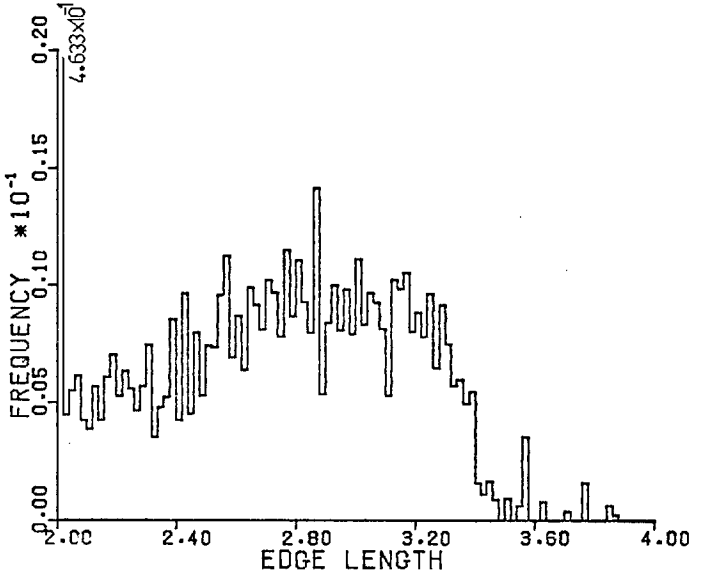


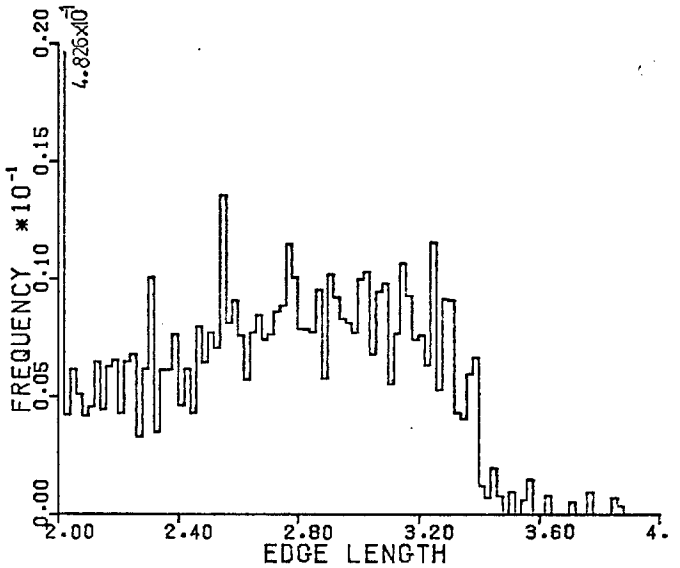
FIG.4.19 THE NORMALISED CELL VOLUME DISTRIBUTIONS FOR SIX DEGREES OF DISTURBANCE



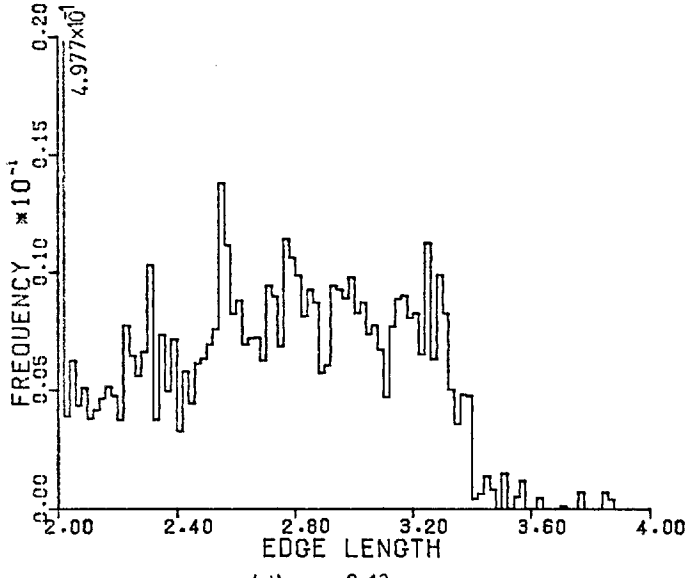
(a) x = 0.06



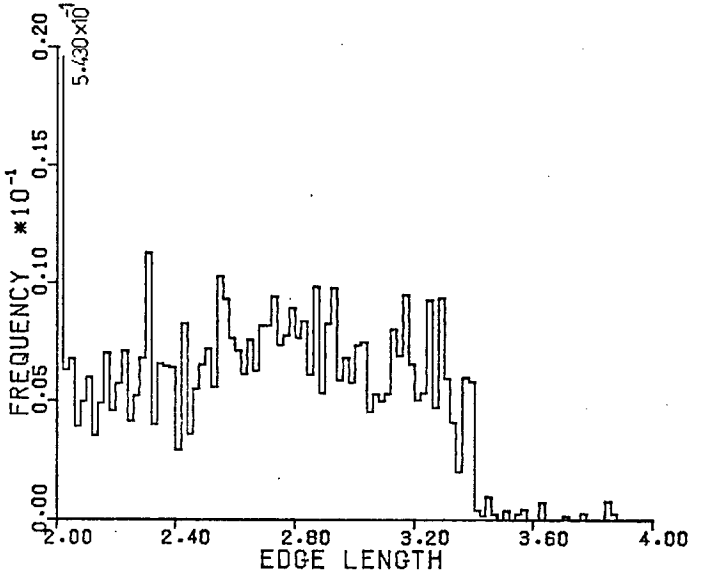
(b) x = 0.07



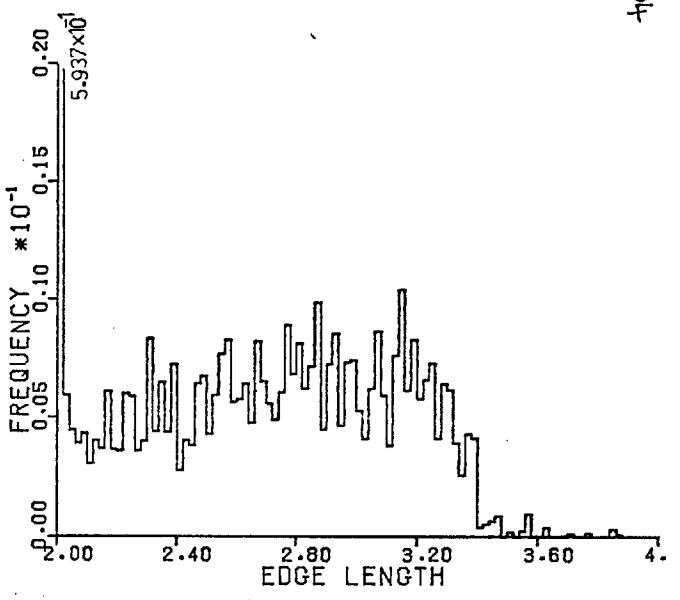
(c) x = 0.10



(d) x = 0.13



(e) x = 0.20



(f) x = 0.27

FIG. 4.20 THE NORMALISED EDGE LENGTH DISTRIBUTIONS FOR SIX DEGREES OF DISTURBANCE

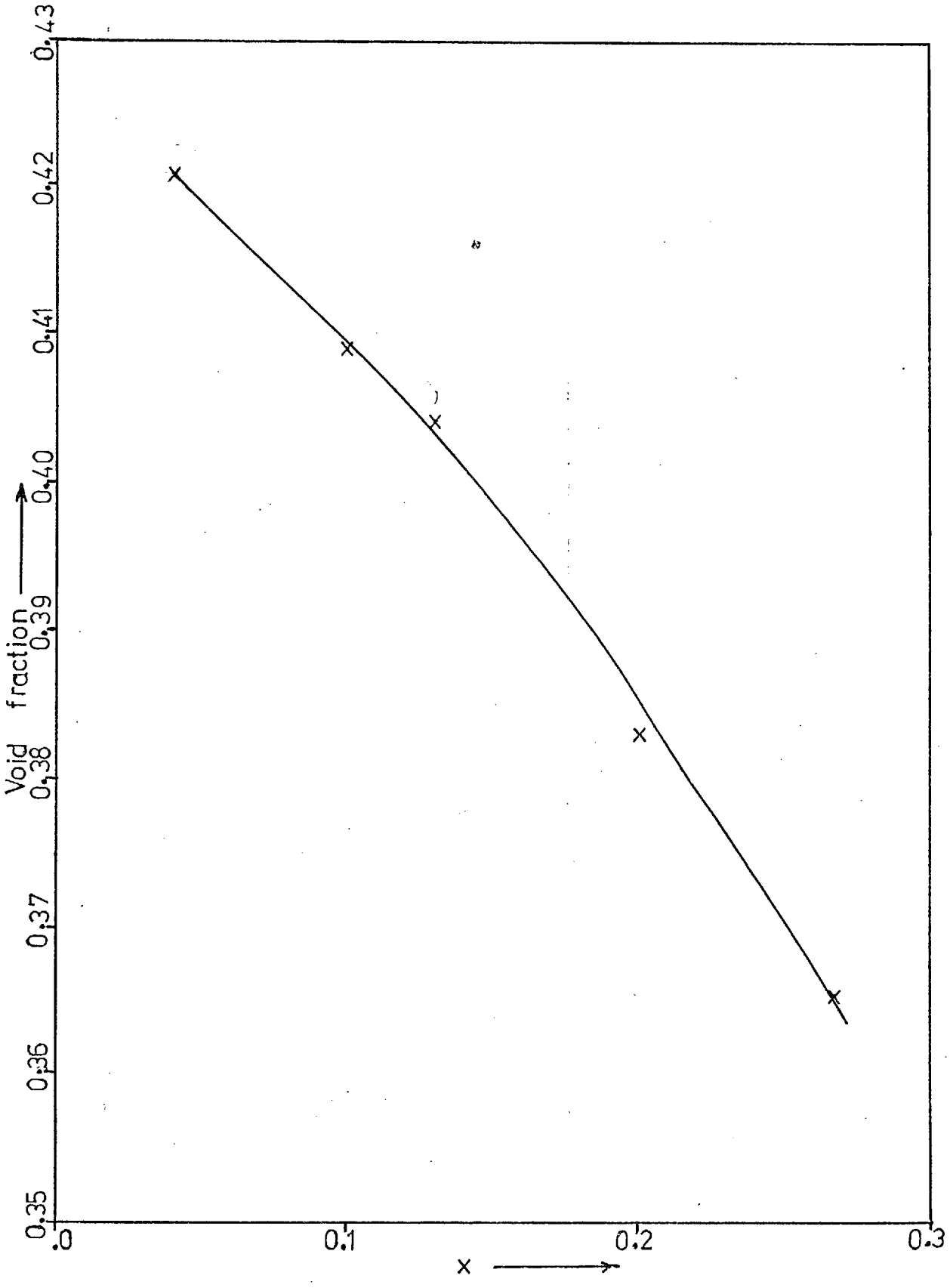


FIGURE 4.21
Variation of void fraction with x.

The vibration experiments of Kolbuszewski were analogous to those carried out by Debbas and Rumpf (50). The results of the two sets of experiments gave a similar pattern of porosity variation with the time of disturbance hence indicating that a large disturbance factor results in a low void fraction. A minimum value of the voidage was reached after prolonged vibrations. The void fractions decreased when the duration times of vibration of the bed were increased until the minimum value was attained. The existence of a limiting value of void fraction could be explained as being a result of geometrical constraints preventing any further relative movement of the particles in the packing. For consolidated packings, larger values of edge lengths could be expected to be less frequent and a lower value for the upper limit of the edge length could be more appropriate. Mason (149) used an upper limit of the edge length as 1.4 times the diameter of a particle in his model of a packed bed and obtained a void fraction of 0.365.

An upper limit of the voidage was found (Section 4.10) to be 0.4212 for a disturbance factor of 0.04. The value of 0.04 of the disturbance factor was derived for a gently formed bed using the method described in Section 4.10. However, this result does not exclude the possibility of the existence of larger void fractions. Other metastable configurations, specially for packings of particles with rough surfaces, could lead to larger voidage values.

The theory could also be employed to explain the consolidation under external loads and settling which usually occurs in packed beds. In both cases changes in the disturbance factor x causes changes in voidages.

The theory derived in this chapter could be assumed to be applicable to beds of smooth particles or to beds which approximate these. The theory can be extended to packings of mixtures of different sizes of particles, but a further study of geometry of packings is needed for this purpose.

CHAPTER 5

The Moisture Distribution Under Imbibition : The Rise Curve.

5.1 The Movement and Distribution of Moisture Under Imbibition.

5.1.1 A Qualitative Analysis

The types of distribution of moisture encountered in a porous body under imbibition have been discussed in Section (2.2). Even though the discussion has been of a qualitative nature, an insight to the problem of imbibition could be obtained from it. A quantitative approach to the problem, especially with a study of the physical phenomena occuring at different stages of the filling-up of the pores in a porous medium, could lead to a generalised description of the phenomenon of imbibition.

In a packed bed of particles, the distances between the surfaces of the neighbouring particles vary. The gaps between the solid surfaces form the channels for liquid to rise into the body and some of the gaps are responsible for liquid hold-up due to capillary action. When a packed bed is placed in a pool of a wetting liquid, the liquid tends to rise faster through regions in which the capillaries, are small. During imbibition the pores of a porous body are liable to be filled up either by a saturated front or by the growth of pendular rings which are connected to the bulk of the liquid.

5.1.2 A theoretical analysis

5.1.2.1 The Capillary pressure of moisture in a partially saturated pore.

Consider a small cell which is saturated partially by moisture. Let G be the free energy of moisture in the cell, V the volume of moisture in the cell, p the capillary pressure of moisture, s the entropy, T the temperature, σ' the surface tension and A the area of air-water interface. Then these quantities can be related by the difference equation

$$dG = Vdp - sdT + \sigma' dA \qquad (5.1)$$

When the moisture in the cell is in equilibrium, free energy is constant. ($dG = o$). Hence for isothermal conditions the equation (5. 1) can be modified:

$$- Vdp = \sigma' dA \quad \ldots\ldots\ldots\ldots\ldots\ldots\ldots\ldots\ldots\ldots \quad (5.2)$$

Let V_p be the pore volume and V_A the volume of air confined in the pore.

Then $$V = V_p - V_A \quad \ldots\ldots\ldots\ldots\ldots\ldots\ldots\ldots\ldots\ldots \quad (5.3)$$

Hence $$-dp = \sigma' \frac{dA}{V_p - V_A} \quad \ldots\ldots\ldots\ldots\ldots\ldots\ldots\ldots\ldots\ldots \quad (5.4)$$

σ' is in general a function of the temperature.

For capillary bodies σ' is generally a constant for isothermal conditions. Therefore equation (5.4) can be integrated from capillary pressure of zero to a pressure p as:

$$-p = \sigma' \int_o^A \frac{dA}{V_p - V_A} \quad \ldots\ldots\ldots\ldots\ldots\ldots\ldots\ldots\ldots\ldots \quad (5.5)$$

If the air core in the pore is assumed to be approximately spherical, then

$$A = kV_A^{2/3} \quad \ldots\ldots\ldots\ldots\ldots\ldots\ldots\ldots\ldots\ldots\ldots\ldots \quad (5.6)$$

Where k is a constant i.e. $3\left(\frac{4\Pi}{3}\right)^{\frac{1}{3}}$ for a spherical core.

Hence $$- p = k\sigma' \int_o^{V_A} \frac{2}{3} \frac{1}{(V_p - V_A)V_A^{\frac{1}{3}}} dV_A \quad \ldots\ldots\ldots\ldots \quad (5.7)$$

or $$p = \frac{2}{3} \frac{k\sigma'}{V_p^{\frac{1}{3}}} \int_o^{V/V_p} \frac{d\left(V/V_p\right)}{V/V_p\left(1 - V/V_p\right)^{\frac{1}{3}}} \quad \ldots\ldots\ldots \quad (5.8)$$

Let the fractional saturation be denoted by X.

Then $$X = V/V_p \quad \ldots\ldots\ldots\ldots\ldots\ldots\ldots\ldots\ldots\ldots \quad (5.9)$$

Therefore eq. (5. 8) can be written as

$$p = \frac{2}{3} \frac{k\sigma'}{V_p^{\frac{1}{3}}} \int_o^X \frac{dX}{X(1-X)^{\frac{1}{3}}} \quad \ldots\ldots\ldots\ldots\ldots\ldots \quad (5.10)$$

Equation (5. 10) can be integrated to give

$$p = \tfrac{2}{3}k\frac{\sigma'}{V_p^{\frac{1}{3}}}\left[\ln\sqrt{\frac{X}{\left\{1-(1-X)^{\frac{1}{3}}\right\}^3}} - \sqrt{3}\ \mathrm{Tan}^{-1}\left\{\frac{2(1-X)^{\frac{1}{3}}+1}{\sqrt{3}}\right\} + \frac{\sqrt{3}\Pi}{6}\right] \quad \ldots\ldots\ldots\ldots\ldots\ldots \quad (5.11)$$

Where $k = 3\left(\frac{4\Pi}{3}\right)^{\frac{1}{3}}$ for an ideal spherical core.

The shape of the capillary pressure curve given by equation (5. 11) is shown in fig. (5. 1).

A similar equation can be developed for a cylindrical cell with a cylindrical air core and the capillary pressure for such a model can be expressed as

$$p = \frac{\sigma'}{a}\ln\left[\frac{1+(1-X)^{\frac{1}{2}}}{1-(1-X)^{\frac{1}{2}}}\right] \quad \ldots\ldots\ldots\ldots\ldots\ldots\ldots\ldots \quad (5.12)$$

where 2a is the diameter of the cylindrical cell.

The shape of the moisture distribution curve given by equation (5. 12) is shown in figure (5. 2).

5. 1. 2. 2 Void Space in a porous body.

The void space in a porous body can be divided into three groups : pores, interconnections and corners, of which the definitions are given below.

Corners: Corners can be defined as that part of the void space in a porous medium which is occupied by the irreducible or trapped moisture when it is desaturated under gravity. A major part of the volume of moisture in the pore corners is in the form of pendular bridges.

Pores: In equation (5. 11) V_p was defined as the pore volume and X the moisture content as the fraction V/V_p where V is the volume of moisture in the pore.

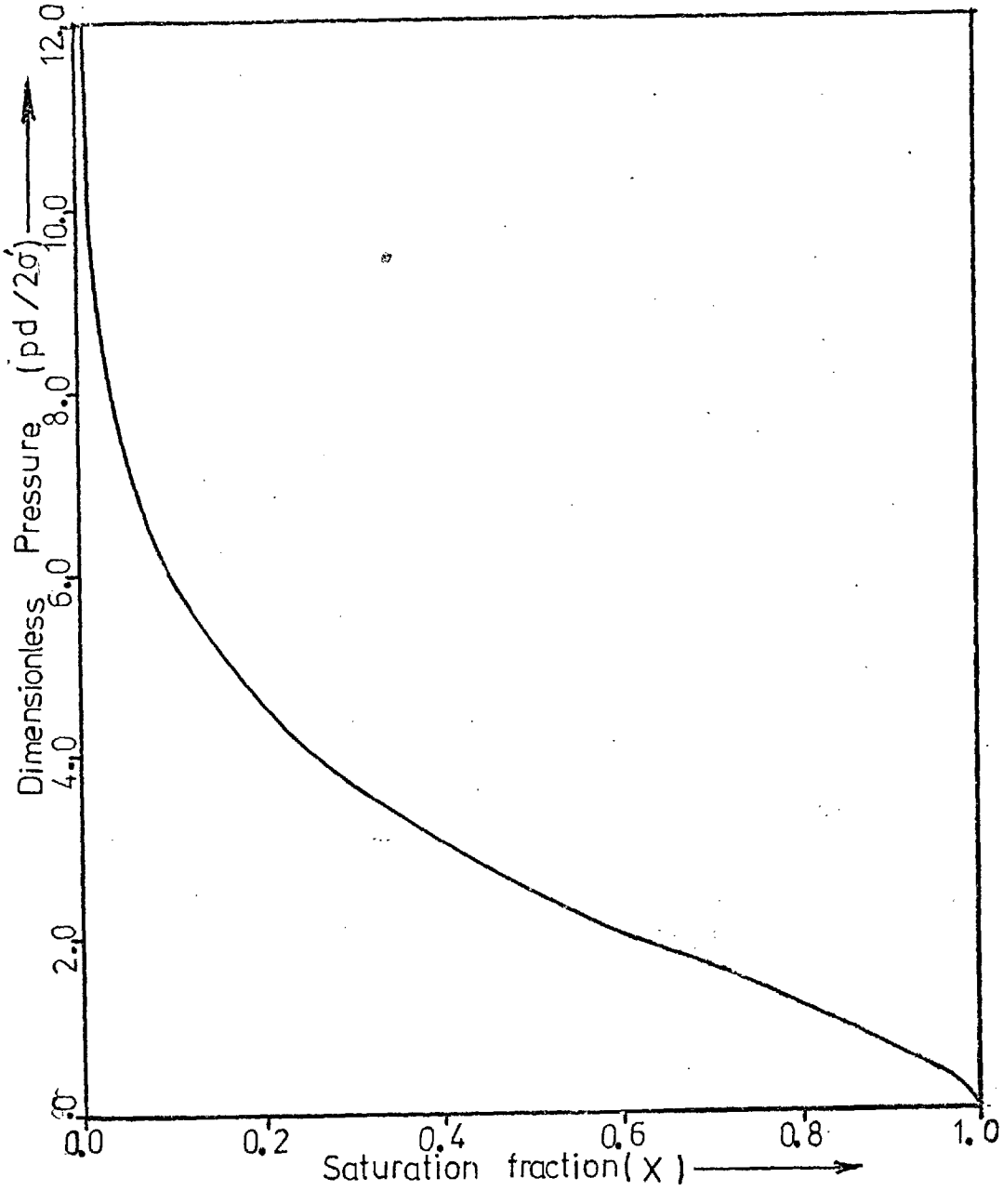


FIGURE 5.1

Capillary pressure curve for a spherical pore.

(d=diameter of pore)

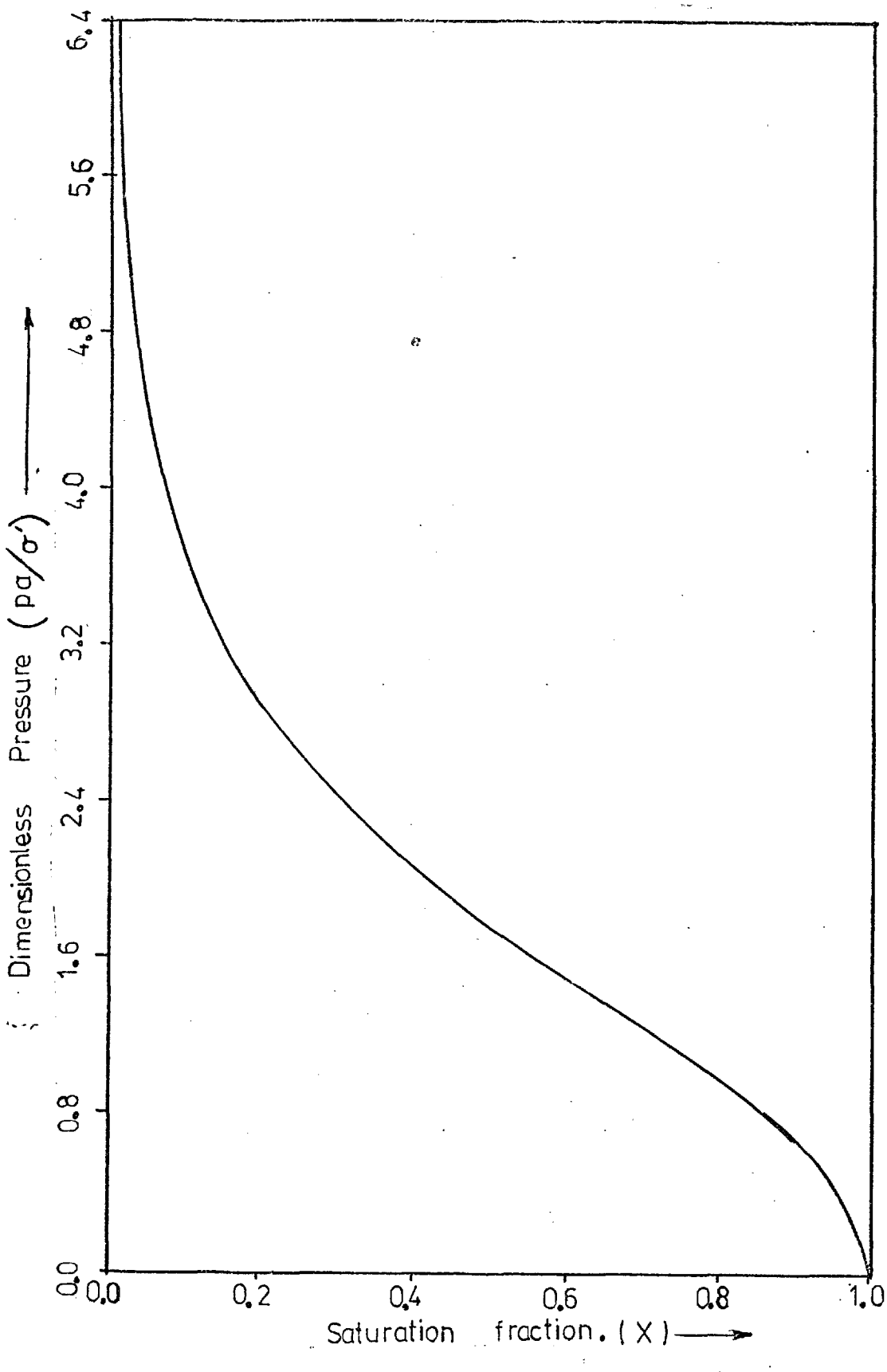


FIGURE 5.2

Capillary Pressure Curve for a Cylindrical Pore. (a = radius of cylinder)

However, eq. (5. 11) was developed without attaching a specific physical meaning to the term pore volume. An investigation of the physical meaning of pore volume is undertaken in the following discussion.

Consider a partially saturated cell A (Fig. 5.3) at a height h above a free surface level. If the cell is raised to a higher position from its present position (ie., if h is increased), the saturation of moisture in the cell decreases thus giving rise to a larger air/water interface and a larger air space in the cell. Suppose the cell is raised gradually away from the free liquid surface, the air core becomes larger and larger. At a very large height, the moisture saturation will be very low, so that the continuous phase of moisture becomes disconnected and forms discontinuous regions of moisture in narrow regions between the cell walls (e.g. pendular regions in a tetrahedral cell in a packing). Theoretically this happens at an infinite capillary pressure or when h =∞. It can be assumed that the continuous moisture phase breaks up just after thc air-water interface merges with the cell walls.

If the air space in a partially saturated tetrahedral cell in a packing is assumed to be approximately spherical, the air space in the cell when the air/water interface just merges with the surfaces of the spheres surrounding the tetrahedral cell can be assumed to take the form of the insphere of the tetrahedral cell. (i. e. the largest sphere which can be fitted in the tetrahedral cell).

However, equation (5. 11) implies that when p =∞ the saturation X = O.

Therefore, in order to have a definition of pore volume which is consistent with equation (5. 11), the pore volume of a tetrahedral cell can be defined as the corresponding tetrahedral insphere volume. A similar definition for the pore size has been given by some authors (43) who have defined pore size as being the diameter of the largest sphere which can be fitted into the space surrounded by a group of spheres in a packing.

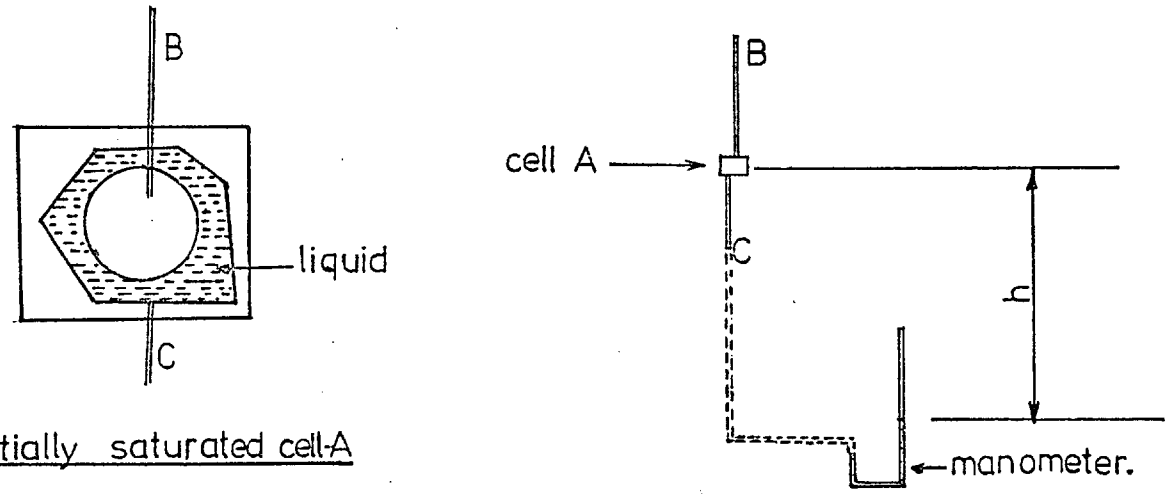


FIGURE 5.3

Cell A connected with tubes B and C

Each pore in a porous body can be connected to its surrounding pores through one or more openings. When a pore has only a single opening, then it is called a blind pore or a dead pore. For non-consolidated porous media, the dead pore volume can be regarded to be negligible (59). The dead pore volume of packed beds of spherical particles can be assumed to be negligible because each tetrahedral subunit in such packings has four openings.

Interconnections

When the pore volume and the volume of pendular bridges have been subtracted from the total void space in a packing, the remaining volume can be regarded as the volume of the void space which interconnect the pores of the packing. Two tetrahedral cells in a packing are usually interconnected by a tetrahedral face common to both tetrahedra. Therefore, it can be assumed that the filling of interconnections is governed by the sizes of the faces of the tetrahedral cells. The size of a face has been defined as the diameter of the circle inscribed in the tetrahedral face (149).

It is suggested that the equilibrium moisture distribution in a porous body under a specified set of conditions is definite and non-random. The non-randomness is a result of the deterministic behaviour of the physical phenomenon occuring in the porous body and of the specific pore geometry associated with a given porous body. A packed bed, once formed, has its own pore geometry. However, if the particles are repacked, the new bed will have its own pore geometry, which could be different from that of the previous bed, although it could be assumed that in each repacking the pore properties vary about mean values.

5. 1. 2. 3 The equivalent radius and the critical radius

The pore channels in a porous body are generally irregular in shape and a mathematical analysis of capillary effects in such irregular channels becomes cumbersome. It has been a common practice to approximate the sizes of these channels by equivalent radii which can easily be used to calculate the capillary effects of moisture in such channels. The size of a tetrahedral face in a tetrahedral cell has usually been denoted by the face insphere radius, which is the radius of the sphere which just passes through the face and touch the three spheres at the corners of the triangular face. Similarly the size of a pore

in a packed bed has been denoted by the radius of the sphere which can just be fitted into a tetrahedral cell of a packing so that the sphere touches all the four spheres situated at the corners of the tetrahedron.

It has been common to assume that the curvature of a meniscus passing through a face of a tetrahedral cell is equal to the curvature of the face insphere (149). The meniscus curvature of a liquid when it enters a pore has been assumed to be the curvature of the tetrahedron insphere.

The face insphere radius and the tetrahedron insphere radius will be referred to as the equivalent radius of the face and equivalent radius of the pore respectively in the following sections.

Suppose a pore or an interconnection of equivalent radius r_e is in contact with moisture at a height h above a free surface, then a meniscus can travel through the pore or through the interconnection thus filling up the pore or the interconnection, if

$$\frac{2\sigma \operatorname{Cos}\Theta}{r_e} \geqslant h \qquad (5.13)$$

where σ is the surface tension and Θ is the contact angle of the wetting liquid. The inequality (5.13) can be re-arranged as

$$\frac{2\sigma \operatorname{Cos}\Theta}{h} \geqslant r_e \qquad (5.14)$$

The term $2\sigma\operatorname{Cos}\Theta/h$ can therefore be regarded as representing a critical value of the equivalent radius for a given height. All pores and interconnections which are in contact with moisture at a height h and the sizes of which are smaller than the critical radius can be assumed to undergo filling.

For water the contact angle Θ, can be assumed to be 0^{o}, so that the critical radius at a height h simplifies to $2\sigma/h$.

5.2 Description of the model and the prediction of the Imbibition curve.

5.2.1 Basic equation for the determination of a capillary pressure curve of a porous body.

The average moisture saturation ($\overline{X}$), in a given section of a porous body can be expressed as

$$\overline{X} = (V_{pw} + V_{cw} + V_{iw} + V_{tw}) / (V_p + V_c + V_i) \ldots . (5.15)$$

where V represents the volume with the subscripts p, c, i, t and w representing pores, corners, interconnections, trapped and water respectively.

If the porous body, the condition of which is represented by equation (5.15), is drained under gravity, part of the moisture which initially belonged to the continuous phase can become trapped as a result of the breaking up of the continuous phase. Let the volume of moisture trapped in this way be denoted by ΔV_{tw}.

Then the irreducible saturation $\overline{X}_i$ can be expressed as

$$\overline{X}_i = (V_{cw} + V_{tw} + \Delta V_{tw}) / (V_p + V_c + V_i) \ldots . (5.16)$$

Equations (5.15) and (5.16) can be combined together to yield

$$\frac{\overline{X} - \overline{X}_i}{1 - \overline{X}_i} = \left(\frac{V_{pw}/V_p + V_{iw}/V_p - \Delta V_{tw}/V_p}{1 + V_{i}/V_p - (V_{tw} + \Delta V_{tw})/V_p} \right) \ldots (5.17)$$

It has been shown by Morrow and Harris (159) that the trapped moisture content is less than about 2 per cent of the void space and hence the term $(V_{tw} + \Delta V_{tw})/V_p$ has been found to be less than 0.03 for the pore size model described in chapter 4. Thus, the two terms $\Delta V_{tw}/V_p$ and $(V_{tw} + \Delta V_{tw})/V_p$ can be neglected, compared with $(V_{pw}/V_p + V_{iw}/V_p)$ and 1 respectively.

Therefore eq. (5. 17) can be modified as follows:

$$\frac{\bar{X} - \bar{X}_i}{1 - \bar{X}_i} = \frac{V_{pw/V_p} + V_{iw/V_p}}{1 + V_{i/V_p}} \quad \ldots\ldots\ldots\ldots \quad (5.18)$$

Or

$$\frac{\bar{X} - \bar{X}_i}{1 - \bar{X}_i} = \frac{V_{pw/V_p} + V_{iw/V_i} \cdot V_{i/V_p}}{1 + V_{i/V_p}} \quad \ldots\ldots\ldots \quad (5.19)$$

The term V_{i/V_p} is the ratio of the volume of interconnections to the volume of the pores of the porous body. For a given liquid, the term V_{i/V_p} can be regarded as a constant for the porous body. The term V_{i/V_p} will be denoted by δ .

Hence, equation (5. 19) can be written in the form

$$\frac{\bar{X} - \bar{X}_i}{1 - \bar{X}_i} = \frac{V_{pw/V_p} + \delta V_{iw/V_i}}{1 + \delta} \quad \ldots\ldots\ldots\ldots \quad (5.20)$$

Equation (5. 20) can be regarded as the basic equation which determines the capillary pressure curves of a porous body. The term V_{pw}/V_p is the ratio of total volume of moisture in the pores to the total pore volume and the term V_{iw}/V_i is the total volume of moisture in the interconnections divided by the total volume of the interconnections in the section of the porous body under consideration.

In general, the terms V_{pw}/V_p and V_{iw}/V_i are functions of capillary pressure and depend on the distribution of the moisture in the pores and interconnections within the porous body.

Therefore it is seen that in order to evaluate the terms V_{pw}/V_p and V_{iw}/V_i for a given capillary pressure the distribution of moisture in the pores and interconnections has to be studied.

5. 2. 2 Description of the model

5. 2. 2. 1 Packed bed

The void space of a porous body can be divided into pores, corners and interconnections. The corners of the void space of a packing is usually occupied by pendular moisture.

The model of a packed bed which is used for the prediction of rise curves assumes the pores of the packed bed to be interconnected and to be arranged in layers within the packing. The distance between each layer is assumed to be a constant for a given packing and is assumed to be the average height of the tetrahedra in the packing. A similar model has been described by Mason (150) in his studies of desaturation of porous media. However, interconnectivity between the pores in a given layer has not been considered by Mason (150).

The sizes of pores and interconnections are assumed to be distributed randomly so that depending on the pore size distribution, a given pore is allowed to be a neighbour of any other pore and depending on the interconnection size distribution to be interconnected by any of the interconnections. Mason (150) has discussed the limitations of the above assumptions and has suggested that the error involved in approximating a packed bed to the model described above can be negligible.

5. 2. 2. 2 Model of the mechanism of Imbibition

When a dry porous body is dipped in a pool of a wetting liquid, moisture starts moving along the pores and interconnections of the porous body.

If a pore in a porous body is saturated with moisture during imbibition, it is most likely that it transfers moisture to some of its neighbouring pores. However, if a pore in a porous body is prevented from filling with imbibed moisture, then this pore can prevent moisture reaching some of its neighbouring pores by breaking the moisture path to these pores. This suggests that saturated and empty pores can occur as separate clusters in a porous body. Clustering of saturated pores and empty pores in a porous body can lead to wet regions and dry regions in a packing.

The existence of wet and dry regions in packed beds under imbibition was observed in the imbibition experiments described in later sections of this chapter. Wet patches of ballotini were distinctly observed in these experiments when the rise columns were dismantled; specially in the regions of low moisture content.

However, the possibility of the existence of unfilled pores and unfilled interconnections in a wet region cannot be excluded.

5.2.2.3 Calculation of V_{pw}/V_p and V_{iw}/V_i in Equation (5.20)

Let a horizontal plane be drawn between two layers of pores in order to intersect the interconnections joining the two layers. Let h be the height of the plane above the free liquid surface and let ψ_h be the fraction of interconnections intersected by the plane in wet regions out of the total number of interconnections intersected by the plane. Therefore, fraction ψ_h of the pores which belong to the layer just above the plane can be assumed to be accesible by moisture from the interconnections below.

All interconnections and pores of equivalent radii (approx.) $2\sigma/h$ and less can be assumed to be filled in a wet region.

Let u(r) and v(R) be the functions relating the volume of any pore and of any interconnection to their radii r and R, respectively.

Hence, the volume of moisture V_{pw} in the completely saturated pores in a layer at a height h can be written as

$$V_{pw} = \psi_h \cdot \int_0^{2\sigma/h} g(R)\, v(R)\, dR \quad \ldots\ldots\ldots\ldots\ldots\ldots \quad (5.21)$$

Similarly, the volume of moisture V_{iw} in completely saturated interconnections at a height h can be expressed as:

$$V_{iw} = \psi_h \cdot \int_0^{2\sigma/h} f(r)\, u(r) dr \quad \ldots\ldots\ldots\ldots\ldots\ldots\ldots\ldots \quad (5.22)$$

(For definitions of $f(r)$ and $g(R)$ see Sect. 5.2.2.4)

The total volume of pores (V_p) and interconnections (V_i) in the section can be written as:

$$V_p = \int_0^{\infty} g(R)\ v(R)dR \quad \ldots\ldots\ldots\ldots\ldots\ldots \quad (5.23)$$

and $$V_i = \int_0^{\infty} f(r)\ u(r)\ dr \quad \ldots\ldots\ldots\ldots\ldots\ldots \quad (5.24)$$

Hence $$V_{pw}/V_p = \psi_h \left[\int_0^{2\sigma/h} g(h)\ v(R)dR \ / \ \int_0^{\infty} g(R)\ v(R)\ dR \right] \ldots (5.25)$$

and $$V_{iw}/V_i = \psi_h \left[\int_0^{2\sigma/h} f(r)\ u(r)\ dr \ / \ \int_0^{\infty} f(r)\ u(r)\ dr \right] \ldots (5.26)$$

By the definition of a pore

$$v(R) = \frac{4}{3}\Pi R^3 \quad \ldots\ldots\ldots\ldots\ldots\ldots\ldots\ldots \quad (5.27)$$

If a relationship of u(r) with r is assumed, then:

$$u(r) = a\, r^2 \quad \ldots\ldots\ldots\ldots\ldots\ldots\ldots\ldots\ldots\ldots \quad (5.28)$$

where a is a constant. Equation (5.28) assumes the behaviour of the volume of interconnections with respect to their equivalent radii to be similar to that of circular cylinders. The equations (5.25) and (5.26) can thus be modified to the form:

$$V_{pw}/V_p = \psi_h \left\{ \int_0^{2\sigma/h} g(R)R^3 dR \ / \ \int_0^{\infty} g(R)R^3 dR \right\} \ldots\ldots\ldots (5.29)$$

and $$V_{iw}/V_i = \psi_h \left\{ \int_0^{2\sigma/h} f(r)r^2 dr \ / \ \int_0^{\infty} f(r)r^2 dr \right\} \ldots\ldots\ldots (5.30)$$

Equation (5.20) can thus be modified as

$$\frac{\overline{X} - \overline{X}_i}{1 - \overline{X}_i} = \frac{\psi_h}{1+\delta} \left[\frac{\int_0^{2\sigma/h} g(R)R^3 dR}{\int_0^{\infty} g(R)R^3 dR} + \frac{\int_0^{2\sigma/h} f(r)r^2 dr}{\int_0^{\infty} f(r)r^2 dr} \right] \ldots (5.31)$$

where $\overline{X}$ is the fractional saturation and $\overline{X}_i$ is the fractional irreducible saturation averaged over a given cross-section. Equation (5.31) is applicable as long as there are wet regions in the packed bed. ie. equation (5.31) is true if $\psi_h > O$. However, moisture cannot reach the pores, which are situated above the height at which $\psi_h = O$. Therefore,

if $\psi_h = O$ at $h = h'$

then $\overline{X} = O$ for $h > h'$ ..... (5.32)

5.2.2.4 Calculation of ψ_h

Let f(r) be the distribution function of equivalent radii (r) of interconnections and g(R) be the distribution function of equivalent radii (R) of pores in a given packing.

Let I_h and J_h be defined as follows.

$$I_h = \int_0^{2\sigma/h} f(r)dr \quad \text{..... (5.33)}$$

$$\text{and } J_h = \int_0^{2\sigma/h} g(R)dR \quad \text{..... (5.34)}$$

Where h is the height of a given layer of pores and interconnections in a packing above a free liquid surface and σ is the surface tension of liquid.

If f(r) and g(R) are normalised distributions, then I_h and J_h represent the number of interconnections and pores which would undergo filling due to capillary action as a fraction of the total number of interconnections and pores existing in a wet region of a packing at a height h above a free liquid surface.

Consider a layer of pores situated at a height h above the free liquid surface and let Ψ_h be the fraction of the above pores which belong to wet regions. Therefore, Ψ_h fraction of interconnections which join the pores

of the present layer to the pores that exist in the layer just above the present layer, can be regarded as being accesible to moisture.

Let Δh be the average thickness of a layer of pores. Then, out of the above interconnections, only those of which the equivalent radii are less than $2\sigma / (h + \Delta h)$ can be regarded being capable of transfering moisture to the upper layer of pores at a height $h + \Delta h$ above the free liquid surface. Thus only $\Psi_h I_{h + \Delta h}$ fraction of interconnections are active in transferring moisture to the upper layer of pores at height $h + \Delta h$. Interconnecting windows of a tetrahedral pore always neighbour the pendular regions or corners of the pore. Therefore, once an opening of a tetrahedrai pore is filled it can be assumed that its corners or pendular regions would have undergone filling. Therefore, it can be assumed that once moisture reaches a pore through one of its interconnections, the incoming moisture will occupy the corners which surround the pore irrespective of whether the size of the pore permits filling up of the pore or not. Hence, the fraction of pores which would be filled or would be surrounded by moisture in the upper layer can be expresses as: $\Psi_h I_{h + \Delta h}$.

However, the fraction of $\Psi_h I_{h + \Delta h}$ pores which are in contact with moisture can transfer moisture to the empty pores in the same layer or to the corners or pendular regions which surround the empty pores, if the sizes of the interconnections which connect these pores permit the transfer.

If a fraction of $\Psi_h I_{h + \Delta h}$ pores are in contact with moisture in a given layer, then a fraction of $(1.0 - \Psi_h I_{h + \Delta h})$ pores in the same layer will be free from moisture and will be empty. Therefore, the probability of an empty pore being a neighbour to a pore which is in contact with moisture can be expressed as $\Psi_h I_{h+\Delta h} \cdot (1.0 - \Psi_h I_{h + \Delta h})$.

Hence, the probability of moisture being transferred from pores already in contact with moisture to the empty pores in the same layer can be expressed as:

$$\Psi_h I_{h + \Delta h} \cdot (1.0 - \Psi_h I_{h + \Delta h}) \cdot I_{h + \Delta h}$$

Therefore, the total fraction of pores in the upper layer (at a height $h + \Delta h$ above the free liquid surface) which would be in contact with moisture can be expressed as:

$$\psi_h I_{h+\Delta h} + \psi_h I_{h+\Delta h} (1.0 - \psi_h I_{h+\Delta h}) I_{h+\Delta h}$$

From the definition of ψ, the above quantity is equal to $\psi_{h+\Delta h}$.

Hence $$\psi_{h+\Delta h} = \psi_h I_{h+\Delta h} \left[1.0 + (1.0 - \psi_h I_{h+\Delta h}) I_{h+\Delta h} \right] \quad \ldots\ldots\ldots\ldots (5.35)$$

Equation (5.35) enables values of ψ to be calculated for different layers of the model from a knowledge of a single value of ψ at a known height and from a knowledge of the distributions g(R) and f(r).

5.2.2.5 Calculation of the Imbibition curve

For a porous body in which one of the faces just dips into a pool of a liquid, ψ_o can be regarded as unity. Therefore the values of ψ for heights Δh, $2\Delta h$, $3\Delta h$, ... etc., can be calculated by the repeated application of equation (5.35).

Each of these values of ψ can be used in equation (5.31) in order to calculate the quantity $(\overline{X} - \overline{X}_i)/(1 - \overline{X}_i)$ for each of the chosen heights. Thus the variation of moisture content with height, can be obtained so giving the imbibition curve.

In all the above equations, a prior knowledge of the distributions g(R) and f(r) is required. A knowledge of the quantity Δh, which can be assumed to be the average tetrahedron height of the packing is also required in order to predict the imbibition curve.

5.3 Experimental

5.3.1 Preliminary

Several sets of experiments have been carried out in order to obtain the rise and drain curves of packed beds of ballotini. Ballotini of grades 6, 7, 8, 9, 10 and 11 were used in these experiments. The reproducibility of the capillary pressure curves has been checked by repeating the experiments for random samples.

It was observed that the commercial ballotini used was contaminated by an impurity which was sparingly soluble in cold water, a cold dilute solution of the impurity indicated an electrical conductivity (Approx. 30×10^{-3} $Ohm^{-1}cm^{-1}$) considerably different from that of pure deionised distilled water. When the ballotini was washed with hot deionised distilled water and the solution evaporated to dryness a residue was obtained indicating the existence of an impurity. It was observed that the impurity could be removed by washing ballotini with dilute hydrochloric acid and then several times by deionised distilled water. At the end of the final washing, the solution gave an electrical conductivity nearly equal to that of deionised distilled water.

A quantity of ballotini which would fill a column of 10 cm. diameter upto a pre-determined height was first soaked in dilute hydrochloric acid and left for a few days. The ballotini was washed by placing the ballotini in a large flask and by adding an approximately equal volume of deionised distilled water and then shaking thoroughly for about 3-4 minutes. The efficiency of washing was increased by draining the wet ballotini through a sintered glass filter. The solution obtained after the fifth washing had an electrical conductivity approximately equal to that of deionised distilled water. The conductivity was measured using a 'Sproule Electrolytic conductivity cell - Model EDB/01/A' of cell constant 0.1, together with a 'Philips PR9501' conductivity meter. The latter measured conductivities in twelve different ranges from 0 to 300 $Ohm^{-1}cm^{-1}$ and in steps of 0.05×10^{-6} $Ohm^{-1}cm^{-1}$ in the range 0 to 3×10^{-6} $Ohm^{-1}cm^{-1}$. The conductivity of the deionised distilled water used in the experiments varied from 15×10^{-6} upto 20×10^{-6} $Ohm^{-1}cm^{-1}$.

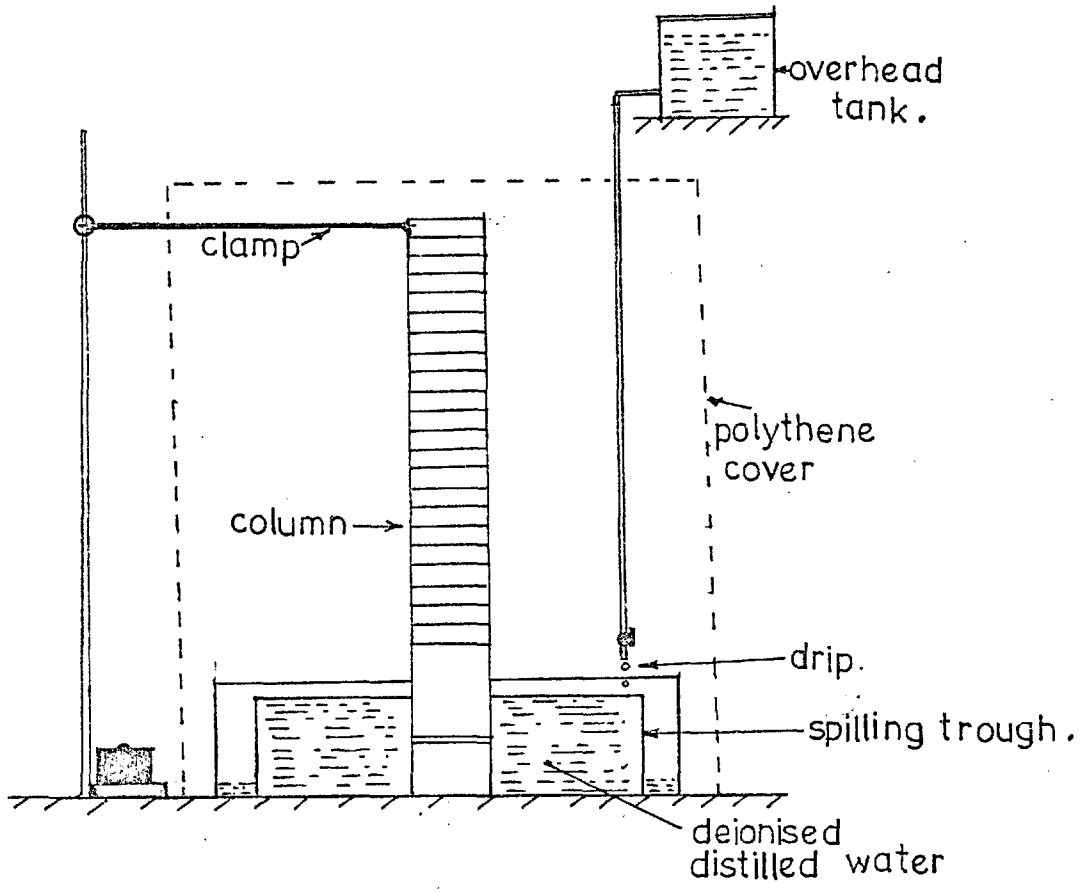
The wet ballotini in the final washing was mixed with more deionised distilled water and slowly poured into a column of 10cm. diameter. (see Fig. 5.4). The column was made of 10 cm. internal diameter and approximately 1 cm. thick perspex rings with a thin rubber lining of about 0.1 cm. thick at one of its edges. The rubber lining served as a seal to prevent water leaking through the gaps between the rings. The ballotini was supported by means of a clean wire gauze attached to a perspex ring, which was situated below the free liquid surface in the trough, and above the bottom of the trough.

5.3.2 Determination of the Drain Curve

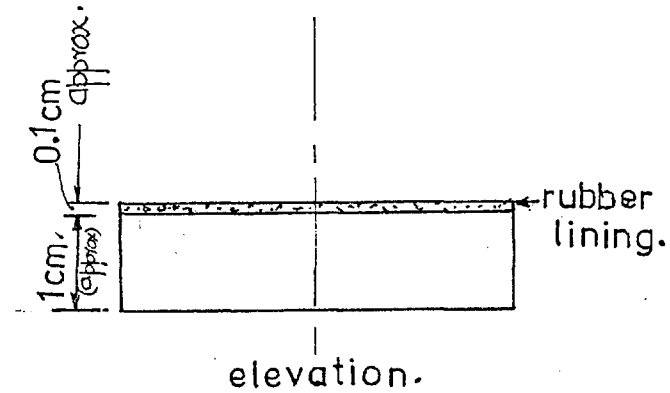
The column was erected vertically on a brim-full trough of de-ionised distilled water. The level of water in the trough was maintained constant throughout the experiment by allowing de-ionised distilled water to drip at a slow rate into the trough from an overhead tank, so that water was always spilling from the trough at a very slow rate. A plumb line and a cathedoscope was used to check whether the column was vertical. Once the column was packed, the whole column was rewetted by a gentle stream of deionised distilled water for about 10-15 minutes. Precautions were taken not to disturb the packing and disturb its internal structure while rewetting. The whole column and the trough were then covered with polythene paper, to prevent dust and to minimise unnecessary evaporation. The column was kept in a constant temperature room in which the temperature varied by upto a maximum of $\pm 2^{o}C$ during the experiments.

When two perspex rings were placed one on top of the other, a line of separation between the two rings was clearly observed. Similar lines were observed between perspex rings in the experimental column. The heights of these lines above the free liquid surface were measured using a cathedoscope with an accuracy of 0.001 cm. These measurements were later used to calculate the average height of each perspex ring in the column.

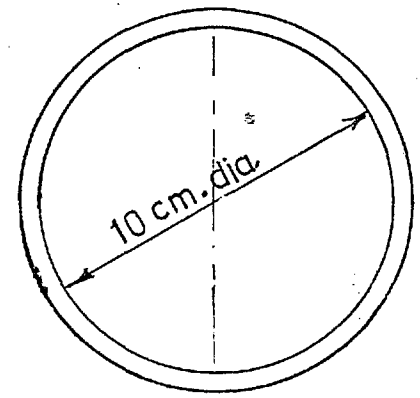
The columns were allowed to stand for a few days for moisture in the columns to attain equilibrium. The contents in each ring were then carefully taken into a previously weighed petri dish by slowly shearing each ring off the column



COLUMN



elevation.



plan

PERSPEX RING

FIGURE 5.4 Details of experimental column.

starting with the top ring of the column.

The petri dishes with the wet ballotini were then weighed. These were then dried at a temperature of approximately 110^{o}C for about 10 to 15 hours until no further reduction in weight of each petri dish was observed. The petri dishes with the dry ballotini were weighed.

At the end of the above experiment, a pure dry quantity of ballotini was obtained.

5.3.3 Determination of the Imbibition Curve

A column was filled with pure dry ballotini upto a pre-determined height in an empty trough using perspex rings as described in the last experiment. De-ionised distilled water was slowly let into the trough until the trough just start to overflow. The supply of distilled water was then restricted and the column was allowed to remain undisturbed for a few days in order that equilibrium conditions would be obtained. The de-ionised distilled water in the trough was kept at the spilling level throughout the experiment by allowing de-ionised distilled water to drip at a slow rate on to the pool. The average heights of each ring and the moisture contents in the ballotini were measured in exactly the same way as described in the previous section.

In each of the above cases, the number of days required for equilibrium was determined by repeating the experiment but varying the time between the start of the experiment and the dismantling of the column. Any number of days equal to or more than the minimum number of days required for consistent moisture distributions for packings of a given grade of ballotini, was regarded as a satisfactory period for moisture to reach its equilibrium distribution.

A mean void fraction of 0.4044 $\pm$ 0.0037 was observed in the above experiments. The particle size distribution of each grade of ballotini was obtained by measuring the diameters of about 50 particles of each grade of ballotini under a microscope.

5.4 A Computer program to calculate the imbibition curve

A computer program was developed to predict the capillary pressure curve for a packed bed of particles of known diameter. The calculations started from the free surface level at which the whole cross section of the bed was in contact with the wetting liquid. At this section $\psi_o = 1.0$. The average distributions of face radii and tetrahedron insphere radii which were predicted as described in chapter 4 for a packing of mean void fraction 0.4045 were used in the calculations. These distributions are given in Appendix 6.

Equations (5.31) and (5.35) were employed to predict the quantity $(\overline{X} - \overline{X}_i)/(1 - \overline{X}_i)$ for different layers Δh apart, thus giving the capillary imbibition curve for the packed bed.

Commercial ballotini was observed to be composed of particles of a distribution of sizes (see Appendix 3). However, the particle size distributions were such that each grade of ballotini could be regarded as consisting of approximately equal size particles (Section 7.2.2). Therefore it can be expected that a packed bed of a given grade of ballotini can be represented by a uniform sphere packing. (Section 7.3.2). The computer program was therefore developed to calculate the theoretical imbibition curve based on previously predicted (Chapter 4) pore size distributions of uniform sphere packings in order to obtain the minimum root mean square deviation of the quantity $(\overline{X} - \overline{X}_i)/(1 - \overline{X}_i)$ from a given set of imbibition data. The only variable parameter in the above calculations was the particle diameter of the packing. The particle diameter at the minimum root mean square deviation of the quantity $(\overline{X} - \overline{X}_i)/(1 - \overline{X}_i)$ can be regarded as the average capillary particle diameter which represents the packed bed of ballotini for imbibition of moisture. The average capillary particle diameter was seen (Table 5.1) to be slightly less than the volume mean particle diameter for each grade of ballotini as expected (Section 7.3.2). A flow diagram of the computer program is shown in figure 5.5.

NAME-LIST

DH — Δh
SO — ψ_o
H — h

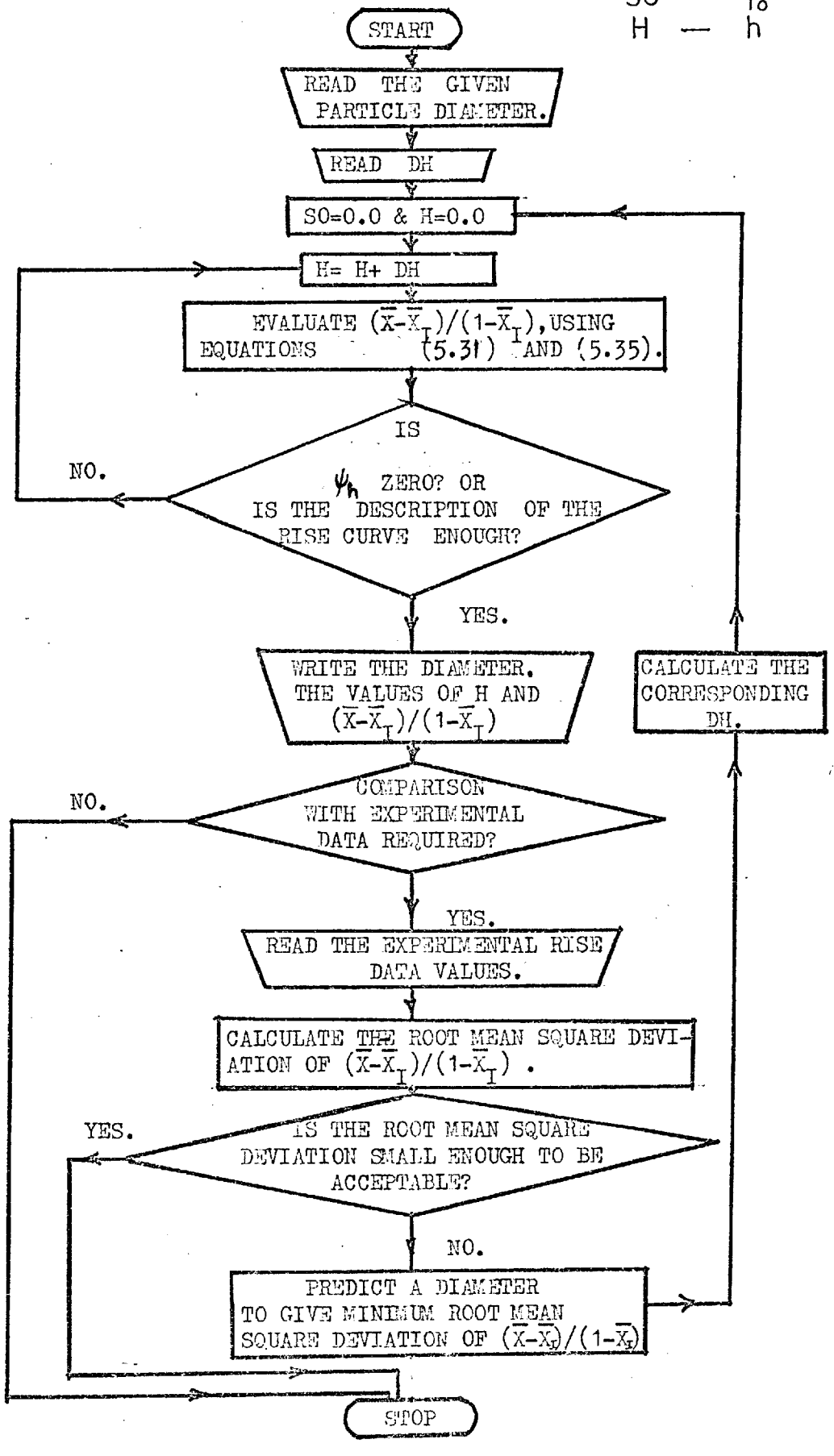


FIGURE 5.5
FLOW DIAGRAM OF THE COMPUTER PROGRAM FOR THE PREDICTION OF RISE CURVE.

5.5. Results and Discussion

The experimental data for rise curves obtained for different grades of ballotini are given in appendix 1. Table 5.1 gives the mean particle diameter, the volume mean diameter, the average diameter calculated from the computer program for the minimum variance between the experimental observations and the theory, and the root mean square deviation of $(\overline{X} - \overline{X}_i)/(1 - \overline{X}_i)$ between experiments and the corresponding theoretical imbibition values for each grade of ballotini.

Table 5.1

Particle mean diameter, volume mean particle diameter, average capillary particle diameter and the root mean square deviation of $(\overline{X} - \overline{X}_i)/(1 - \overline{X}_i)$ between theory and the experimental points for six grades of ballotini.

GRADE OF BALLOTINI	PARTICLE-MEAN DIAMETER (cm.)	VOLUME-MEAN PARTICLE DIAMETER (cm.)	CALCULATED AVERAGE CAPILLARY PARTICLE DIAMETER (cm.)	ROOT MEAN SQUARE DEVIATION IN $(\overline{X} - \overline{X}_i)/(1 - \overline{X}_i)$
6	0.07466	0.07486	0.06813	0.043
7	0.06490	0.06530	0.06383	0.022
8	0.05972	0.05990	0.05966	0.040
9	0.04154	0.04173	0.03604	0.037
10	0.02785	0.02854	0.02577	0.039
11	0.02240	0.02282	0.02154	0.048

The mean particle diameter for a given grade of ballotini was obtained by choosing a random sample of ballotini and then measuring diameters of about 50 particles under a microscope. (See Appendix 3). Fig. 5.6 (a) - (f) compares the computed imbibition curve with the experimental points for the six grades of ballotini.

The average capillary diameter calculated for each grade of ballotini was found to be less than the volume mean particle diameter for each grade. (See Section 7.3.2). This is to be expected, as it will be shown in Section 7.3.2 that the equivalent particle diameter of a packing consisting of spheres of approximately

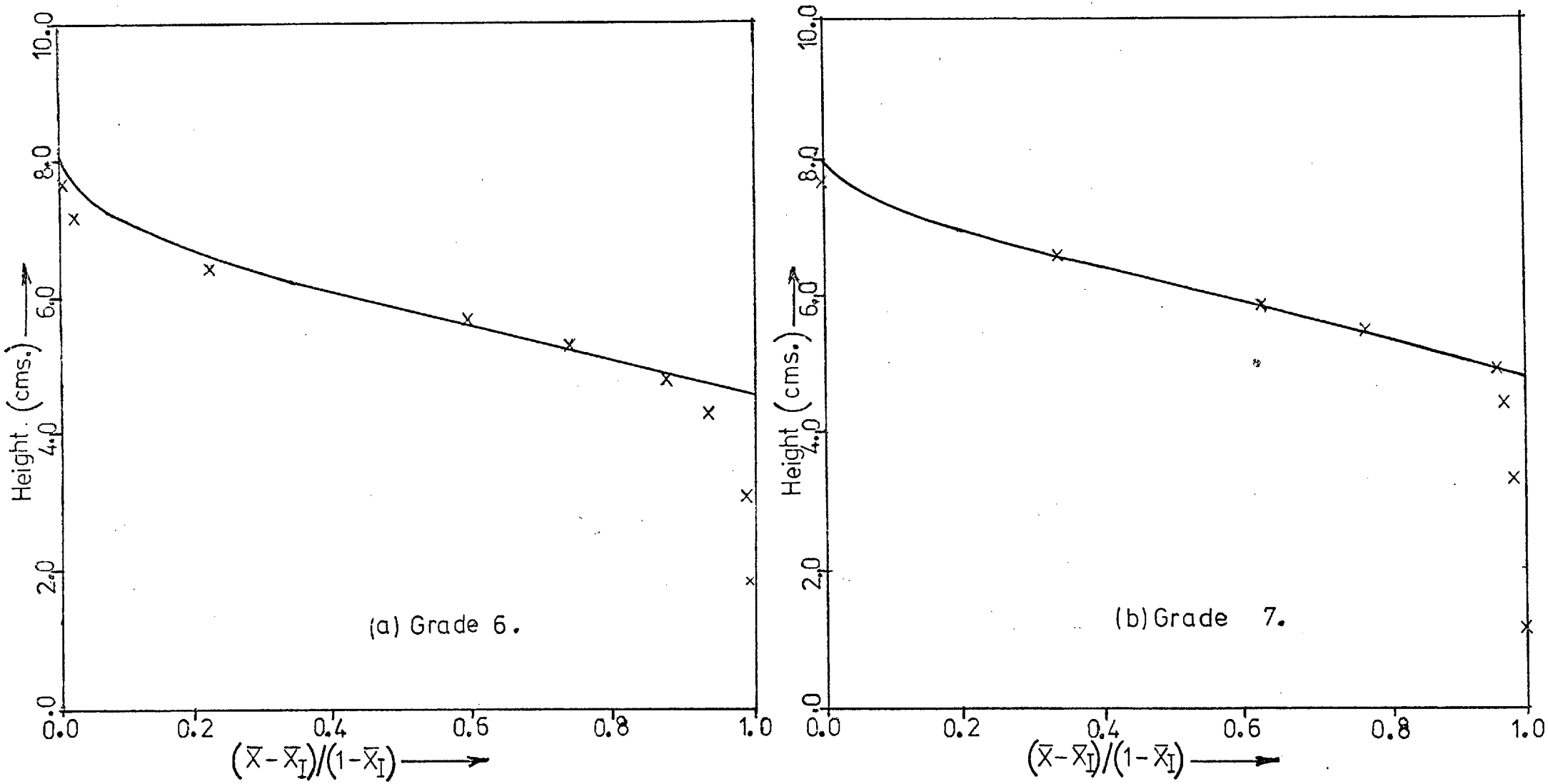


FIGURE 5.6

Comparison of experimental rise values with theoretical curve.
(× – experimental points, —— – theoretical curve.)

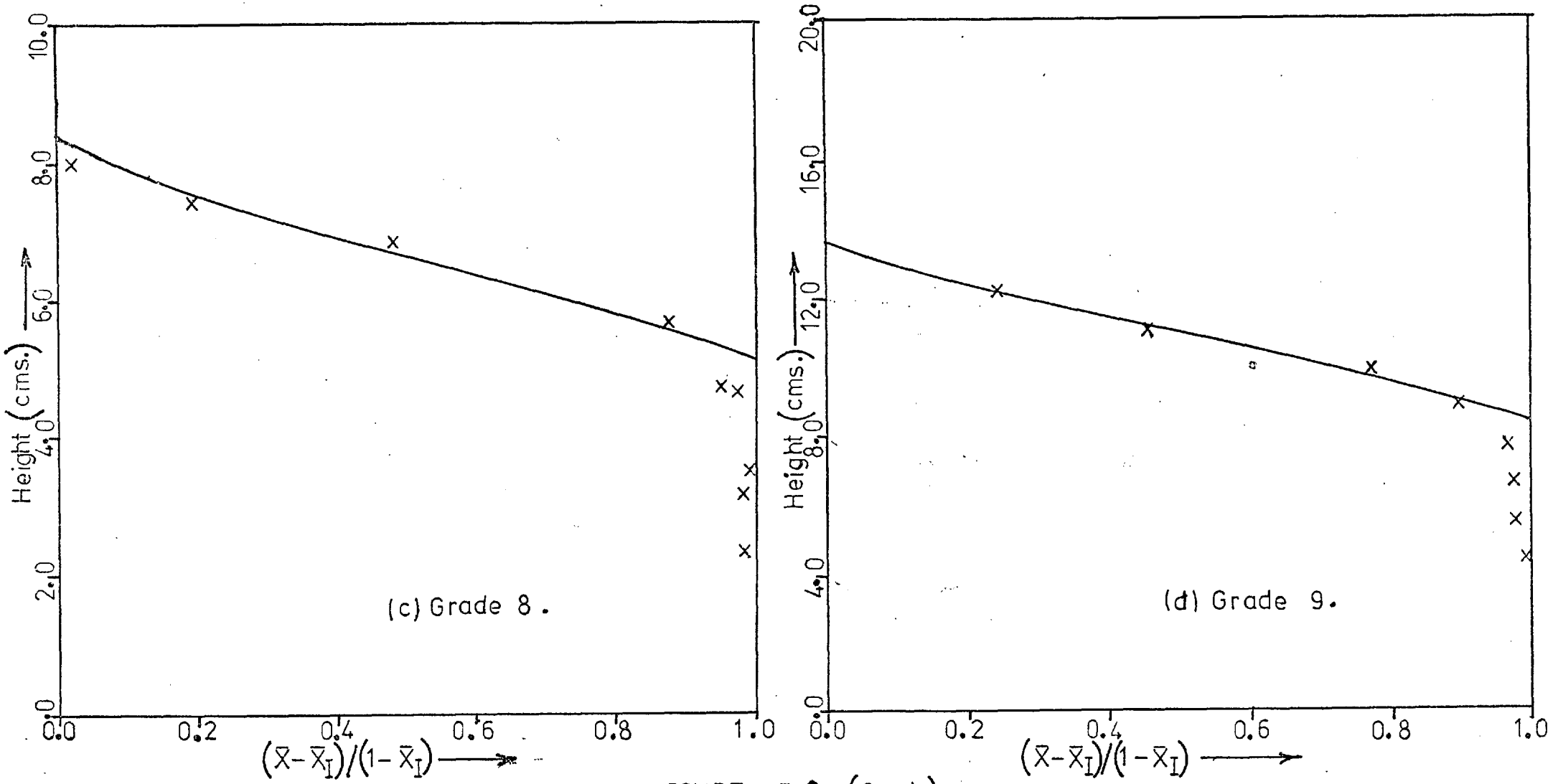


FIGURE 5.6 (Cont.)

Comparison of experimental rise values with theoretical curve.
(x experimental points, —— theoretical curve.)

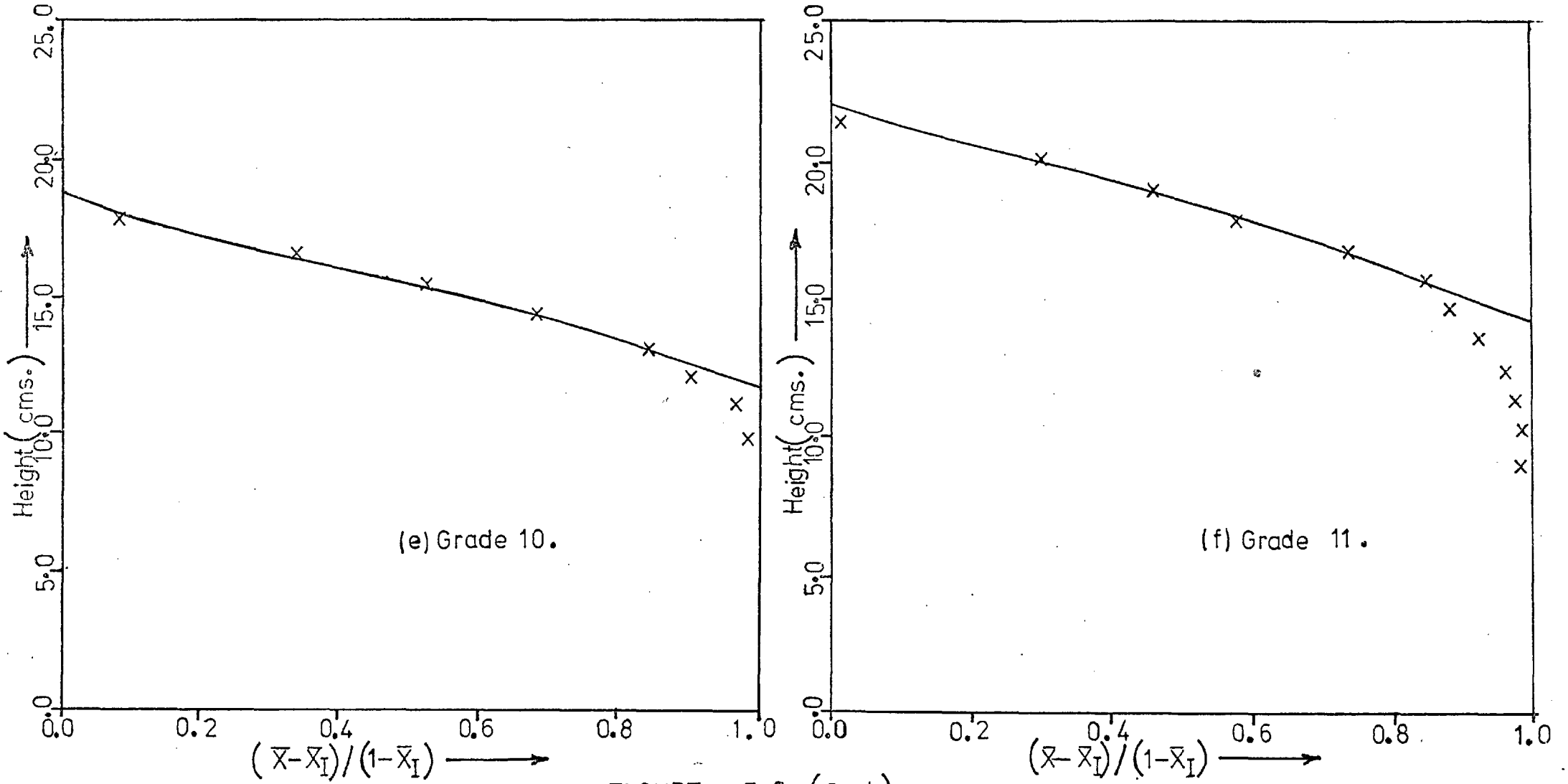


FIGURE 5.6 (Cont.)

Comparison of experimental rise values with theoretical curve.
(x experimental points, — theoretical curve.)

equal size can be expected to be less than the volume mean diameter of the particles of the packing. The six grades of ballotini used in the experiments can be regarded as consisting of approximately equal size spheres. (see Section 7. 2. 2).

The predicted theoretical curve was found to be satisfactory for beds of all the six grades of ballotini. The largest root mean square deviation of $(\overline{X} - \overline{X}_i)/(1 - \overline{X}_i)$ between the experimental values and the theoretical values was found to be 0. 048 for a bed of grade 11 ballotini.

The deviation of the theoretical curve from the corresponding experimental curve was found to be prominent for values of $(\overline{X} - \overline{X}_i)/(1 - \overline{X}_i)$ near unity, for all six grades of ballotini. The experimental entry capillary pressure (ie., the capillary pressure above which the moisture saturation starts to depart from unity) was found to be always less than the theoretically predicted entry capillary pressure. This showed that some of the pore sizes and window sizes that existed in the packing were larger than the sizes assumed in the packings.

The computer program which has been developed to predict the pore size distributions (Chapter 4)considered tetrahedron edge lengths only upto a value of $\sqrt{3}$ times a particle diameter in its calculations. This limitation of the edge length value made it possible to make the computer calculations (Chapter 4) efficient without significantly affecting the calculated value of the overall void fraction.

Further, particles of larger size than the average particle diameter (d_{av}) calculated from the computer program which predicted the imbibition curve were seen to be present in all the six grades of ballotini.

The above two effects might have caused the existence of a few larger pores and a few larger windows than those used in the calculated pore size and window size distributions.

The difference between the theoretical curve and the experimental points near moisture contents of unity might also have been a result of the above.

Apart from the above differences, the overall description of the experimental imbibition values by the predicted curve was seen to be good.

CHAPTER 6

The Moisture Distribution Under Drain Conditions : The Drain Curve.

6.1 The Movement and Di stribution of Moisture under drain:

The structure of packed beds and the types of void spaces in them have already been discussed in chapters 4 and 5. The mechanism of drainage is different from that of imbibition mainly in that the invading fluid is nonwetting with respect to the displaced fluid. However, it can not be suggested that the mechanism of drainage is the reverse process of imbibition with the invading and displaced fluids interchanged. An investigation of the nature of the two phenomena suggest that drainage of a wetting liquid cannot be considered as the reverse process of imbibition.

Under normal conditions of drainage, the invading fluid is abundant and the porous medium is wholly immersed in the invading fluid unlike in the case of imbibition. Because of this, it is likely that the nonwetting fluid can diffuse rapidly into the porous medium through the sides of the porous body. The nonwetting phase can be prevented from entering a certain location in the porous medium if the geometry of the openings surrounding that location prevent draining of the wetting liquid from that location.

When a completely saturated porous body is allowed to drain under gravity with one of its faces dipping in a pool of a wetting liquid, moisture starts moving in some regions as a result of an imbalance between gravitational and the capillary potential of moisture in these regions. This is accompanied by movement of menisci into the porous body through openings at the top face of the porous body. If openings in the sides of the porous body permit entry of the non-wetting fluid, then movement of menisci into the porous body can occur through these openings as well. The movement of the non-wetting phase and the wetting phases continues until a complete balance between the capillary and gravitational forces is established in all regions of the porous body.

6.2 A model for drainage : Prediction of Drain Curve.

In the following discussion it is assumed that drainage of moisture takes place as outlined in the previous section. A model will be constructed which will lead to the prediction of the drain curve for a given packing based on a probability study of moisture retention in the pores of a packing.

Let n pores of a certain region of a porous body be completely saturated out of a total of N pores.

Then, the probability for two completely saturated pores to be situated adjacent to each other is given by $n(n-1)/N^2$. If both n and N are large, the limit of the probability (P) can be given by

$$P = \lim_{\substack{n \to \infty \\ N \to \infty}} \left\{ \frac{n(n-1)}{N^2} \right\} \tag{6.1}$$

$$\text{i.e} \quad P = \frac{n^2}{N^2} \tag{6.2}$$

But $\frac{n}{N}$ is the number of pores completely saturated as a fraction of the total number of pores present in a given region of a porous body. Let the fraction n/N be denoted by x_f. Hence

$$P = x_f^2 \tag{6.3}$$

Using the same notation as in chapter 5,

$$I_h = \int_0^{2\sigma/h} f(r)\, dr \tag{6.4}$$

Where I_h represents the fraction of completely saturated interconnections at a height h above the free liquid surface level in which the moisture can refrain from draining and f(r) is the equivalent radii (r) distribution of the interconnections.

Let the quantities η and P* be defined as $\frac{r}{d}$ and $\frac{hd}{2\sigma}$ respectively where d is a linear dimension which is characteristic of the porous medium and which is usually taken to be the particle diameter in the case of a packed bed. The term P* is a dimensionless quantity and can be termed the dimensionless capillary pressure. Also let I_{P*} represent the fraction of completely saturated interconnections which can hold capillary moisture against gravity at a dimensionless capillary pressure P*.

$$\text{Thus } I_{P*} = \int_0^{1/P*} f(\eta)\,d\eta \qquad (6.6)$$

Similar expressions can be obtained by considering the distribution of equivalent radii of the pores. i.e.,

$$J_h = \int_0^{2\sigma/h} g(R)\,dR \qquad (6.7)$$

$$\text{and } J_{P*} = \int_0^{1/P*} g(\mu)\,d\mu \qquad (6.8)$$

where $\mu = R/d$

J_{P*} represents the probability of holding a meniscus in a pore against draining at a dimensionless capillary pressure P*. Similarly I_{P*} can be interpreted as the probability of holding a meniscus in an interconnection against draining at a dimensionless capillary pressure P*.

The probability ρ_h that a pore can hold a meniscus against draining either as a result of capillary forces within the pore or within a single interconnection can be given by $\rho_h = 1.0 - (1.0 - I_h)(1.0 - J_h)$ (6.9(a))

A term ρ_{P*} can be similarly defined as the probability that a pore can hold a meniscus against draining either as a result of capillary forces within a pore or within a single interconnection at a dimensionless capillary pressure P*. Thus ρ_{P*} can be written as

$$\rho_{P*} = 1.0 - (1.0 - I_{P*})(1.0 - J_{P*}) \qquad (6.9(b))$$

For a pore with n windows, the probability that r windows are completely saturated because the adjacent pores are completely saturated is given by ${}^nC_r P^r (1.0 - P)^{n-r}$ where $n \geqslant r$. This is the same as the probability of (n - r) windows being open to unsaturated or partially saturated pores.

Hence the probability that a pore in which (n - r) windows are open to unsaturated or partially saturated pores can exist and the moisture in which will not drain is given by ${}^nC_r P^r (1.0 - P)^{n-r} \rho_{P*}^{n-r}$ at a given dimensionless capillary pressure P*. This assumes that the menisci in all the pore window combinations which are open to empty pores are capable of holding the wetting - non wetting liquid interfaces receding into the pore. The existence of a single meniscus in

a pore-window combination which could allow the wetting - non wetting fluid interface to recede into the pore through the window is assumed to cause the pore to empty no matter what the conditions of the menisci at the other windows.

Thus the overall probability (x_f) that completely saturated pores can exist within a porous body at a dimensionless capillary pressure P* is given by:

$$x_f = \sum_{r=1}^{n} {}^{n}C_r P^r (1.0 - P)^{n-r} \rho_{P*}^{n-r} \quad \ldots\ldots \qquad (4.10(a))$$

For a tetrahedral subunit system, n = 4. Therefore, the probability that completely saturated pores can exist within a porous body at a dimensionless capillary pressure P* is given by:

$$x_f = \sum_{r=1}^{4} {}^{n}C_r P^r (1.0 - P)^{n-r} \rho_{P*}^{n-r} \qquad (4.10(b))$$

This expression, in fact gives the fraction of completely saturated pores to the total number of pores in the region under consideration.

$$\text{Hence} \quad x_f = P^4 + 4P^3(1 - P)\rho_{P*} + 6P^2(1 - P)^2\rho_{P*}^2 + 4P(1 - P)^3\rho_{P*}^3 + (1 - P)^4\rho_{P*}^4 \ldots\ldots\ldots\ldots \qquad (6.11)$$

Equations (6-3) and (6-11) are two simultaneous equations which can be solved for x_f for a given ρ_{P*}. However, ρ_{P*} is a function of h , the distributions f(r) and g(R). Hence, the fraction (x_f) can be evaluated from a knowledge of the height, and the distributions of the equivalent radii of pores and interconnections. The solution of the two equations in terms of x_f for various values of ρ_{P*} is given in appendix 4.

The fraction x_f represents the ratio of the number of completely saturated pores (n) to the total number of pores in a given region. There is a certain amount of selectivity in the size of the pores which are completely saturated. Moisture may be trapped in a pore for one of three reasons. A meniscus might enter a pore but because of the small size of the pore the meniscus might not be able to pass through the pore, or the meniscus might not be able to enter the pore at all because of the small aperture of the interconnections. Otherwise the moisture within a pore might be trapped because moisture is trapped in all adjacent pores, thus eliminating the possibility of a meniscus entering the pore. Selectivity of the size of a trapped pore occurs when the meniscus enters

the pore but does not pass through it because of its small size.

The fraction (x_f') of the number of pores trapped because of the moisture held up by interconnections alone divided by the total number of pores in the region being considered can be derived in a similar manner to the derivation of equation (6. 11). Thus x_f' could be expressed as follows:

$$x_f' = P^4 + 4P^3(1 - P)I_{P*} + 6P^2(1 - P)^2 I_{P*}^2 + 4P(1 - P)^3 I_{P*}^3 + (1 - P)^4 I_{P*}^4 \quad \ldots\ldots\ldots\ldots\ldots \quad (6\text{-}12)$$

Hence the fractional selectivity in the completely saturated pores could be expressed as:

$$x_f - x_f' = 4P^3(1 - P)(\rho_{P*} - I_{P*}) + 6P^2(1 - P)^2(\rho_{P*}^2 - I_{P*}^2) + 4P(1 - P)^3(\rho_{P*}^3 - I_{P*}^3) + (1 - P)^4(\rho_{P*}^4 - I_{P*}^4) \quad (6\text{-}13)$$

The values of P, ρ_{P*}, I_{P*} are all fractional quantities and are less than unity. For values of P near unity ρ_{P*} and I_{P*} both approach unity and $x_f - x_f'$ becomes neglegibly small. For small values of P, ρ_{P*} and I_{P*} are small and all the terms in equation (6-13) become small making $x_f - x_f'$ negligible. For intermediate values of P, the only significant term in equation (6-13) is $4P^3(1 - P)(\rho_{P*} - I_{P*})$. The term $\rho_{P*} - I_{P*}$ will be assumed to be small so that the term $4P^3(1 - P)(\rho_{P*} - I_{P*})$ becomes negligible compared with x_f. Thus x_f' is approximately equal to x_f under most circumstances.

Therefore, it can be assumed that the selectivity in the pore sizes of the completely saturated pores is negligible and the pore size distribution of the completely saturated pores can be assumed to be the same as the pore size distribution of the porous body. The fraction x_f could therefore be assumed to represent the ratio of the volume of completely saturated pores to the total volume of the pores in the region under consideration.

The basic equation, equation (5. 20) which can be used for the determination of a capillary pressure curve, can be applied in the case of drainage in order to predict the drain curve.

The notation which will be used in the following analysis is similar to that defined in Section (5.2.1). Equation (5.20) is as follows:

$$\frac{\overline{X} - \overline{X}_i}{1 - \overline{X}_i} = \frac{V_{pw}/V_p + V_{iw}/V_i}{1 + \delta} \qquad (6.14)$$

From the definition of x_f it is clear that

$$x_f = V_{pw}/V_p \qquad (6.15)$$

If randomness is assumed in the distribution of pores and interconnections in the porous body, the number of completely saturated interconnections can be assumed to be proportional to the number of completely saturated pores. This assumption holds if the number of pores and the number of interconnections in the region of the porous body under consideration is large.

Under such conditions, V_{iw}/V_i can be expressed as:

$$V_{iw}/V_i = x_f \qquad (6.16)$$

Therefore equation (6.14) reduces to the simple form

$$\frac{\overline{X} - \overline{X}_i}{1 - \overline{X}_i} = x_f \qquad (6.17)$$

If ρ_{p*} is known at a given dimensionless pressure P*, then x_f can be calculated using the simultaneous equations (6.3) and (6.11). This enables the term $(\overline{X} - \overline{X}_i)/(1 - \overline{X}_i)$ to be related to the dimensionless capillary pressure P*, thus giving the drain curve in a dimensionless form.

6.3 Computer program for the prediction of drain curves.

The calculations were carried out in two stages. Preliminary calculations were made using a computer program to solve equations (6.3) and (6.11) in order to obtain x_f for different values of ρ_{p*}. The solutions are given in Appendix 4. These results were then stored in the computer.

The main computer program was designed to calculate the quantity x_f for given values of the dimensionless capillary pressure P*. The distributions of the face insphere radii f(r) and the tetrahedron insphere radii g(R) obtained in Chapter 4 for a mean voidage of 0.4045 were used in order to evaluate ρ_{P*} for each section of the packed bed. A value of x_f was evaluated for the value of ρ_{P*} obtained by interpolation of the stored values, thus giving the value of $(\overline{X} - \overline{X}_i)/(1 - \overline{X}_i)$ for the height considered.

A flow-chart of the main computer program is shown in fig. 6-1.

6.4 Discussion

Unlike in the case of imbibition, the steps of calculation of the drain curve were able to be carried out without the use of the average height of tetrahedra in the packing. For a given type of packing consisting of a given type of particles and for a given degree of disturbance of the packing, the variation of the dimensionless capillary pressure with $(\overline{X} - \overline{X}_i)/(1 - \overline{X}_i)$ is to be expected to be universal and to be independent of the characteristic dimension of the particles of the packing. This hypothesis was tested for spherical ballotini. Experiments were carried out as described in Section (5.3) to obtain moisture saturations with height for six grades of ballotini. The results were compared with the theoretical drain curve and an average capillary diameter of the particles of the packing was evaluated for each grade of ballotini such that the root mean square deviation between the experimental and theoretical values of $(\overline{X} - \overline{X}_i)/(1 - \overline{X}_i)$ was minimised. Table (6.1) gives the mean particle diameter, the volume mean particle diameter, the average capillary diameter for the best fit and the root mean square deviation of $(\overline{X} - \overline{X}_i)/(1 - \overline{X}_i)$ for each grade of ballotini.

It can be seen from table (6.1) that for drainage the average capillary diameter of the particles in the packing is less than the volume mean diameter of the particles in the packing. As in the case of imbibition, this is to be expected. (see Section 5.5).

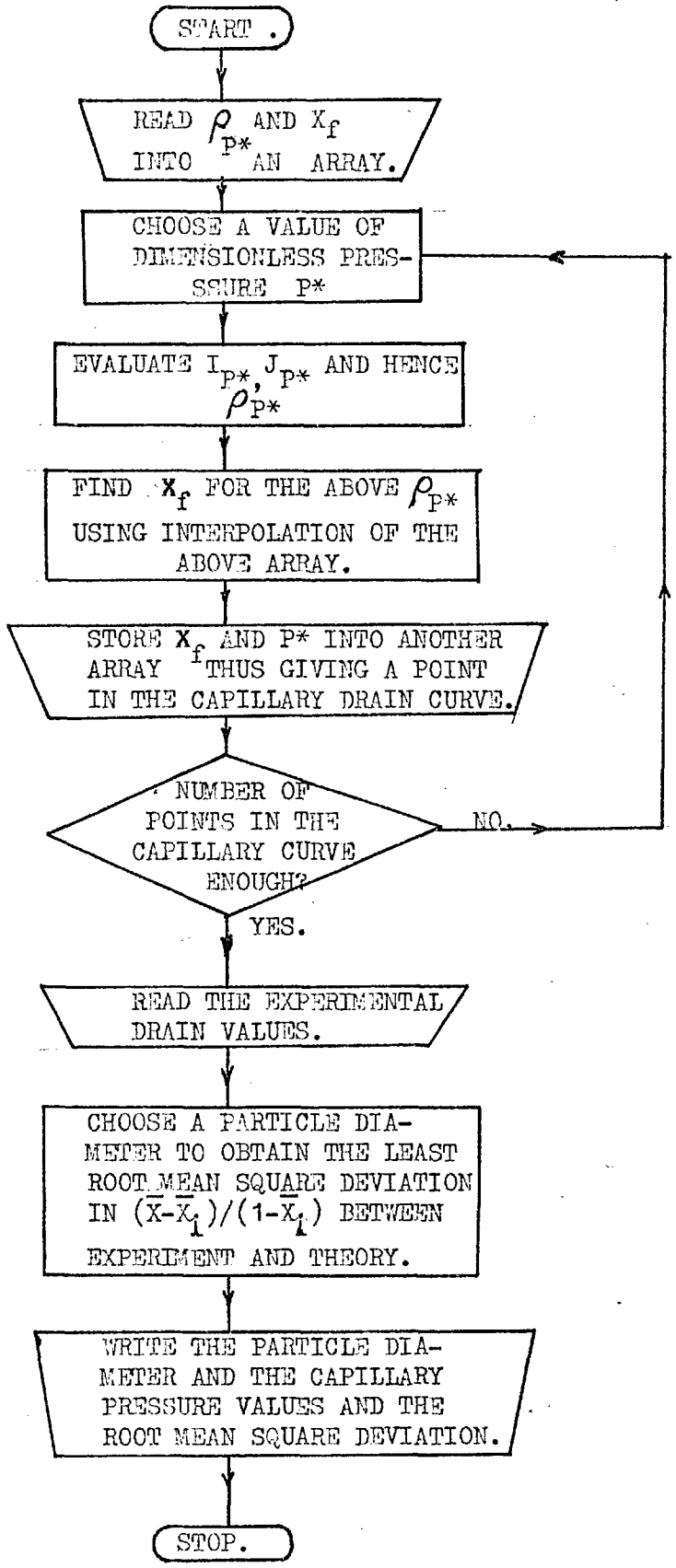


FIGURE 6. 1

FLOW-CHART OF THE COMPUTER PROGRAM WHICH EVALUATES THE DRAIN CURVE.

Table 6.1

Particle mean diameter, volume mean particle diameter, average capillary particle diameter and the root mean square deviation of $(\overline{X} - \overline{X_i})/(1 - \overline{X_i})$ between the theoretical values and the experimental points for six grades of ballotini.

GRADE OF BALLOTINI.	PARTICLE-MEAN DIAMETER	VOLUME-MEAN PARTICLE DIAMETER	CALCULATED AVERAGE CAPILLARY DIAMETER	ROOT-MEAN SQUARE DEVIATION IN $(\overline{X} - \overline{X_i})/(1 - \overline{X_i})$
6	0.07466	0.07486	0.06695	0.0452
7	0.06490	0.06530	0.06446	0.0246
8	0.05972	0.05990	0.05186	0.0329
9	0.04154	0.04173	0.03717	0.0215
10	0.02785	0.02854	0.02485	0.0440
11	0.02240	0.02282	0.02153	0.0281

Table (6. 2) gives the values of the dimensionless capillary pressure $(\frac{pd}{2\sigma'})$ where p is the capillary pressure, d is the average capillary diameter of the particles of the packing and σ' is the surface tension of the wetting liquid.

Fig (6. 2) compares the experimental dimensionless capillary pressure values for the six grades of ballotini with the theoretical curve. It can be seen that the theoretical curve describes the actual behaviour of drainage moisture distribution with capillary pressure satisfactorily with a maximum root mean square deviation of the term $(\overline{X} - \overline{X_i})/(1 - \overline{X_i})$ of 0. 0452 for grade 6 ballotini. The results show that unlike the case of imbibition, it may be possible to represent the drain curve for a given type of packing by a universal curve. The characterization of packed beds by an average capillary diameter, particularly in cases of unimodal particle size distributions or in cases where packed beds consist of approximately equal size spheres could be a useful tool in studies of drying rates etc. in such beds.

The slight departure of the theoretical curve from the experimental values at low capillary pressures indicates the existence of larger pores and larger face openings than assumed in the theory.

It has been shown in Section (5. 5) that the packed beds used in the experiments could have had a few pores and a few windows which were larger than those predicted by the respective distributions obtained in Chapter 4.

However, the overall representation of the experimental data by the theoretical curve was found to be satisfactory.

Table 6-2

Theoretical variation of $(\overline{X} - \overline{X}_i)/(1 - \overline{X}_i)$ with the dimensionless pressure $\frac{pd}{2\sigma'}$

$pd/2\sigma'$	$(\overline{X} - \overline{X}_i)/(1 - \overline{X}_i)$	$pd/2\sigma'$	$(\overline{X} - \overline{X}_i)/(1 - \overline{X}_i)$
3.25	1.000	6.05	0.031
3.35	0.902	6.15	0.028
3.45	0.765	6.25	0.025
3.55	0.655	6.35	0.022
3.65	0.572	6.45	0.020
3.75	0.497	6.55	0.017
3.85	0.432	6.65	0.015
3.95	0.373	6.75	0.013
4.05	0.327	6.85	0.012
4.15	0.290	6.95	0.010
4.25	0.256	7.05	0.009
4.35	0.226	7.15	0.007
4.45	0.199	7.25	0.006
4.55	0.176	7.35	0.006
4.65	0.154	7.45	0.005
4.75	0.136	7.55	0.004
4.85	0.122	7.65	0.004
4.95	0.110	7.75	0.003
5.05	0.098	7.85	0.003
5.15	0.086	7.95	0.003
5.25	0.077	8.05	0.003
5.35	0.067		
5.45	0.060		
5.55	0.053		
5.65	0.048		
5.75	0.043		
5.85	0.039		
5.95	0.035		

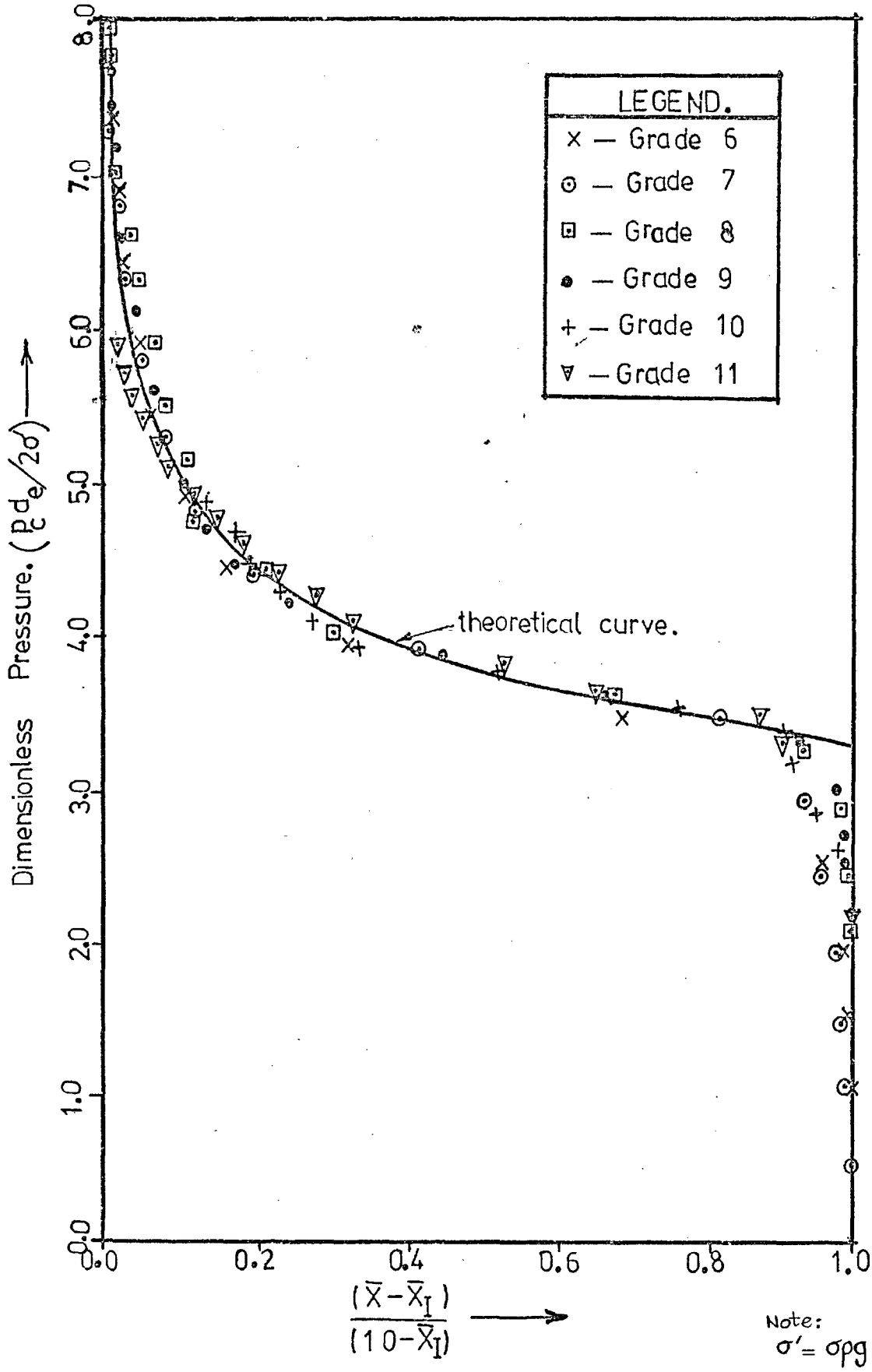


FIGURE 6.2

Comparison of the experimental drain values with the theoretical drain curve.

CHAPTER 7

The Effect of Mixing different size spherical particles on the capillary pressure curves in a bed.

7.1 Introduction

When two sets of uniform spheres are mixed and randomly packed to form a bed, the structure of the packing can be similar to that of a random packing of uniform spheres or the spheres can arrange themselves to form a structure which is different to that of a uniform sphere packing. If the difference in the particle diameters of the two sets is large, some of the smaller spheres are liable to be trapped in the large pores of the packing. The trapped spheres do not transmit any load from the upper layers of the bed and the trapped spheres do not take part in determining the equilibrium structure of the bed.

On the other hand, if the difference in the particle sizes is small the randomly packed bed can have a structure similar to that of a random packing of uniform spheres. The trapping of smaller particles in the large pores can then be assumed to be insignificant.

In general, when two sets of spheres are mixed and a random packing is formed, some of the smaller spheres can take part in determining the equilibrium structure of the packing, while the rest of the smaller spheres can be trapped in the pores of the equilibrium determining structure. The proportion in which the smaller spheres are distributed between being trapped and taking part in the equilibrium determining structure is determined partly by the relative particle sizes of the two sets and partly by the relative proportion of the smaller particles in the mixture.

Therefore, it can be expected that capillary pressure curves would be dependent on the relative particle sizes and on the proportions in which they are mixed in the packing. Thus, the capillary pressure curves in packed beds of mixtures of spheres, could be studied by classifying the mixtures in terms of the particle size distributions in the mixtures.

7.2 Definitions

7.2.1 A complete Mixture; Uniform Mixture or a Homogeneous Mixture.

Suppose m sets of spheres, each set consisting of n_i uniform spheres of diameter d_i where $i = 1, \ldots m$ and all n_i are large, are mixed and packed, a mixing index M for the packing can be defined (40) as

$$M = \frac{\sigma}{\sigma_e} \qquad \ldots\ldots\ldots\ldots\ldots\ldots\ldots\ldots\ldots\ldots \quad (7.1)$$

Where σ is the theoretical standard deviation of the particle diameters and σ_e is the standard deviation of particle diameters obtained experimentally by studying a random sample from the packing. If M has a value of unity, the packing is said to be of a complete or uniform or homogeneous mixture. A value of $M = \infty$ corresponds to a state of complete segregation whereas $M = 1$ implies spacial randomness of the particles on a macroscopic scale.

7.2.2 A classification of mixtures of hard spheres according to the particle size distribution.

Suppose two sets of uniform spheres of diameters d_1 and d_2 (where $d_1 > d_2$) are mixed homogeneously and packed randomly to form a bed, the structure of the resulting bed will be similar to that of a uniform sphere packing, provided that the particle sizes d_1 and d_2 are approximately equal.

Suppose $f_r(\delta)$ is defined as the pore size distribution of the equilibrium determining structure of the bed (ie., neglecting the presence of trapped spheres), the fraction ψ_{d^*} of the pores, which are larger than a given diameter d* can be expressed as

$$\psi_{d^*} = \int_{d^*}^{\infty} f_r(\delta)\, d\delta \qquad \ldots\ldots\ldots\ldots\ldots\ldots\ldots\ldots \quad (7.2)$$

Hence, the fraction of pores in the bed which can hold the smaller spheres in them can be expressed as

$$\psi_{d_2} = \int_{d_2}^{\infty} f_r(\delta)\, d\delta \ldots\ldots\ldots\ldots\ldots\ldots\ldots\ldots \quad (7.3)A$$

If the two particle sizes are approximately equal, the pore size distribution $f_r(\delta)$ of the bed can be approximated to the pore size distribution $f_1(\delta)$ of a uniform sphere packing of particle diameter d_1.

Thus, equation (7.2) can be modified in the form:

$$\Psi_{d_2} = \int_{d_2}^{\infty} f_1(\delta)\, d\delta \qquad \text{..... (7.3)B}$$

Let us denote ϕ as the fraction of pores of the equilibrium determining structure, which can be occupied by the smaller particles, without significantly affecting the capillary properties of the bed.

If the two particle sizes are approximately equal

$$\phi > \Psi_{d_2} \qquad \text{..... (7.4)}$$

$$\text{i.e., } \phi > \int_{d_2}^{\infty} f_1(\delta)\, d\delta \qquad \text{..... (7.5)}$$

Expression (7.5) can be modified as follows.

$$\phi > \int_{d_2/d_1}^{\infty} f_1\left(\frac{\delta}{d_1}\right) d\left(\frac{\delta}{d_1}\right) \qquad \text{..... (7.6)}$$

The distribution $f_1(\frac{\delta}{d_1})$ (i.e., the tetrahendron insphere radii distribution) for a random packing of uniform spheres has already been evaluated in chapter 4.

Hence, if ϕ is known, a ratio d_{2/d_1} can be calculated, below which the inequality (7.6) is not satisfied. A small value (say $\phi = 0.15$) will be assumed for ϕ. This assumption will be later shown to be reasonable by comparing results which will be derived based on the assumption, with the corresponding experimental observations. Using the tetrahedron insphere radii distribution predicted in chapter 4 (see Appendix 6), for a value of $\phi = 0.15$,

$$\frac{d_2}{d_1} > 0.75 \quad \ldots\ldots\ldots\ldots\ldots\ldots\ldots\ldots \quad (7.7)$$

Therefore, based on the above assumed value of 0.15 for $\emptyset$, two particle sizes can be said to be approximately equal, if the ratio of the diameter of the smaller particle to the diameter of the larger is greater than 0.75. Otherwise the two particle sizes will be said to be different.

However, when a range of particle sizes exists in a packing the above definition has to be modified. However, equation (7.2) can still be applied and the pore size distribution of the resulting bed $f_r(\delta)$ can be approximated to the pore size distribution $f_m(\delta)$ of a random packing of uniform spheres of diameter equal to the average particle diameter (μ) of the packing. Hence, equation (7.3)B can be modified to the form:

$$\Psi_{d_2} = \int_{d_2}^{\infty} f_m(\delta)\, d\delta \quad \ldots\ldots\ldots\ldots\ldots\ldots\ldots \quad (7.8)\,A$$

and hence,

$$\Psi_{d_2} = \int_{d_2/\mu}^{\infty} f_m\left(\frac{\delta}{\mu}\right) d\left(\frac{\delta}{\mu}\right) \quad \ldots\ldots\ldots\ldots\ldots \quad (7.8)B$$

Thus, a lower limit for the quantity $d_{2/\mu}$ can be chosen, above which the quantity Ψ_{d_2} does not exceed $\emptyset$. In such a case

$$d_{2/\mu} > 0.75 \quad \ldots\ldots\ldots\ldots\ldots\ldots\ldots\ldots \quad (7.9)$$

Hence, if a packing consists of spheres of approximately equal sizes, the ratio of the smallest significant diameter to the mean particle diameter can be expected be greater than 0.75.

Because of the possibility of the existence of a variety of distributions of particle sizes in a packing, the mean particle size (μ) and the variance (σ) of the distribution will be introduced in order to obtain a generalisation of inequality (7.9). If the particle size distribution approximates a Gaussian distribution, then it can be shown that 88 per cent of the particles lie within the particle diameters

Table 7.1

Values of μ, σ and μ/σ for different grades of ballotini

Grade of ballotini	μ (cm.)	σ (cm.)	μ/σ
6	0.0747	0.0039	19.39
7	0.0649	0.0051	12.63
8	0.0597	0.0036	16.79
9	0.0415	0.0028	14.73
10	0.0279	0.0045	6.23
11	0.0224	0.0031	7.32

$d = \mu + 1.555\sigma$ and $d = \mu - 1.555\sigma$ so that the smallest significant particle diameter can be expressed as $\mu - 1.555\sigma$.

Therefore, inequality (7.9) can be modified to obtain

$$\frac{\mu - 1.555\sigma}{\mu} > 0.75 \quad \text{..... (7.10)}$$

or

$$\frac{\mu}{\sigma} > 6.22 \quad \text{..... (7.11)}$$

Assuming that the inequality (7.11) can be applied in general, a mixture of spherical particles can be said to be composed of approximately equal size spheres, if the ratio of the mean particle size to the variance of the particle size distribution exceeds 6.22. Otherwise the particle sizes can be said to be different.

Table 7.1 shows the values of μ/σ for different grades of ballotini used in the experiments described in chapters 5 and 6. The μ/σ values have been calculated using the corresponding particle size distributions (Appendix 3) obtained by measuring particle diameters from random samples of ballotini, under a microscope. It is seen that μ/σ factors of all grades of ballotini, shown in Table 7.1 satisfy the inequality (7.11) thus indicating that each grade of ballotini used in the experiments can be considered to be composed of approximately equal size particles.

It has already been observed (Chapters 5 and 6) that packed beds of a given grade of ballotini can be represented by a uniform sphere packing to describe each case of rise and drain distribution of moisture in the beds. i.e., Each grade of ballotini used in earlier experiments (Chapters 5 and 6) can be regarded to consist of approximately equal size spheres. These experimental observations verify that when the factor μ/σ exceeds 6.22, packed beds of each grade of ballotini used in the experiments is able to be represented by an approximately equal size sphere packing. Therefore, the assumption that $\emptyset = 0.15$, on which the definition of approximately equal size spheres was based can be regarded to be reasonable.

7.3 The effect of mixing on pore-size

7.3.1 Void fraction

The void fraction of a random packing of uniform spheres is shown (Chapter 4) to be dependent on the mode of packing and on the degree of disturbance applied during and after the formation of the packing. However, beds formed under the same conditions have void fractions which vary about a mean value although the variance is often small.

If two sets of uniform spheres of different diameters are mixed homogeneously to form a packed bed, its void fraction varies considerably depending on the composition of the mixture (84). Investigations on the variation of the void fraction with the composition of mixtures have been carried out by Furnas (84). Binary systems were studied and it was observed that the void fractions of the mixtures were always less than the void fraction of the uniform sphere packings packed under the same conditions. Fig. 7.1 shows a typical variation of void fraction with composition. A minimum void fraction is seen to exist at a certain composition. The mixture at this composition has been termed the critical composition. The critical composition has been found (84) to consist of between 65 and 70 percent by volume of large constituents.

Theoretical studies have been made (48) to evaluate the composition at the minimum void fraction by assuming that smaller particles fit in the interstices formed by larger particles. The smaller particles were not considered to take part in forming the structure of the bed. Therefore, the theory can be considered to be applicable when the difference between the sizes of particles is large. Hard sphere mixtures have been studied in gas and liquid state physics in order to co-relate the physical properties of mixtures of gases and liquids (154, 165). Application of models of sphere packings formed in complete absence of the gravitational force in order to describe real packed beds has already been shown to be questionable (Chapter 3). Manglesdorf and Washington (142) studied the shrinkage in volume on mixing two different sizes of spheres, but unfortunately their studies were made upto a maximum size ratio of 1.6 : 1 only.

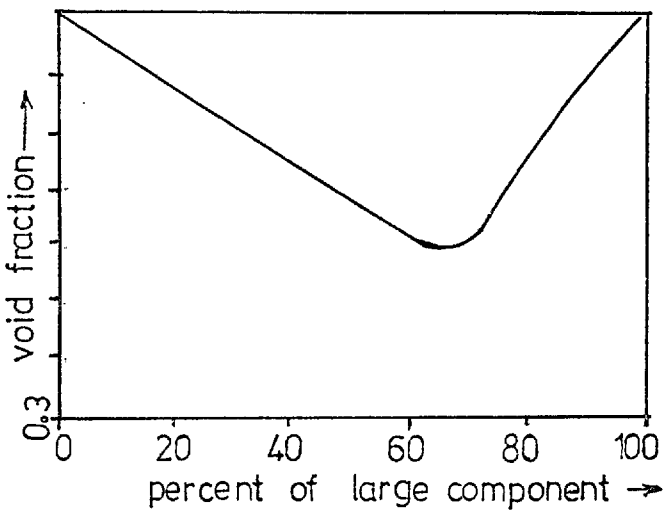


FIGURE 7.1

Typical variation of void fraction with composition for two component mixtures of spheres.

Upto present day, no satisfactory theory for the determination of either the pore size distribution or the void fraction of beds of mixtures of spheres exist.

7.3.2 Representation of beds of approximately equal size spheres by an equivalent uniform sphere packing.

From the above discussion it is seen that the void fraction of a bed which consists of a mixture of sphere sizes is always less than the void fraction of a uniform sphere packing.

If N sets of spheres, each set consisting of n_i uniform spheres of diameter d_i, where all n_i are large, were to be mixed homogeneously and packed in a column, the overall voids in the mixture would be less than or equal to the total sum of the voids in each uniform sphere packing. This can be expressed as follows:

$$\sum_{i=1}^{N} \frac{4}{3}\pi \; n_i d_i^3 \; \frac{\varepsilon}{1-\varepsilon} \geq \frac{4}{3}\pi \left(\sum_{i=1}^{N} n_i d_i^3\right) \frac{\varepsilon'}{1-\varepsilon'}, \quad \ldots\ldots\ldots \quad (7.12)$$

where ε is the void fraction of a uniform sphere packing and ε' is the void fraction of the mixture. The equality in statement (7.4) applies when all d_i are equal.

If the packing were to consist of approximately equal size spheres, it could be assumed that the overall structure of the packing would be close to that of an ensemble of equal size spheres of a certain diameter (d_e). This diameter could be termed the equivalent diameter of a particle representing the packing. In order to have an equivalent structure, it is necessary that the total number of spheres in each bed to be the same. The total voids in the equivalent bed can therefore be expressed as $\frac{4}{3}\pi \left(\sum_{i=1}^{N} n_i\right) d_e^3 \; \frac{\varepsilon}{1-\varepsilon}$

If equivalence is sought in terms of the void sizes in the two beds, the two void volumes can be equated.

Hence

$$\frac{4}{3}\pi \left(\sum_{i=1}^{N} n_i d_i^3\right) \frac{\varepsilon'}{1-\varepsilon'} = \frac{4}{3}\pi \left(\sum_{i=1}^{N} n_i\right) d_e^3 \; \frac{\varepsilon}{1-\varepsilon} \quad \ldots\ldots \quad (7.13)$$

Expressions (7.12) and (7.13) can be combined to give

$$\sum_{i=1}^{N} \frac{4}{3}\pi n_i d_i^3 \frac{\varepsilon}{1-\varepsilon} \geqslant \frac{4}{3}\pi \left(\sum_{i=1}^{N} n_i\right) d_e^3 \frac{\varepsilon}{1-\varepsilon} \quad \ldots\ldots\ldots\ldots\ldots \quad (7.14)$$

$$\text{i.e.,} \quad d_e \leqslant \left(\sum_{i=1}^{N} n_i d_i^3\right) / \left(\sum_{i=1}^{N} n_i\right) \quad \ldots\ldots\ldots\ldots\ldots \quad (7.15)$$

$$\text{or} \quad d_e \leqslant d_c \quad \ldots\ldots\ldots\ldots\ldots\ldots\ldots\ldots\ldots \quad (7.16)$$

Where d_c is the volume mean diameter of the particles.

Hence, if a packed bed of spheres of approximately equal sizes is represented by an equivalent bed of uniform spheres then in order to describe the properties of the void space, the equivalent diameter would have to be less than the volume mean diameter of the particles of the bed. Since the capillary properties are dependent on the void space, it could be expected that the representation of the capillary curves by those of an equivalent bed would have a relationship similar to that of the inequality (7.16)

It has already been observed (Chapters 5 and 6) that representation of the capillary rise and drain curves for six grades of ballotini by the corresponding equivalent diameters satisfies the inequality (7.16) in each case.

7.3.3 Beds consisting of Mixtures of spheres of different diameters.

7.3.3.1 General

When a mixture of spheres in which the diameters differ widely is mixed homogeneously and packed the structure of the packing cannot be regarded as being similar to that of a random packing of equal size spheres. This is because some of the smaller particles can occupy interstices without taking part in the primary equilibrium determining structure of the bed. Hence, such a bed could be regarded as being a combination of an equilibrium determining structure similar to that described for equal size sphere packing in Chapter 4 together with collections of smaller particles trapped in the larger pores of the structure.

7.3.3.2 Mixtures of two or more components

When a packing consists of two components of different sizes, the primary equilibrium determining structure will contain more small pores than the random packing of the single size larger spheres, but more large pores than the single size random packing of the smaller spheres. In effect this widens the spread of pore sizes over that for a single random uniform sphere packing.

The overall pore size distributions can thus be regarded as having relatively wider ranges of pore sizes than would be exhibited by a random uniform sphere packing. The average height of a tetrahedron in a mixture could be regarded to be larger than that for the corresponding smaller size sphere random packing but smaller than that for the corresponding larger size sphere random packing.

Generalisation of these results could be extended to a mixture of more than two components and would suggest that a wider range of pore sizes and relatively more smaller pores than in the case of a random uniform sphere packing.

7.4 Experiments

The changes in void fractions and pore size distributions on mixing particles of different sizes have been discussed in previous sections. The behaviour of capillary pressure curves of packed beds consisting of different proportions of the constituents can be expected to be interpreted in terms of the respective pore size distributions. Therefore, experiments were carried out to obtain the capillary pressure curves of packed beds of mixtures of ballotini and are described below.

7.4.1 Mixing

Experiments were carried out using mixtures of various proportions of purified Grade 6 and Grade 10 ballotini. Mixing was carried out in a fluidised bed using air from a compressed air cylinder. The required proportions of the two grades were placed in a column and fluidised for about five to ten minutes. As the density of both grades of the material was the same, fluidisation was expected to give a uniform mixture of the two grades.

Preliminary tests of mixing were carried out using the two grades of ballotini in a large bottle and then shaking thoroughly for five to ten minutes. The mixture when packed in a glass cylinder showed segregation patches indicating that the mixing was inadequate. However, the fluidised mixtures did not show any segregation effect indicating that the mixture could be regarded as being close to homogeneous.

Fig. 7.2 shows the variation of the void fraction of uniformly mixed random packings with composition for mixtures of Grade 10 and Grade 6 ballotini. The critical mixture was found to be approximately 37.5 per cent by weight of grade 10 ballotini. Two mixtures below the critical composition, two above the critical composition and another mixture of approximate critical composition were chosen to study the rise and drain curves (described in section 7.4.2.). Table 7.2 shows the composition of the mixtures and their corresponding mean particle sizes (μ), the variances (σ) of the distribution and the μ/σ factors.

7.4.2 The Determination of the Rise and Drain curves.

The experiments were carried out in the same manner as described in Section 5.3, but using the mixtures specified in Table 7.2. Mixtures 1, 2, 3, 4, 5, 7 and 8 were used in the rise experiments and mixtures 1, 2, 3, 4, 6, 7 and 8 in the drain experiments. Appendix 5 gives the observations in these experiments.

7.5 Results and Discussion

7.5.1 The Irreducible Saturation

The irreducible saturation obtained in the experiments were found not to vary appreciably with the composition of the mixture. This result agrees with the findings of Morrow (165) who observed that the residual saturation is independent of the particle size and the composition of the mixtures of particles. The observed average residual saturation was found to be 5.36 per cent of the void space, the value somewhat less than Morrow's (165) result (7.2 per cent), but was in reasonable agreement with the observations of Harris and Morrow (109),

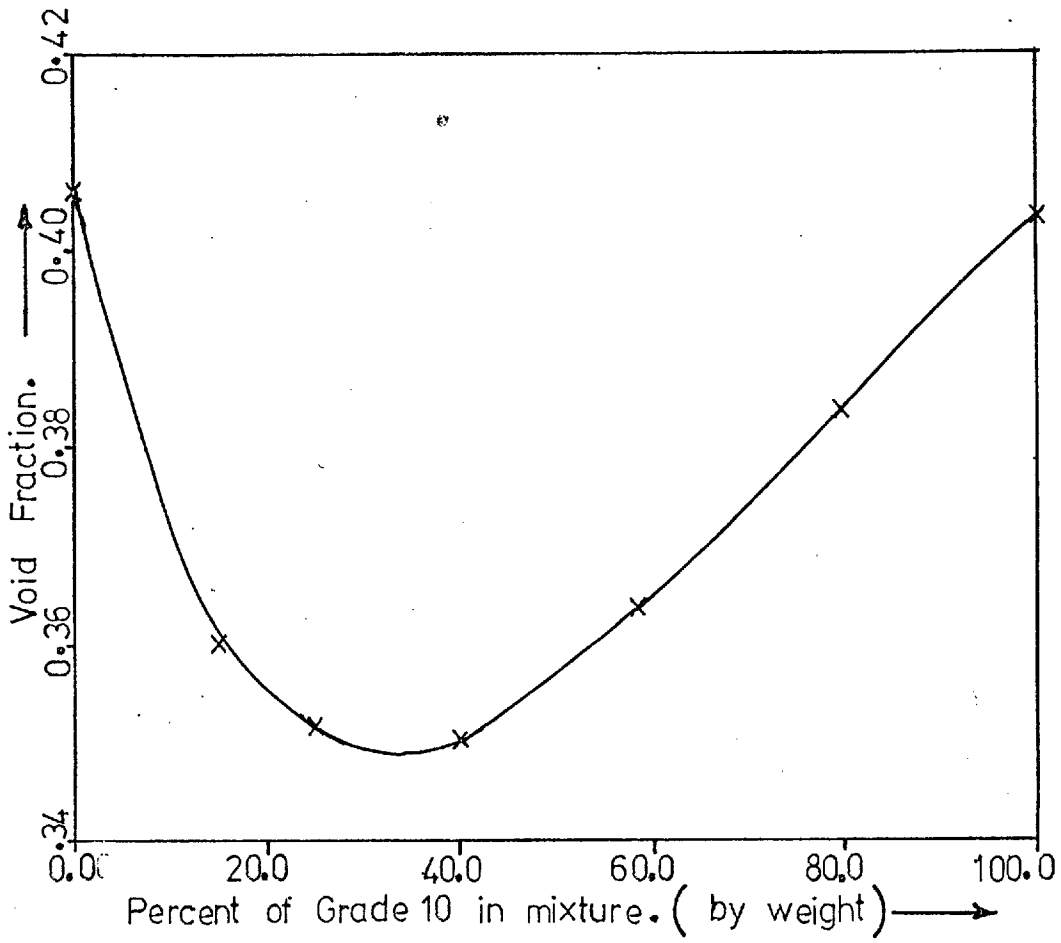


FIGURE 7.2

Variation of void fraction with composition for mixtures of grade 6 and grade 10 ballotini.

Table 7.2

MIXTURE	COMPOSITION OF MIXTURE (PERCENT-GRADE 10)	μ (cm.)	σ (cm.)	μ/σ
1	0.0	0.07466	0.00385	19.39
2	14.9	0.03910	0.02047	1.91
3	24.9	0.03455	0.01698	2.04
4	40.0 (APPROXIMATELY CRITICAL MIXTURE)	0.03144	0.01323	2.38
5	58.2	0.02964	0.01003	2.96
6	58.9	0.02959	0.00993	2.98
7	79.1	0.02853	0.00716	3.98
8	100.0	0.02785	0.00447	6.23

who obtained a value of 4.5 to 5.0 percent of the void space excluding the volume of trapped moisture. The moisture trapped in isolated pores were found by Harris and Morrow to be 1 to 2 percent of the pore space. (see Section 2.6.2). The beds used by Morrow (165) and by Harris and Morrow (109) can not be regarded as gently formed. However, the experiments described in Section 5.3 and in Section 7.4 were carried out with carefully formed unconsolidated beds. Unconsolidated beds can be expected to contain relatively fewer smaller pores than for the corresponding consolidated beds. Therefore, the volume of moisture trapped in isolated spots can be regarded to be small for unconsolidated beds when compared with the corresponding values of consolidated beds. The difference between the values of irreducible saturations obtained in the above experiments and obtained by Morrow (165) and Harris and Morrow (109) may be a result of this.

7.5.2 Pore sizes

The effects of mixing particles of two different sizes on the sizes of the pores have been discussed in earlier sections can be summarised as follows:

(1) Packed beds consisting of particles of two different sizes contain larger pores and openings than would be exhibited by a single size small sphere packing. Therefore it can be expected that entry capillary pressure (59) of the largest opening of a packed bed of a mixture is smaller than the entry capillary pressure of the largest opening of a packing consisting of single size small spheres.

(2) Packed beds consisting of particles of two different sizes contain more smaller pores than would be exhibited by a single size large sphere packing.

(3) The pore size distributions of randomly formed packed beds consisting of mixtures of spherical particles have wider ranges of pore sizes than can be expected for a random uniform sphere packing. Therefore it can be expected that changes of the quantities I_h and J_h (eq. 5.33 and eq. 5.34) with h, when h is increased from the entry capillary pressure of the largest opening to large values, are small compared with the corresponding changes for a uniform sphere packing.

and

(4) The average height of a tetrahedron of a packed bed of a mixture can be regarded as larger than the corresponding value of a single size small sphere packing but smaller than the corresponding value of a single size large sphere packing.

7.5.3 Behaviour of Rise Curves

To investigate the behaviour of the rise curves with mixing, the basic equations (5.31), (5.33) and (5.35) which describe the imbibition curve will be recalled. The equations are as follows:

$$(\bar{X} - \bar{X}_i)/(1 - \bar{X}_i) = h/(1+\bar{\delta}) \left[\frac{\int_0^{2\sigma/h} g(R)\, R^3 dR}{\int_0^{\infty} g(R) R^3 dR} + \frac{\int_0^{2\sigma/h} f(r) r^2 dr}{\int_0^{\infty} f(r) r^2 dr} \right] \cdots \quad (7.17)$$

$$I_h = \int_0^{2\sigma/h} f(r)dr \quad \cdots\cdots\cdots\cdots\cdots\cdots \quad (7.18)$$

$$\text{and} \quad \psi_{(h+\Delta h)} = \psi_h \cdot I_{h+\Delta h} \cdot (1.0 + (1.0 - \psi_h I_{h+\Delta h}) I_{h+\Delta h}) \quad \cdots\cdots\cdots\cdots \quad (7.19)$$

It has also been discussed that relatively more smaller pores and a wider spread of pore sizes can be expected in packed beds of mixtures of spherical particles than would be expected for a uniform sphere packing. Therefore changes of I_h when h is increased in steps to large values (eq. 7.18) can be expected to be smaller for packed beds of mixtures than the corresponding changes that could be expected for a uniform sphere packing. Thus, it can be expected that changes in the values of ψ with h in repetitive calculations using equation (7.19), to be smaller than the corresponding changes for a uniform sphere packing. Further, the integrals $\int_0^{2\sigma/h} g(R)R^3 dR$ and $\int_0^{2\sigma/h} f(r)r^2 dr$ in equation (7.17) can be expected to change relatively slowly with h when calculated for a mixture than for a uniform sphere packing. As a result of these, the factor $(\bar{X} - \bar{X}_i)/(1 - \bar{X}_i)$ in equation (7.17) can be expected to change with h by relatively smaller amounts for a mixture than for a uniform sphere packing. Therefore, rise curves of packings consisting of mixtures of spheres of different sizes can be expected to be steeper than the rise curves of uniform sphere packings.

This is clearly seen from fig. 7.3, which compares the rise curves for various mixtures of Grade 6 and Grade 10 ballotini. The variation of the capillary rise curves did not show any abrupt changes in behaviour as the compositions of the mixtures of packings were changed. The curves for the different mixtures were bounded by the rise curves for grade 6 and grade 10 ballotini. (i.e., curves for mixture 1 and mixture 8 respectively, of fig. 7.3). The curve for the mixture of approximately the critical composition (i.e., mixture 4) was seen to be steeper for a considerable range of moisture saturations, than the curves on either side of it. This could be explained as being the result of the critical mixture having the largest proportion of small pores that could be made from mixtures of the two sizes of spheres. The steep nature of the curves for small proportions (e.g., 14.9 per cent of Grade 10, i.e., Mixture 2) of the smaller size spheres gives an indication of the extent of influence of mixing small particles to a collection of large particles, on the pore sizes. The rise curves for mixture 1 (i.e., grade 6) and for mixture 2 (i.e., 14.9 percent of grade 10) is seen to be distinctly different. However, the rise curves for mixture 8 (i.e., grade 10) and for mixture 7 (i.e., 79.1 of grade 10) is seen to be similar in behaviour. This suggests that it may be possible to represent packed beds of mixtures of spheres with even large differences in sizes but with a small proportion of the larger component by an equivalent uniform sphere packing.

7.5.4 Behaviour of drain curves

The basic equations which determine the drain curve (from Chapter 6) are:

$$x_f = P^4 + 4P^3(1-P)\rho_h + 6P^2(1-P)^2\rho_h^2 + 4P(1-P)^3\rho_h^3 + (1-P)^4\rho_h^4 \quad \ldots\ldots\ldots\ldots (7.20)$$

Where $$\rho_h = 1.0 - (1.0 - I_h)(1.0 - J_h) \quad \ldots\ldots\ldots\ldots\ldots\ldots (7.21)$$

$$P = x_f^2 \quad \ldots\ldots\ldots\ldots\ldots\ldots (7.22)$$

and $$\frac{\overline{X} - \overline{X}_i}{1 - \overline{X}_i} = x_f \quad \ldots\ldots\ldots\ldots\ldots\ldots (7.23)$$

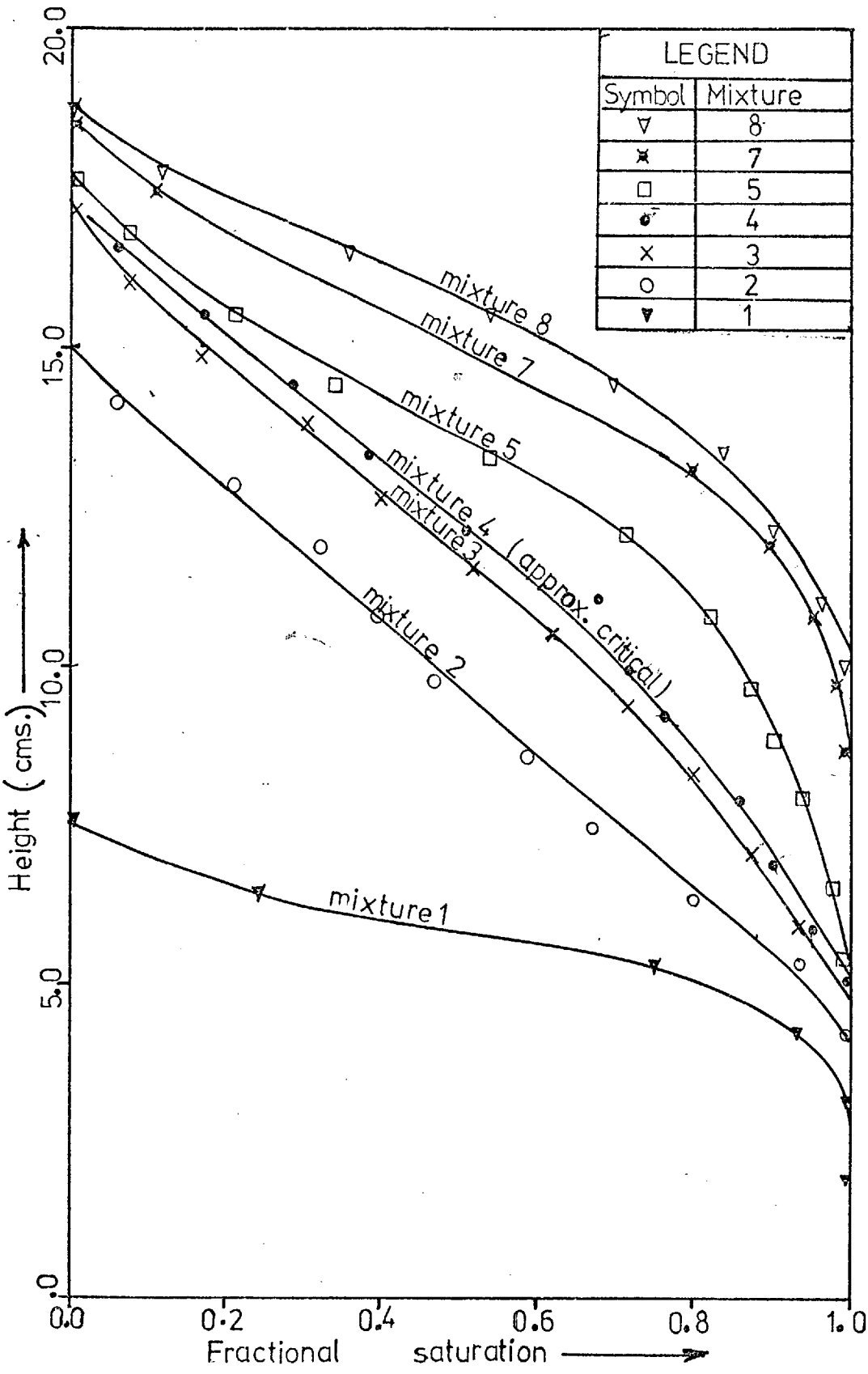


FIGURE 7.3

Rise curves for mixtures of grade 6 and grade 10 ballotini.

It has been shown that when h is changed from a certain value to a larger value I_h can be expected to change by relatively smaller amounts for packings of mixtures of spheres than for uniform sphere packings. By a similar argument, values of J_h (equation 5.34) can be shown to change with h relatively slowly for packed beds of mixtures than for uniform sphere packings. It can be seen from appendix 4 (i.e., solution of equations (7.20) and (7.22)) that x_f increases from 0.0 to 1.0 as ρ_h is increased from 0.0 to 1.0. Therefore it can be expected that x_f changes with h by relatively smaller amounts for packed beds of mixtures than for uniform sphere packings. Therefore, it can be expected from equation (7.23), that the quantity $(\overline{X} - \overline{X}_i)/(1 - \overline{X}_i)$ changes with h by relatively smaller amounts for packed beds of mixtures than for single size sphere packings. Thus the drain curve (i.e., h vs $(\overline{X} - \overline{X}_i)/(1 - \overline{X}_i)$) can be expected to be steeper for packed beds consisting of mixtures of particles than for single size sphere packings.

Fig. 7.4 shows drain curves for packed beds of different proportions of grade 6 and grade 10 ballotini. As expected the drain curves of packed beds of mixtures of grade 6 and grade 10 ballotini are seen to be steeper than the drain curves of packed beds of either grade 6 or grade 10 ballotini. Therefore steeper drain curves and steeper rise curves are to be expected for mixtures than for packings of approximately uniform size particles. The steepest curve is seen to be that of the packed bed of approximately critical composition. This is to be expected as in the case of rise curves. The behaviour of drain curves did not show any abrupt changes when composition was changed.

The drain curves for mixtures with small proportions of larger constituent are seen to be similar to those of packed beds composed of the smaller constituents alone (see curves for mixture 7 and mixture 8 of Fig. 7.4) but with lower capillary pressure values. Once again, this indicates the possibility of the representation of this type of mixture by a packing of uniform spheres of an equivalent diameter. The appreciable difference between the drain curves for mixtures with smaller proportions of the smaller constituent (e.g., drain curve for mixture 2 in Fig. 7.4) and the drain curve of the larger constituent alone (drain curve for mixture 1 of Fig. 7.4) indicates the influence of the presence of small particles in a packing on the pore sizes and hence on the capillary properties of the packing.

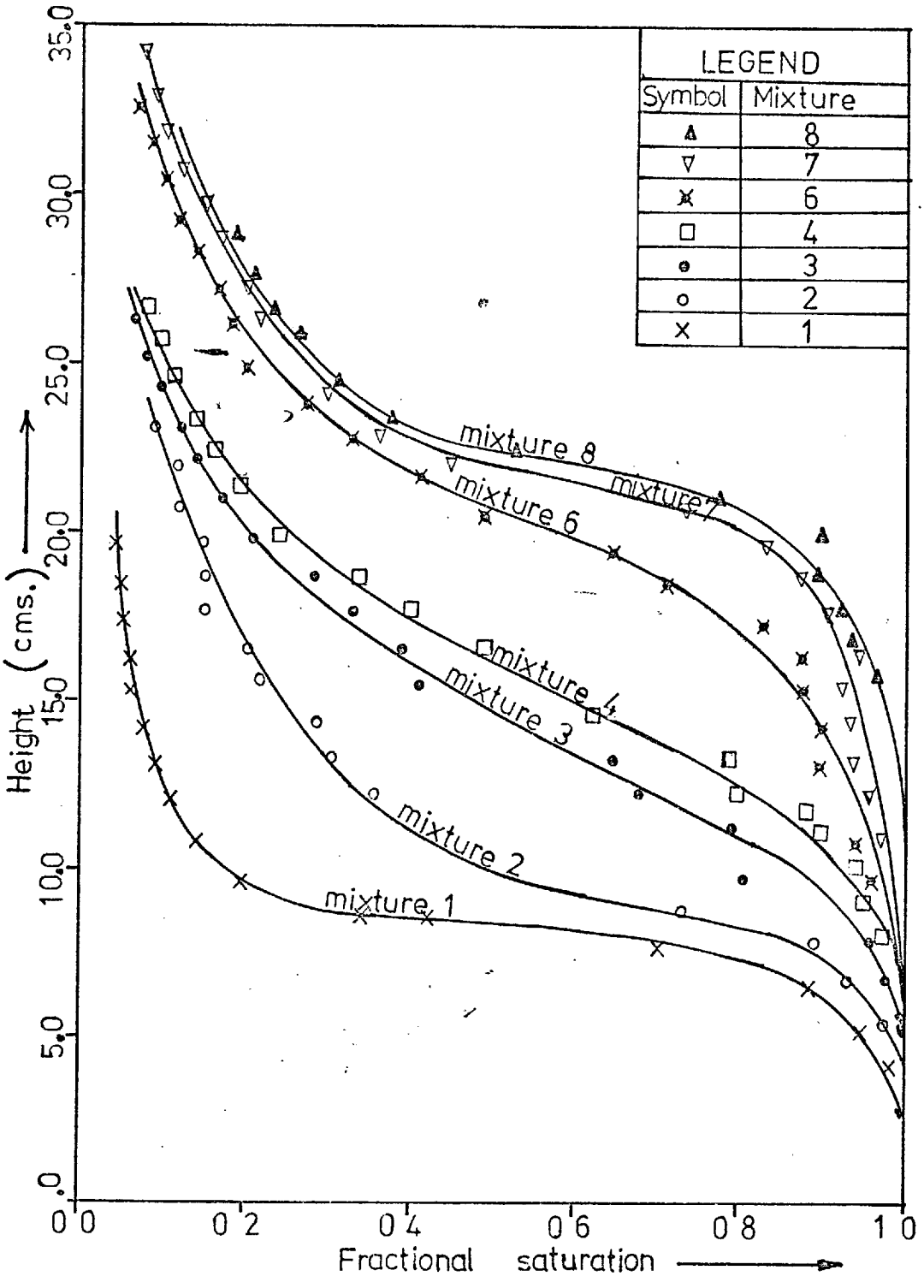


FIGURE 7.4

Drain curves for mixtures of grade 6 and grade 10 ballotini.

7. 5. 5 Other comments

For a complete description of the capillary pressure curves for packed beds consisting of mixtures of spheres, a model for such beds needs to be developed from which the pore size distributions can be predicted. These distributions could be employed in order to obtain the rise and drain curves for the mixtures. Such an analysis would need further study of the properties of packed beds of mixtures. The results obtained in this work show that the behaviour of packings made up of mixtures of particle sizes is in accordance with the expected behaviour based on the application of general theoretical concepts.

CHAPTER 8

Conclusion

The work presented in this thesis can be summarised as follows.

The distribution of moisture in porous bodies under rise and drain conditions can be predicted satisfactorily only if the behaviour of capillary moisture in the pores of the porous body is properly included in the calculations leading to these predictions. For such calculations the pore size distributions of the porous body are needed.

Development of a general model to predict the pore size distributions to cover the whole range of porous media is impractical. This is because the structure of the pore spaces differ widely for different porous bodies. Pore size distributions of different random packings of a given set of particles packed under the same conditions each time, can be regarded as varying about a mean pore size distribution.

A literature survey has been made (Chapter 3) of previous models which have been developed to represent packed beds. A model for the prediction of the distribution of pore sizes in random packings of equal size spheres has been developed. (Chapter 4). The statics of a packing formed under gravity and the geometry of packing were coupled together to develop a Monte Carlo method for the above prediction. The pore size distributions thus obtained are applicable to regions in a packed bed, far away from the walls and the base of the packing. The method takes into account the effect of consolidation in a packed bed. Consolidation could arise either as a result of vibrations or of other disturbances incurred during the formation of the packing and afterwards. The method thus enables pore size distributions to be predicted for different levels of consolidation. Extension of the model to packed beds of mixtures of spheres needs further study on the packing arrangement of spheres in such beds.

The packing becomes more complex when the particle sizes differ widely. The pore size distribution model may be useful in other fields of engineering such as compaction and strength of packings, flow through packed beds etc, when the particles of the packing can be considered to be approximately equal size spheres. The average pore size distributions obtained by averaging the respective distributions from five Monte-Carlo computer runs, were used to predict the rise and drain curves in packed beds of uniform spheres.

An outline of the previous work that has been carried out to describe capillary pressure curves in porous media was given. (Chapter 2). Experiments have been carried out to obtain the rise and drain moisture distributions with height for packed beds, each bed consisting of ballotini of a given grade. Six grades of commercial ballotini were used in these experiments. Experiments have also been carried out to determine the rise and drain moisture distributions with height in packed beds consisting of mixtures of various proportions of grade 6 and grade 10 ballotini.

A basic equation for the determination of a capillary pressure curve was developed (Chapter 5) based on the assumption that a porous body can contain pores and interconnections some of which may be completely saturated, some are partially saturated, and the rest unsaturated.

An integral equation has been developed (Chapter 5) which could be used for the prediction of capillary pressure curves for a pore of any shape. Solutions of the equation for the spherical and cylindrical pores were obtained. The behaviour of the capillary pressure - moisture saturation relationship for spherical and cylindrical pores was seen to be similar to the behaviour of capillary pressure - moisture saturation relationship for a porous body.

A model has been developed (Chapter 5) for the prediction of rise curves in terms of the pore size distributions. The model was based on the approximation that a porous body consists of layers of interconnected pores, the thickness ($\triangle h$) of each layer being regarded as a characteristic of the porous medium. The

method enables the saturation fractions at different heights to be predicted from a knowledge of the particle diameter of packing. The computations involve a step by step calculation for layers Δh of the characteristic thickness. For a given packing, the calculations start from the level of the free surface of the liquid pool.

It has been observed that the capillary rise curve for a given packed bed of approximately equal size spheres can be predicted reasonably accurately from a knowledge of a single parameter (i.e. an average particle diameter of the packing) using the developed model. The largest discrepancies in the predicted moisture contents at a given height were found to be for fractional moisture contents (i.e. the volume of moisture divided by the volume of pores) in the range 0.95 - 1.00.

A model for the prediction of drain curves for a given packed bed has been developed (Chapter 6). A study of the probability of retention of moisture in pores of a packed bed was made in the calculations for the predictions. It was shown that the drain curve for a uniform sphere packing can be expressed in terms of a dimensionless curve, which is applicable to beds of different particle sizes and to different wetting liquids. The validity of the above dimensionless drain curve was checked using packed beds of approximately equal size spheres. Water was the wetting liquid. It was shown that for such beds, the capillary drain curve can be predicted from a knowledge of a single parameter, i.e. an average particle diameter of the packing. The largest difference between the predictions and the experimental observations was found to occur at fractional moisture contents between 0.95 and 1.0.

A possible method for the classification of packed beds consisting of mixtures of different size particles was introduced (Chapter 7). Studies of capillary pressure curves in packed beds of mixtures of different size particles would be made easier to carry out by the use of such a classification. The pore size distributions that could be expected by mixing particles of different sizes have been studied. The behaviour of capillary pressure curves based on these pore size distributions have been discussed. The expected behaviour of capillary pressure curves were compared with the experimental observations, and were found to be in agreement.

APPENDIX 1.

THE EXPERIMENTAL RESULTS OF RISE COLUMNS FOR DIFFERENT GRADES OF BALLOTINI.

GRADE 6 .		GRADE 7.	
Height h(cms.) above free surface level.	$\frac{\bar{X} - \bar{X}_I}{1 - \bar{X}_I}$	Height h(cms.) above free surface level	$\frac{\bar{X} - \bar{X}_I}{1 - \bar{X}_I}$
8.634	0.000	8.760	0.000
7.559	0.003	7.681	0.001
7.134	0.013	6.605	0.340
6.467	0.206	5.860	0.622
5.681	0.583	5.497	0.780
5.364	0.737	4.936	0.961
4.809	0.872	4.386	0.967
4.265	0.934	3.326	0.979
3.145	0.997	1.103	1.000
1.931	1.000		

APPENDIX 1.(cont.)

GRADE 8.

Height h(cms.) above free surface level.	$\frac{\bar{X} - \bar{X}_I}{1 - \bar{X}_I}$
9.124	0.000
7.977	0.024
7.422	0.186
6.826	0.484
5.719	0.880
4.753	0.952
4.640	0.971
3.531	0.991
3.203	0.984
2.398	0.987
2.098	1.000

GRADE 9.

Height h(cms.) above free sufrace level.	$\frac{\bar{X} - \bar{X}_I}{1 - \bar{X}_I}$
14.496	0.000
13.385	0.018
12.272	0.244
11.153	0.449
10.032	0.766
8.946	0.890
7.857	0.958
6.742	0.969
5.643	0.972
4.450	0.989
3.245	1.000

APPENDIX 1.(cont.)

GRADE 10.

Height h(cms.) above free surface level.	$\frac{\bar{X} - \bar{X}_I}{1 - \bar{X}_I}$
18.868	0.000
17.765	0.079
16.638	0.327
15.519	0.520
14.418	0.680
13.317	0.842
12.185	0.902
11.051	0.958
9.944	0.976
8.839	1.000

GRADE 11.

Height h(cms.) above free surface level.	$\frac{\bar{X} - \bar{X}_I}{1 - \bar{X}_I}$
22.316	0.000
21.197	0.016
20.107	0.294
18.992	0.458
17.864	0.581
16.756	0.740
15.667	0.850
14.603	0.884
13.517	0.924
12.395	0.956
11.276	0.964
10.138	0.982
8.987	0.987
7.853	1.000

APPENDIX 1 (cont.)

Mean pool temperature during imbibition experiments.

GRADE.	Mean pool temperature. (^{o}C)
6	19.8
7	19.5
8	20.3
9	19.9
10	19.2
11	21.2

APPENDIX 2.

THE EXPERIMENTAL RESULTS OF DRAIN COLUMNS FOR DIFFERENT GRADES OF BALLOTINI.

GRADE 6.		GRADE 7.	
Height h (cms.) above free surface level.	$\frac{\bar{X} - \bar{X}_I}{1 - \bar{X}_I}$	Height h (cms.)above free surface level.	$\frac{\bar{X} - \bar{X}_I}{1 - \bar{X}_I}$
19.770	0.007	17.753	0.005
18.632	0.008	16.647	0.005
17.515	0.010	15.520	0.019
16.428	0.013	14.412	0.036
15.345	0.017	13.329	0.057
14.254	0.034	12.221	0.083
13.152	0.052	10.098	0.118
12.061	0.075	9.988	0.207
10.950	0.106	8.887	0.420
9.846	0.163	7.798	0.824
8.738	0.311	6.696	0.928
7.612	0.692	5.586	0.954
6.512	0.882	4.486	0.974
5.444	0.951	3.397	0.980
4.382	0.981	2.305	0.983
3.268	0.996	1.140	1.000
2.223	1.000		

APPENDIX 2. (cont.).

GRADE 8.		GRADE 9.	
Height h(cms.) above free surface level.	$\frac{\bar{X} - \bar{X}_I}{1 - \bar{X}_I}$	Height h(cms.) above free surface level.	$\frac{\bar{X} - \bar{X}_I}{1 - \bar{X}_I}$
23.406	0.004	30.862	0.016
22.324	0.003	29.754	0.015
21.250	0.010	28.648	0.015
20.158	0.019	27.536	0.018
19.067	0.037	26.453	0.027
17.989	0.052	25.412	0.034
16.870	0.071	24.354	0.044
15.780	0.083	23.272	0.050
14.725	0.110	22.169	0.065
13.625	0.119	21.059	0.084
12.511	0.207	19.968	0.103
11.417	0.303	18.887	0.130
10.312	0.685	17.784	0.167
9.237	0.934	16.629	0.241
8.131	0.978	15.496	0.446
7.051	0.994	14.376	0.667
5.966	1.000	13.220	0.923
		12.073	0.970
		10.942	0.991
		9.841	0.991
		8.770	1.000

APPENDIX 2.(cont.).

GRADE 10.

Height h (cms.) above free surface level.	$\frac{\bar{X} - \bar{X}_I}{1 - \bar{X}_I}$
28.905	0.135
27.738	0.168
26.561	0.195
25.467	0.228
24.382	0.271
23.255	0.333
22.168	0.505
21.091	0.764
19.963	0.901
18.865	0.902
17.772	0.914
16.677	0.938
15.587	0.972
14.461	1.000

GRADE 11.

Height h (cms.) above free surface level.	$\frac{\bar{X} - \bar{X}_I}{1 - \bar{X}_I}$
39.945	0.011
38.841	0.023
37.730	0.033
36.628	0.053
35.520	0.073
34.417	0.080
33.308	0.121
32.223	0.141
31.116	0.180
30.008	0.231
28.939	0.282
27.834	0.333
26.721	0.420
25.602	0.532
24.510	0.656
23.429	0.874
22.326	0.906
14.614	1.000

APPENDIX 2. (cont.)

Mean pool temperature during drain experiments.

GRADE.	Mean pool temperature. (^{o}C)
6	20.4
7	21.9
8	20.0
9	19.5
10	19.9
11	19.9

APPENDIX 3.

MICROSCOPIC ANALYSIS OF DIFFERENT GRADES OF BALLOTINI.

GRADE 8.		GRADE 9.	
DIAMETER. (cms.)	NO.OF SPHERES OBSERVED.	DIAMETER (cms.)	NO.OF SPHERES OBSERVED.
0.053	1	0.035	1
0.054	3	0.036	2
0.055	2	0.037	1
0.056	2	0.038	4
0.057	1	0.039	4
0.058	10	0.040	6
0.059	3	0.041	5
0.060	12	0.042	6
0.061	3	0.043	9
0.062	2	0.044	3
0.063	4	0.045	6
0.064	2	0.046	2
0.065	2	0.047	1
0.066	3	TOTAL	50
0.067	0		
TOTAL	50		

APPENDIX 3 . (Cont.)

MICROSCOPIC ANALYSIS OF DIFFERENT GRADES OF BALLOTINI.

GRADE 7		GRADE 6	
DIAMETER (cms.)	NO.OF SPHERES OBSERVED	DIAMETER (cms.)	NO.OF SPHERES OBSERVED
0.053	1	0.068	2
0.054	1	0.069	3
0.055	1	0.070	3
0.056	0	0.071	5
0.057	1	0.072	3
0.058	2	0.073	2
0.059	2	0.074	5
0.060	1	0.075	6
0.061	2	0.076	5
0.062	2	0.077	6
0.063	6	0.078	4
0.064	4	0.079	2
0.065	3	0.080	0
0.066	5	0.081	0
0.067	5	0.082	3
0.068	3	0.083	0
0.069	4	0.084	0
0.070	1	0.085	1
0.071	2	TOTAL	50
0.072	0		
0.073	1		
0.074	0		
0.075	2		
0.076	0		
0.077	1		
TOTAL	50		

APPENDIX 3. (cont.)

MICROSCOPIC ANALYSIS OF DIFFERENT GRADES OF BALLOTINI.

GRADE 10.		GRADE 11.	
DIAMETER. (cms.)	NO.OF SPHERES OBSERVED.	DIAMETER (cms.)	NO.OF SPHERES OBSERVED.
0.015	1	0.016	1
0.021	5	0.017	3
0.022	2	0.018	1
0.023	0	0.019	2
0.024	2	0.020	8
0.025	3	0.021	6
0.026	1	0.022	2
0.027	7	0.023	6
0.028	5	0.024	10
0.029	5	0.025	6
0.030	1	0.026	2
0.031	8	0.027	1
0.032	3	0.028	1
0.033	1	0.029	0
0.034	1	0.030	0
0.035	1	0.031	0
0.036	1	0.032	1
0.037	0	TOTAL	50
0.038	1		
TOTAL	50		

APPENDIX 3. (cont.)

MICROSCOPIC ANALYSIS OF DIFFERENT GRADES OF BALLOTINI.

MEAN PARTICLE DIAMETERS.

GRADE OF BALLOTINI	MEAN PARTICLE DIAMETER.(cms.)	VOLUME MEAN PARTICLE DIAMETER. (cms.)
6	0.0747	0.0749
7	0.0649	0.0653
8	0.0597	0.0599
9	0.0415	0.0417
10	0.0279	0.0285
11	0.0224	0.0228

APPENDIX 4.

SOLUTION OF EQUATION (6.11)

(Values of x_f for various values of ρ_{P*} . Equation (6.11))

ρ_{P*}	x_f	ρ_{P*}	x_f
0.00	0.000	0.28	0.006
0.01	0.000	0.29	0.007
0.02	0.000	0.30	0.008
0.03	0.000	0.31	0.009
0.04	0.000	0.32	0.011
0.05	0.000	0.33	0.012
0.06	0.000	0.34	0.013
0.07	0.000	0.35	0.015
0.08	0.000	0.36	0.017
0.09	0.000	0.37	0.019
0.10	0.000	0.38	0.021
0.11	0.000	0.39	0.023
0.12	0.000	0.40	0.026
0.13	0.000	0.41	0.028
0.14	0.000	0.42	0.031
0.15	0.001	0.43	0.034
0.16	0.001	0.44	0.038
0.17	0.001	0.45	0.041
0.18	0.001	0.46	0.045
0.19	0.001	0.47	0.049
0.20	0.002	0.48	0.054
0.21	0.002	0.49	0.058
0.22	0.002	0.50	0.064
0.23	0.003	0.51	0.069
0.24	0.003	0.52	0.075
0.25	0.004	0.53	0.081
0.26	0.005	0.54	0.087
0.27	0.005	0.55	0.094

APPENDIX 4(CONT).

ρ_{p*}	x_f	ρ_{p*}	x_f
0.56	0.102	0.79	0.508
0.57	0.109	0.80	0.546
0.58	0.118	0.81	0.588
0.59	0.127	0.82	0.634
0.60	0.136	0.83	0.685
0.61	0.146	0.84	0.742
0.62	0.157	0.85	0.805
0.63	0.168	0.86	0.876
0.64	0.180	0.87	0.956
0.65	0.193	0.88	1.000
0.66	0.207	0.89	1.000
0.67	0.222	0.90	1.000
0.68	0.237	0.91	1.000
0.69	0.254	0.92	1.000
0.70	0.272	0.93	1.000
0.71	0.291	0.94	1.000
0.72	0.312	0.95	1.000
0.73	0.334	0.96	1.000
0.74	0.357	0.97	1.000
0.75	0.383	0.98	1.000
0.76	0.411	0.99	1.000
0.77	0.440	1.00	1.000
0.78	0.473		

APPENDIX 5.

Experimental results for packed beds of mixtures of grade 6 and grade10 ballotini.

(1) Imbibition Experiments.

MIXTURE 1.		MIXTURE 2.	
Height. (cms.)	Fractional Saturation.	Height. (cms.)	Fractional Saturation.
8.634	0.000	14.090	0.060
7.559	0.056	12.965	0.204
7.134	0.066	11.843	0.324
6.467	0.249	10.726	0.385
5.681	0.605	9.610	0.465
5.364	0.751	8.530	0.583
4.809	0.879	7.459	0.669
4.265	0.938	6.368	0.800
3.145	0.997	5.304	0.940
1.931	1.000	4.206	1.000

APPENDIX 5 (cont.)

Experimental results for packed beds of mixtures of grade6 and grade 10 ballotini.

(1) Imbibition Experiments.

MIXTURE 3.

Height. (cms.)	Fractional Saturation.
17.102	0.009
16.008	0.077
14.975	0.164
13.862	0.302
12.713	0.397
11.598	0.515
10.481	0.622
9.374	0.711
8.254	0.798
7.138	0.873
5.990	0.934
4.891	1.000

MIXTURE 4.

Height. (cms.)	Fractional Saturation.
17.729	0.005
16.643	0.061
15.558	0.165
14.426	0.281
13.291	0.382
12.210	0.510
11.100	0.679
9.999	0.724
8.920	0.758
7.811	0.864
6.732	0.908
5.653	0.950
4.556	0.992
3.438	1.000

APPENDIX 5. (cont.).

Experimental results for packed beds of mixtures of grade 6 and grade 10 ballotini.

(1) Imbibition experiments.

MIXTURE 5.

Height. (cms.)	Fractional Saturation.
17.693	0.004
16.582	0.065
15.501	0.211
14.425	0.340
13.307	0.540
12.142	0.714
10.964	0.822
9.865	0.868
8.799	0.907
7.686	0.941
6.553	0.978
5.444	0.988
4.342	1.000

MIXTURE 7.

Height. (cms.)	Fractional Saturation.
18.597	0.005
17.482	0.112
15.371	0.242
14.213	0.481
13.108	0.797
11.913	0.904
10.808	0.956
9.717	0.988
8.619	1.000

MIXTURE 8.

Height. (cms.)	Fractional Saturation.
18.868	0.000
17.765	0.128
16.638	0.363
15.519	0.546
14.418	0.697
13.317	0.850
12.185	0.907
11.051	0.960
9.944	0.977
8.839	1.000

APPENDIX 5.(cont.).

Experimental results for packed beds of mixtures of grade6 and grade 10 ballotini.

(2) Drain experiments.

MIXTURE 1.		MIXTURE 2.	
Height. (cms.)	Fractional Saturation.	Height. (cms.)	Fractional Saturation
19.770	0.060	23.113	0.095
18.632	0.061	22.009	0.120
17.515	0.063	20.898	0.121
16.428	0.066	19.817	0.147
15.345	0.070	18.741	0.152
14.254	0.086	17.682	0.153
13.152	0.103	16.625	0.213
12.061	0.124	15.555	0.221
10.950	0.154	14.439	0.294
9.846	0.207	13.318	0.311
8.738	0.348	12.214	0.362
7.612	0.708	11.096	0.407
6.512	0.888	9.960	0.492
5.444	0.954	8.805	0.737
4.382	0.982	7.677	0.895
3.268	0.996	6.590	0.937
2.223	1.000	5.510	0.975
		4.423	1.000

APPENDIX 5.(cont.)

Experimental results for packed beds of mixtures of grade6 and grade 10 ballotini.

(2) Drain experiments.

MIXTURE 3.		MIXTURE 4.	
Height. (cms.)	Fractional Saturation.	Height. (cms.)	Fractional Saturation.
26.403	0.072	26.817	0.079
25.317	0.081	25.728	0.099
24.241	0.099	24.619	0.112
23.128	0.118	23.428	0.139
22.071	0.142	22.316	0.161
21.006	0.166	21.224	0.193
19.919	0.211	20.102	0.221
18.840	0.285	19.952	0.242
17.745	0.326	18.858	0.337
16.628	0.391	17.716	0.408
15.539	0.411	16.644	0.487
14.472	0.610	15.581	0.460
13.385	0.649	14.520	0.615
12.285	0.683	13.438	0.791
11.175	0.793	12.337	0.813
10.042	0.805	11.230	0.912
8.909	0.957	10.100	0.952
7.814	0.960	8.980	0.947
6.729	0.982	7.877	0.974
5.634	1.000	6.763	1.000

APPENDIX 5. (cont.)

Experimental results for packed beds of mixtures of grade6 and grade10 ballotini.

(2) Drain experiments.

MIXTURE 6.		MIXTURE 7.	
Height. (cms.)	Fractional Saturation.	Height. (cms.)	Fractional Saturation.
32.781	0.073	34.008	0.078
31.568	0.085	32.916	0.090
30.411	0.103	31.811	0.100
29.302	0.122	30.703	0.122
28.281	0.143	29.684	0.149
27.175	0.170	28.571	0.172
26.074	0.179	27.463	0.196
24.970	0.201	26.354	0.224
23.891	0.270	25.227	0.268
22.770	0.333	24.028	0.304
21.635	0.415	22.962	0.361
20.543	0.489	21.854	0.452
19.469	0.646	20.778	0.741
18.424	0.710	19.681	0.841
17.379	0.832	18.615	0.879
16.336	0.874	17.549	0.907
15.248	0.876	16.479	0.945
14.141	0.903	15.405	0.925
13.034	0.894	14.312	0.934
11.888	0.886	13.203	0.936
10.739	0.936	12.100	0.954
9.614	0.956	10.970	0.973
8.534	0.932	9.834	0.960
7.447	0.960	8.695	0.961
6.334	1.000	7.548	0.996

APPENDIX 5.(cont.)

Experimental results for packed beds of mixtures of grade 6 and grade 10 ballotini.

(2) Drain experiments.

MIXTURE 8.

Height. (cms.)	Fractional Saturation.
28.905	0.182
27.738	0.212
26.561	0.238
25.467	0.270
24.382	0.310
23.255	0.369
22.168	0.532
21.091	0.776
19.963	0.906
18.865	0.907
17.772	0.919
16.677	0.942
15.587	0.973
14.461	1.000

APPENDIX 5.(cont.)

Experimental results for packed beds of mixtures of grade 6 and grade 10 ballotini.

(3) Composition of mixtures and mean pool temperatures.

MIXTURE.	PERCENT OF GRADE 10 IN MIXTURE. (by weight.)	MEAN POOL TEMPERATURE DURING EXPERIMENT. (°C)	
		IMBIBITION	DRAINAGE
1	0.0	19.8	20.4
2	14.9	19.5	19.6
3	24.9	21.2	19.8
4	40.0	19.6	20.8
5	58.2	19.2	-
6	58.9	-	20.6
7	79.1	20.7	21.1
8	100.0	19.2	19.9

APPENDIX 6

PREDICTED NORMALISED MEAN PORE SIZE AND INTERCONNECTION SIZE DISTRIBUTIONS

FOR A DISTURBANCE FACTOR X=0. 13.

FACE INSPHERE RADIUS DISTRIBUTION		TETRAHEDRON INSPHERE RADIUS DISTRIBUTION	
Face insphere radius /particle radius	Frequency x1000	Tetra. insphere radius/particle radius	Frequency x1000
0. 15 - 0. 16	69. 2915	0. 15 - 0. 16	0. 0000
0. 16 - 0. 17	16. 4327	0. 16 - 0. 17	0. 0000
0. 17 - 0. 18	15. 0111	0. 17 - 0. 18	0. 0000
0. 18 - 0. 19	14. 2898	0. 18 - 0. 19	0. 0000
0. 19 - 0. 20	15. 0463	0. 19 - 0. 20	0. 0000
0. 20 - 0. 21	14. 8813	0. 20 - 0. 21	0. 0000
0. 21 - 0. 22	15. 7441	0. 21 - 0. 22	0. 0000
0. 22 - 0. 23	18. 2941	0. 22 - 0. 23	1. 2718
0. 23 - 0. 24	16. 3936	0. 23 - 0. 24	1. 5068
0. 24 - 0. 25	14. 6370	0. 24 - 0. 25	2. 7124
0. 25 - 0. 26	14. 4739	0. 25 - 0. 26	3. 2743
0. 26 - 0. 27	15. 2805	0. 26 - 0. 27	5. 0459
0. 27 - 0. 28	13. 6394	0. 27 - 0. 28	9. 3059
0. 28 - 0. 29	16. 2992	0. 28 - 0. 29	11. 2212
0. 29 - 0. 30	15. 3847	0. 29 - 0. 30	7. 4037
0. 30 - 0. 31	14. 2186	0. 30 - 0. 31	9. 5695
0. 31 - 0. 32	15. 6439	0. 31 - 0. 32	6. 9117
0. 32 - 0. 33	13. 7049	0. 32 - 0. 33	8. 2652
0. 33 - 0. 34	14. 1625	0. 33 - 0. 34	6. 6009
0. 34 - 0. 35	14. 5473	0. 34 - 0. 35	7. 1117
0. 35 - 0. 36	13. 1873	0. 35 - 0. 36	6. 8274
0. 36 - 0. 37	13. 6067	0. 36 - 0. 37	7. 2327
0. 37 - 0. 38	15. 6913	0. 37 - 0. 38	10. 2602
0. 38 - 0. 39	14. 2603	0. 38 - 0. 39	7. 7178
0. 39 - 0. 40	15. 1433	0. 39 - 0. 40	8. 8211
0. 40 - 0. 41	13. 7622	0. 40 - 0. 41	7. 4289
0. 41 - 0. 42	12. 8051	0. 41 - 0. 42	7. 0035
0. 42 - 0. 43	15. 1411	0. 42 - 0. 43	8. 5249
0. 43 - 0. 44	15. 1191	0. 43 - 0. 44	9. 7424
0. 44 - 0. 45	13. 9251	0. 44 - 0. 45	8. 1366
0. 45 - 0. 46	14. 1124	0. 45 - 0. 46	9. 5576
0. 46 - 0. 47	13. 9465	0. 46 - 0. 47	8. 9442
0. 47 - 0. 48	14. 2262	0. 47 - 0. 48	8. 3062
0. 48 - 0. 49	12. 0856	0. 48 - 0. 49	7. 8560
0. 49 - 0. 50	13. 6145	0. 49 - 0. 50	8. 4414
0. 50 - 0. 51	13. 9500	0. 50 - 0. 51	8. 7524
0. 51 - 0. 52	14. 4896	0. 51 - 0. 52	9. 6448
0. 52 - 0. 53	14. 3141	0. 52 - 0. 53	9. 4747
0. 53 - 0. 54	11. 7529	0. 53 - 0. 54	9. 5711
0. 54 - 0. 55	12. 9637	0. 54 - 0. 55	9. 3183
0. 55 - 0. 56	10. 4613	0. 55 - 0. 56	8. 7456
0. 56 - 0. 57	13. 1129	0. 56 - 0. 57	7. 9928

FACE INSPHERE RADIUS DISTRIBUTION

Face insphere radius /particle radius	Frequency x 1000
0.57 - 0.58	12.7406
0.58 - 0.59	12.5534
0.59 - 0.60	12.7396
0.60 - 0.61	12.3449
0.61 - 0.62	14.3923
0.62 - 0.63	13.0333
0.63 - 0.64	13.0572
0.64 - 0.65	13.0176
0.65 - 0.66	12.6700
0.66 - 0.67	10.9470
0.67 - 0.68	13.0957
0.68 - 0.69	13.4248
0.69 - 0.70	13.6070
0.70 - 0.71	10.8715
0.71 - 0.72	11.5886
0.72 - 0.73	11.2931
0.73 - 0.74	9.1037
0.74 - 0.75	8.5496
0.75 - 0.76	8.8034
0.76 - 0.77	7.2598
0.77 - 0.78	7.4928
0.78 - 0.79	6.3262
0.79 - 0.80	5.9704
0.80 - 0.81	6.0565
0.81 - 0.82	5.9018
0.82 - 0.83	5.7087
0.83 - 0.84	4.0904
0.84 - 0.85	3.3668
0.85 - 0.86	4.8551
0.86 - 0.87	4.3848
0.87 - 0.88	3.8615
0.88 - 0.89	2.3356
0.89 - 0.90	2.3746
0.90 - 0.91	0.1210
0.91 - 0.92	0.1447
0.92 - 0.93	1.3269
0.93 - 0.94	0.1348
0.94 - 0.95	0.0578
0.95 - 0.96	0.0000
0.96 - 0.97	0.0288
0.97 - 0.98	1.0000
0.98 - 0.99	0.0585
0.99 - 1.00	0.0000

TETRAHEDRON INSPHERE RADIUS DISTRIBUTION

Tetra. insphere radius /particle radius	Frequency x 1000
0.57 - 0.58	9.7290
0.58 - 0.59	9.8613
0.59 - 0.60	8.5569
0.60 - 0.61	9.7260
0.61 - 0.62	9.1915
0.62 - 0.63	8.2932
0.63 - 0.64	9.7667
0.64 - 0.65	10.0585
0.65 - 0.66	9.8625
0.66 - 0.67	8.3514
0.67 - 0.68	10.0775
0.68 - 0.69	9.4833
0.69 - 0.70	10.2931
0.70 - 0.71	10.1815
0.71 - 0.72	9.9408
0.72 - 0.73	9.3809
0.73 - 0.74	8.0709
0.74 - 0.75	9.2514
0.75 - 0.76	9.5519
0.76 - 0.77	8.6790
0.77 - 0.78	8.7164
0.78 - 0.79	9.4269
0.79 - 0.80	8.0794
0.80 - 0.81	6.5292
0.81 - 0.82	7.5154
0.82 - 0.83	8.1446
0.83 - 0.84	7.3750
0.84 - 0.85	9.1574
0.85 - 0.86	7.1355
0.86 - 0.87	7.1652
0.87 - 0.88	7.8499
0.88 - 0.89	8.4140
0.89 - 0.90	6.0780
0.90 - 0.91	3.9363
0.91 - 0.92	3.8135
0.92 - 0.93	2.3233
0.93 - 0.94	3.4608
0.94 - 0.95	2.9240
0.95 - 0.96	2.1576
0.96 - 0.97	2.1210
0.97 - 0.98	2.1038
0.98 - 0.99	1.2576
0.99 - 1.00	1.5343

Void Fraction = 0.40453 & Variance = 0.0003

$\frac{\text{Average Height of Tetrahedron}}{\text{Particle Diameter}}$ = 1.5565 & Variance = 0.0012

V_I / V_P = 0.337 for a value of X_i = 0.0536

List of Symbols

A	-	Interfacial Area of Air/Water or wetting/non-wetting meniscus
a	-	radius of cylinder
d	-	diameter of a particle
F	-	Force
F*	-	Critical Reaction
F^*_{max}	-	Maximum Critical Reaction
$f(F^*)^{max}$	-	Frequency distribution function of Critical Reactions
f(r)	-	Capillary radius distribution function (Chapter 2)
f(r)	-	Face insphere radii distribution function (Chapters 5, 6, 7)
$f(\eta)$	-	Distribution function of dimensionless critical reactions (Chapter 4)
$f_r(\delta)$	-	pore diameter distribution function (Chapter 7)
G	-	Gibbs free energy
g	-	Gravitational Acceleration
g(R)	-	Pore radii or tetrahedron insphere radii distribution function
h	-	Height above a free liquid surface
k	-	a constant
M	-	Mixing Index
N	-	Total Number of pores in a given section of a porous body
n	-	Number of saturated pores in a given section of a porous body
P	-	Probability of two saturated pores becoming adjacent
P*	-	Dimensionless Capillary Pressure $= \frac{hd}{2\sigma}$
p	-	porosity (Chapter 2)
p	-	pressure (Chapter 5)
Pc	-	Capillary pressure (Chapter 2)
R	-	radius of a pore
r_e	-	Equivalent radius of a pore or an interconnection
r	-	radius of interconnection
s	-	Entropy
T	-	Temperature
T 1	-	Equilibrium determining tetrahedral Unit (Chapter 4)
T 2	-	A subunit in a packing (Chapter 4)
U 1	-	A subunit in a packing (Chapter 4)
u(r)	-	Function relating Volume of an interconnection to its radius (r)

V	-	Volume
V_A	-	Volume of Air Core
V_P	-	Pore Volume
$\mathcal{V}(R)$	-	Function relating Volume of a pore to its radius R
X	-	Fractional Saturation = V/V_p
$\bar{X}_i$, $\bar{X}_I$	-	Fractional Irreducible Saturation
$\bar{X}$	-	Average Fractional Saturation over a given section of a porous body
x	-	Factor of Disturbance
α	-	An angle (Chapter 4)
α , β	-	Constants of the Weibull distribution (Chapter 2)
γ , σ'	-	Surface tension of liquid (absolute Units)
δ	-	pore size
Θ	-	Angle defined by Figure 2.5
ζ	-	Probability factor for stability
η	-	Dimensionless force or reaction
μ	-	Coefficient of Friction (Chapter 4)
μ	-	Mean particle size (Chapter 7)
ρ	-	density of liquid
σ	-	Surface tension of liquid expressed as $\gamma/\rho g$
ψ	-	Fraction of the porous body belonging to wet regions (Chapter 5)

Subscripts:

c	-	corners
e	-	equivalent
i	-	interconnections
p	-	pores
t	-	trapped
w	-	water or wetting liquid

REFERENCES

1. Ackerman,A.S.E., Nature, 155, 82,(1945).
2. Adams and Matheson, J.Chem. Phys., 56, 1989,(1972).
3. Alder,B.J., J.Chem. Phys., 23, 263-271,(1955).
4. Alkiviades,C.P.,Chi Tien and Raffi, M.T.,A.I.Chem.E.J., 19, 58-66, (1973).
5. American Instruments Co., J.Phys. Chem., 75 , No.4,(1971).
6. Amirsoleymani, T., Ph.D.Thesis, University of Birmingham, (1966).
7. Anderson, A. B. C.,Soil Sci.,56, 29-41, (1943).
8. Anderssen, R. S. and Seneta, E., Pure and Appl. Geophys. J., 91, 5-13, (1971).
9. Archie,G.E., Trans. A. I. M. E., 146,54, (1942).
10. Arthur,J.R.F. and Menzies, B.K., Geotechnique, 22 , No. 3, (1972).
11. Barrer, R.M., Appl. Mater. Res., 2, 129-143, (1963).
12. Barrer,R.M., Barrie, J. A. and Rogers, M.G., Trans. Farad. Soc., 58 , 2473-2483, (1962).
13. Baver, L.D., Soil Physics, John Wiley & Sons Inc.,N.Y., (1946).
14. Benenati, R. F. and Brosilow, C. B., A.I.Chem. E. J., 8 , 359-361, (1962).
15. Beresford, R.H., Disc. Farad. Soc., 43 ,76 ,(1967).
16. Bergelin, O. P., Chem. Eng.,56 ,No. 5, 104, (1949).
17. Bernal, J.D., Nature, 183 , 141-147 ,(1959).
18. Bernal, J. D., Nature , 185 , 68-70 ,(1960).

19. Bernal,J.D., Soviet Physics Crystallography, 7 ,410-417,(1963).

20. Bernal,J.D., Proc. Roy. Soc., A280 ,299-322,(1964).

21. Bernal,J.D. and Finney,J.L., Disc.Farad.Soc., 43 ,62,(1967).

22. Bernal,J.D. and Finney,J.L., Nature, 214 ,No.5085,265-266,(1967).

23. Bernal,J.D. and Mason, J.,Nature, 188 , 910, (1960).

24. Bernal,J.D., Mason, J. and Knight, K.R.,Nature, 194 ,957-958,(1962).

25. Biarez,J., D.Sc. Thesis, University of Grenoble, (1961).

26. Blum,E.H., Ph.D. Thesis, Princeton University,(1964).

27. Bodor,E.E., et.al., J.Coll.& Intf.Sci., 32 ,No.2,367-370,(1970).

28. Briggs, L.J.,U.S.Dept.Agr.Bur.of Soils,Bull.No.10,(1897).

29. Brignole,E.A.,Zacharonek,G. and Mangosio,J., Chem.Eng.Sci., 28 , No.5,1225-1230, (1973).

30. Brooks,R.H. and Corey,T.A.,J.Irrig.& Drainage Div.,Proc.Am.Soc. Civ.Eng, IR2 ,61-88, (1966).

31. Buckingham,E., U.S.Dept.Agr.Bur.Soil Bull., 38 ,(1907).

32. Burdine ,N.T., Trans.A.I.M.E.,198 ,71, (1953).

33. Burdine,N.T.,et.al.,Trans. A.I.M.E., 189 ,195, (1950).

34. Busby,T.S., J. Soc.Glass Technol., 34 ,10,(1950).

35. Calhoun,J.C., Fundamentals of Reservoir Engineering ,p417, Univ.Oklahoma Press, Norman.,(1953).

36. Carman,P.C.,Flow of gases through Porous Media ,Academic Press, N.Y., (1956).

37. Ceaglske,N.H. and Hougen,H.A.,Trans.Am.Inst.Chem.Eng., 33 , 283, (1937).

38. Childs,E.C., Soil Sci., 55 , 219-223, (1943).

39. Claridge, E.L., Soc.Petrol.Eng.J., 12 ,No. 4, 352, (1973).

40. Clyde Orr, Jr.,'Particulate Technology' pp 90-102, McMillan Co.,N.Y.,(1966)

41. Collins, R.E.,' Flow of Fluids Through Porous Materials ' in 'Modern Chemical Engineering ', Ed.by Acrivos,A., Vol.1, Reinhold, N.Y., (1963)

42. Collis-George,N., Soil Sci., 74 , 315-322, (1952).

43. Coulson, J.M. and Richardson, J.F., 'Chemical Engineering ' Vol.2,pp 854 -859, (1955), Pergamon Press, London.

44. Coxeter, H.S.M., ' Introduction to Geometry ', John Wiley & Sons, N.Y., pp 409-412, (1961).

45. Coxeter, H.S.M., Trans.New York Acad.Sci., 24 ,320-331, (1962).

46. Coxeter, H.S.M., Proc. Symp.in Pure Math., Am.Math.Soc., Vol VII, 53-71, (1963).

47. Croney, D., Geotechnique , 3 , 1-16, (1952).

48. Dalavalle, J.M.,'Micromeritics ', 2nd Ed., Pitman Publishing Co., N.Y., (1948).

49. Davies, R., I. & E.C., 62 , No.12, (1970).

50. Debbas, S., and Rumpf, H., Chem.Eng.Sci., 21 , 583, (1966).

51. Delon, J.F., Silicates Ind., 36 ,No.4, 89-93, (1971).

52. Deresiewicz, H., ' Advances in Applied Mechanics ', Vol V, 233-306, Academic Press , N.Y., (1958).

53. Desch, C.H., J.Inst.Metals, 22 ,241, (1919).

54. Diamond, S., Clay Min.,18 , 7, (1970).

55. Dodd, C.G. and Kiel, O.G., J.Phys.Chem., 63 , 1646-1652, (1959).

56. Drake, L.C., Ind.Eng.Chem., 41 , 780, (1949).

57. Dullian, F.A.L. and Batra, V.K., Ind.Eng.Chem., 62 , 25, (1970).

58. Dullian, F.A.L., Dhawan, G.K., Gurak, N. and Babjak, L., Soc.Petrol. Eng.J., 12 ,No.4 ,(1972).

59. Eisenklam, P., 'Porous Masses ' in 'Chemical Engineering Practice ' Ed. by Cremer, H.W. and Davies, T., Vol.2, pp342-463, Butterworths Scientific Publications, London, (1956).

60. El-Sohby, M.A., Ph.D.Thesis, University of Manchester, (1964).

61. El-Sohby, M.A. and Andrawes, K.Z., Can.Geotech.J., (1972).

62. Enderby, A.J., Trans.Farad.Soc., 51 ,835-848, (1955).

63. Enderby, A.J., Trans.Farad.Soc., 52 ,106-120, (1956).

64. Eremenco, V.N., Naidich, Yu.V. and Lavrinenko, I.A.,'Liquid Phase Sintering ',Consultants Bureau, N.Y., (1970).

65. Everett, D.H., Trans.Farad.Soc., 50 ,1077-1096, (1954).

66. Everett, D.H., Trans.Farad.Soc., 51 ,1551-1557 ,(1955).

67. Everett, D.H. and Whitton, W.I., Trans.Farad.Soc., 48 , 749-757,(1952).

68. Everett, D.H. and Smith. F.W., Trans.Farad.Soc., 50 ,187- 197, (1954).

69. Fariborz, R. and Erik, J.S., J.Coll. & Intf.Sci., 39 ,No.2, 367-378, (1972).

70. Fatt, I., Petrol. Trans. Am.Inst.Mining Metall.Engrs., 207 , 144-181, (1956).

71. Fatt,I., Proc. 3rd Int.Congress Fed.Chem.Eng., Inst.Chem.Eng., London, pp 304-311, (1962).

72. Fatt, I. and Dykstra, H., Trans.A.I.M.E. 192 , 249, (1951).

73. Finney, J.L., Disc.Farad.Soc., No.43. pp 83, (1967).

74. Finney, J.L., Ph.D.Thesis, Birkbeck College, University of London, (1968).

75. Fisher, R.A., J.Agr.Sci., 16 ,492-505, (1926).

76. Fisher, R.A., J.Agr. Sci., 18 , 406-410, (1928).

77. Fisher, R.A., Rice, S.A. and Gray,P.,'Statistical Thermodynamics of Liquids ', University Chicago Press,Suppl.,p.212,(1964).

78. Flood, E.A., in ' The Structure and Properties of Porous Materials', ed.by Everett,D.H. & Stone,F.S., Academic Press,N.Y.,pp151-182, (1958).

79. Fluendy, M.A.D. and Smith, E.B., Quarterly Reviews, XI ,241-266,(1962).

80. Foord, S.G., Nature, 155 ,427, (1945).

81. Frevel, L.K. and Kressley, L.J., Analytical Chemistry, 35 ,1492-1502, (1963).

82. Fricke, H.,Physics, I ,106, (1931).

83. Furnas, C.C., U.S.Bur.Mines Bull., 307 ,74, (1929).

84. Furnas, C.C.,Ind.Eng.Chem., 23 ,1052-1058, (1931).

85. Frisch,H.L., in 'Advances in Chem. Physics' ,ed.by Prigogine, I., Vol. VI ,229-290, John Wiley & Sons, N.Y., (1964).

86. Gardner, W., Soil Sci., 7 ,313-317, (1919).

87. Gardner, W., Soil Sci., 7 ,319-324, (1919).

88. Gardner, W., Soil Sci., 10 ,103-126, (1920).

89. Gardner, W., Soil Sci., 10 , 357-358, (1920).

90. Gardner, W., Phys.Rev., 18 ,Ser.2,206-209, (1921).

91. Gardner, W. and Widstoe, J.A., Soil Sci., 11 ,215-232, (1921).

92. Gates, J.I. and Lietz, W.T., A.P.I.Drill.Prod.Pract.,285, (1950).

93. Gilbert,E.W., Can.J.Math., 16 ,286-298, (1964).

94. Gillispie,T. and Settineri, W.J., J.Coll.& Intf.Sci., 24 , 199,(1967).

95. Grachev,G.A., Ione, K.G.,Nosyreva, G.G. and Malinovskaya, O.A., Poristaya Strukt.Katal.Protsessy Perenoska Geterogennom Katal, 106-115,(1970).

96. Graham,H.N. and Walter,K.N., A.I.Chem.E.Journal, 19 ,No.1,112-118, (1973).

97. Graton, L.C. and Fraser,H.J., J.Geology, 43 ,785-909,(1935).

98. Gray, W.A., 'The Packing of Solid Particles', Chapman & Hall Ltd., (1968).

99. Grubisic, G.Z. and Benoit, H., J.Chromatogr. Sci., 9 , No.5, 262-265,(1971).

100. Guin, J.A., Ind. Eng. Chem. Fund., 11 , No.2,282-283, (1972).

101. Gupta, S.C. and Hanks, R.J., Soil Sci.Soc.Amer. Proc., 36 ,No.6, (1972).

102. Hackett, F.E., and Strettan, J.S., J.Agr.Sci., 18 ,671, (1928).

103. Haines, W.B., J.Agr.Sci., 15 ,529-535, (1925).

104. Haines, W.B., J.Agr.Sci., 17 , 264-290, (1927).

105. Haines, W.B., J.Agr.Sci., 20 ,97-116, (1930).

106. Hales, S.Rev., Vegetable Staticks, (1727).

107. Haring, R.E. and Greenkorn,R.A., A.I.Chem.E.J., 16 ,477, (1970).

108. Harris, C.C., Nature, 205, 353-356, (1965).

109. Harris, C.C. and Morrow, N.R., Nature, 203 ,706, (1964).

110. Harris, F.S. and Turpin, H.W., J.Agr.Res., 10 ,113-155,(1917).

111. Hasan,G., Garnet, E.P., and Gilbert, S.B., J.Chem.Ed., 49 , No.6 440, (1972).

112. Hassan, M.E. and Nielsen, R.F., Petrol. Eng., 25 , No.3, B61, (1953).

113. Heller, J.P., Soil Sci. Soc. Amer.Proc., 32 , 778, (1968).

114. Henderson, J.H., Producers Monthly, 14 ,No.1,32, (1949).

115. Henderson, L.M., et.al., Refiner, 19 ,185 ,(1940).

116. Heywood, H.J., Imp. Coll.Chem.Soc.J., 2 ,9-26, (1946).

117. Hilbert, D. and Cohn-Vossen, S.,'Geometry and the Imagination', Chelsea Publishing Co., N.Y.,(1952).

118. Hildebrand, J.H. and Archer, G.,Proc.Nat.Acad.Sci., 47 ,1881-1882, (1961).

119. Holmes, J.W., Aus.J.Appl.Sci., 7 ,45-58, (1956).

120. Holmes, J.W. and Turner,K.G., J.Agr.Eng.Res., 3 ,199-204,(1958).

121. Hrubisek, J., Kolloid-Beihefte, 53 ,385, (1941).

122. Irmay, S., Trans.Am.Geophys.Union, 35 ,463,(1954).

123. Josselin de Jong, G.,Trans.Am.Geophys.Union, 39 ,67,(1958).

124. Kameswara,S.S.V., J.Scientific & Ind.Res., 31 ,No.11,546-550, (1972).

125. Kawakami, M.,J.Chem.Soc.,Japan, 53 ,1085, (1932).

126. Keen, B.A.,J.Agr.Sci., 14 ,170-177, (1924).

127. Keen, B.A., 'The Physical Properties of the Soil',Longmans,Green & Co. Ltd.,London, (1931).

128. Kendall, M.G. and Moran, P.A.P.,'Geometrical Probability', C.Griffin & Co., London, (1963).

129. Khan, J.S., J.Geol., 64 ,385-395,(1956).

130. King, F.H., 'Text Book of the Physics of Agriculture', Madison, Wis.,161-203, (1907).

131. Kolbuszewski, J., 'Sand Particles and their Density',Lect. given to Mat.Sci.club Symp. on densification of particulate materials, London, (1965).

132. Krischer, O. and Sommer, E., Chem.Ing.Tech., 73 ,No.17,967-974, (1971).

133. Ksenzhek, O.S., Russ.J.Phys.Chem., 37 ,691-693, (1963).

134. Kusakov, M.M. and Nekrasov, D.N., 'Capillary Hysteresis in the Rise and wetting liquids in single capillaries and porous bodies.' in 'Research in Surface Forces' ed.by Deryagin, B.V., pp.193-202, Consultants Bureau, N.Y., (1963).

135. Lamb, D.E., Ph.D. Dissertation, Dept. of Chem.Eng.,Princeton University, (1961).

136. Leva, M., and Grummer, M., Chem.Eng.Progress, 43,713-718 ,(1947).

137. Leverett, M.C., Trans.A.I.M.E., 142 , 152,(1941).

138. Loisy, R., Bull.Soc.Chem., 8 ,589, (1941).

139. Luikov, A.V.,'Heat and Mass Transfer in Capillary Porous Bodies', Pergamon Press, (1966).

140. Luikov, A.V., 'Phenomenes des Transport avec Changement de Phase dans les Mileux Poreux ou Colloidaux' pp.21, Editions du Cent. Nat.Rech.Scient.,(1966).

141. MacCrae, J.C., and Gray, W.A., Brit.J.Appl.Phys., 12 ,164-172, (1961).

142. Manglesdorf, P.C. and Washington, E.L., Nature, 187,930, (1960).

143. Manegold, E., Kolloid Z., 81 ,19, (1937).

144. Manegold, E., and Solf, K., Kolloid Z.,89, 36, (1939).

145. Marshall, T.J., ' Relations between Water and Soil', Tech.Comm.No. 50,Commonwealth Bureau of Soils,England,(1959).

146. Marvin, J.W., Am.J.Bot., 26 ,280, (1939).

147. Masmune, S. and Smith, J.M., Ind.Eng.Chem.Fund., 2 ,136-143, (1963).

148. Mason, G.,Disc.Farad.Soc., 75 ,No.43,(1967).

149. Mason, G.,J.Coll.& Intf.Sci., 35 , No.2, (1971).

150. Mason, G.,J.Coll. & Intf.Sci., 41 ,No.2, 208-227, (1972).

151. Mason, G.,Trans. and J.of Brit.Cer.Soc., 71 ,No.3, 93, (1972).

152. Matzke, E.B., Am.J.Bot.,33 ,58, (1946).

153. Mc.Geary, R.K., J.Am.Cer.Soc., 44 ,513-522, (1961).

154. Mc Lellan, A.G., and Alder, B.J., J.Chem.Phys., 24, No.1,115-121, (1956).

155. Meissner,H.P., Michaels, A.S. and Kaiser, R., Ind.Eng.Chem.Process Design and Development, 3 , 202-205, (1964).

156. Melrose, J.C., Soc.Petrol.Eng.J., 5 ,259, (1965).

157. Melrose, J.C., A.I.Chem.E.J., 12 ,986, (1966).

158. Meredith, R.E. and Tobias, C.W., 'Conduction in Heterogeneous Systems' in 'Advances in Electrochemistry and Electrochemical Engineering', Vol 2,pp.15-48,Interscience, N.Y.,(1962).

159. Miller, E.E. and Miller, R.D., J.Appl.Phys., 27 ,324, (1956).

160. Miller, R.D.,Soil Sci.,72 ,291-301, (1951).

161. Molecular Physics Correspondent, Nature, 239, 488-489,(1972).

162. Moore, R.E., Hilgardia, 12,383-426, (1939).

163. Morgenstern, M., Nature, 200 ,559-560, (1960).

164. Morrell, W.E. and Hildebrand, J.H., J.Chem.Phys., 4 ,224, (1936).

165. Morrow, N.R., Chem.Eng.Sci.,25 ,1799, (1970).

166. Morrow, N.R.,Ind.Eng.Chem., 62 ,No.6,32-56, (1970).

167. Morrow, N.R. and Harris, C.C.,Soc.Petrol.Eng.J., 5 ,(1965).

168. Murty, B.G.K., Dimitri,G.,and Dipak,R., A.I.Chem.E.J., 31-37, (1973).

169. Nagive, M.F. and Ibragimov, Ch.Sh., Issled.Obl.Kinet.,Model Optimiz - atsii Khim Protsessov, 1 ,105-115, (1970).

170. Nicholson, D.,Trans.Farad.Soc., 64 ,3416-3424, (1968).

171. Nicholson, D.,Trans.Farad.Soc., 66 ,1713-1719,(1970).

172. Nicholson, D. and Petropoulos, J.H., J.Phys.D:Appl.Phys., 1 ,1379-1385, (1968).

173. Nicholson, D., and Petropoulos, J.H.,J.Phys.D:Appl.Phys., 4 , No.2., 181-189, (1971).

174. Oliver, D.R., Chem.Eng.,No.246, 58-65,(1971).

175. Orr, C.,'Centrifugal Pore size Analyser',USA/Japan Joint Seminar, Kyoto, Japan, (1969).

176. Owen, J.E., Trans. A.I.M.E., 195 ,169, (1952).

177. Palosaari, S.,Ph.D.Thesis, Imperial College, London,(1973).

178. Pavalakis, G. and Barden, L.,J.Soil Sci., 6 ,No.23, (1972).

179. Pickell, J.J., Swanson, B.F. and Hickman, W.B., Soc.Petrol.Eng.J., 6 ,55-61, (1966).

180. Pietsch, W. and Rumpf, H., Chem.Ing.Tech., 89 ,885, (1967).

181. Pople, J., Phil.Mag., 42 ,459, (1951).

182. Porkhaev, A.P., Kolloid.Z., 11 , 346, (1949).

183. Poulovassilis, A., Soil Sci., 93 ,405-412, (1962).

184. Purcell, W.R.,Trans.A.I.M.E., 186 ,39, (1949).

185. Purnell, H., 'Gas Chromatography', p62 , John Wiley & Sons, N.Y., (1962).

186. Rainhard, L.W., Textile Res. J., 17 ,167, (1947).

187. Ralph, S. and Kelsey, F.J., Soc.Petrol.Eng.J., 12 , No.4,345-355, (1972).

188. Rand,B. and Marsh, H., J.Coll.& Intf.Sci., 40 ,No.1, 121-122,(1972).

189. Raymond, P.I., A.I.Ch.E.J., 18 ,No.4,(1972).

190. Rice, O.K., J.Chem.Phys., 12 ,No.1,(1944).

191. Rice, O.K., J.Chem.Phys., 32 ,1277-1278,(1960).

192. Richard, E.M.M., J.of Microscopy, 95 ,Part2, 243-248, (1972).

193. Richards, L.A., Soil Sci., 51 ,377-386, (1941).

194. Richards, L.A., Soil Sci., 68 ,95-112, (1949).

195. Richards, L.A., Agr.Eng., 28 ,451-454, (1947).

196. Ritter, H.L. and Drake, L.C., Ind.Eng.Chem.Anal. Ed., 17 ,782, (1945).

197. Roblee, L.H.S., Baird, R.M. and Tierney, J.W.;A.I.Ch.E.J., 4, 460-464,(1958).

198. Rogers, C.A.,'Packing and Covering', 54, Cambridge Tracts in Mathematics and Mathematical Physics,C.U.P.,(1964).

199. Rose, D.A., Rilem.Bull., 29 ,119-124, (1966).

200. Rose, D.A., J.Soil Sci., 22 , No.4, (1971).

201. Round, G.F. and Newton, R., Nature, 198 ,747-749, (1963).

202. Rowlinson, J.S.,and Buckle, E.R., Nature, 200 ,742-744,(1963).

203. Saffman, P.G.,J.Fluid Mech., 7 ,194, (1960).

204. Scheidegger, A.E., 'The Physics of Flow through Porous Media', MacMillan Co.,N.Y.,(1960).

205. Scheidegger, A.E., Producers Monthly, 17 , No.10,17,(1953).

206. Schofield, R.K., Trans.3rd.Int.Congr.Soil Sci., 2 ,37-48, (1935).

207. Scott, G.D., Nature, 188 , 908-909, (1960).

208. Scott, G.D., Nature, 194 ,956, (1962).

209. Scott, G.D.,Charlesworth, A.M. and Mak, M.K., J.Chem.Phys., 40 , 611-612, (1964).

210. Scott, G.D. and Kilgour, D.M., Brit.J.Appl.Phys., 2 , 863, (1969).

211. Simon, R. and Kelsey, F.J., Soc.Petrol.Eng.J., 12 ,No.4,345-351, (1972).

212. Skalny, J.,Bodor, E.E. and Brunauer, S., J.Coll.& Intf.Sci., 37 , No.2, 476-483, (1971).

213. Slichter,C.S., U.S.Geol.Serv.19th Ann.Report, Part2, 295-301, (1899).

214. Smalley, V. and Smalley, I.J., Nature, 202 ,168, (1964).

215. Smith, C.S., in 'Metal Interfaces',Am.Soc.Metals,Cleveland,p65, (1965).

216. Smith, E.B. and Lea, K.R., Nature, 186 ,714, (1960).

217. Smith, W.O., Physics, 3 ,139, (1932).

218. Smith, W.O., Physics, 4 ,425-438, (1933).

219. Smith, W.O.et.al.,Phys.Rev., 34 ,1271-1274, (1929).

220. Sridharan, A. et.al., J.Soil Mech. and Found. Div., Proc. Am. Soc. Civ.Engrs.,pp. 771-787, (May,1971).

221. Sridharan, A. and Diamond, S., J.Soil Mech.and Found.Div.,Proc. Am.Soc.Civ.Engrs., 98 ,No.SM7,pp.770,(July,1972).

222. Stamm, A.J., Physics, 1 ,116, (1931).

223. Stephen, B.,J.Coll.& Intf.Sci., 39 ,No.2,435-436,(1972).

224. Stone, J.F.,Kirkham,D., and Read,A.A., Soil Sci.Soc.Amer.Proc., 19 ,419-423,(1955).

225. Supnik, F.,Trans.Am.Math.Soc., 65 ,14-26,(1949).

226. Szabo, M.T., Soc.Petrol.Eng.J., 12 ,No.2,85-88,(1972).

227. Tabuchi, T.,Soil Sci., 102 ,329-332, (1966).

228. Tabuchi, T.,Soil Sci., 112 ,448-453, (1971).

229. Tanaeva, S.A., J.Eng.Phys.,(Inzh.Fiz-zh), 9 ,No.5,375-377, (1965).

230. Tanner, C.B. and Hanks, R.J., Soil Sci.Soc.Amer.Proc., 16 ,48-51, (1952).

231. Taylor, S.A. and Kune, J.W., Fundamentals, 335-342.

232. Temperley, H.N.V., Brit.J.Appl.Phys., 14 ,835-839, (1963).

233. Templeton, C.C., A.I.M.E.,T.P.307-G, Trans.A.I.M.E., 201 ,162, (1953).

234. Templeton, C.C., Bull.Amer.Phys.Soc., 29 , No.2, 16,(1954).

235. Terman, M. and Fuller, O.M.,Can.J.Chem.Eng., 51 ,106-110,(1973).

236. Topp,G.C. and Miller,E.E.,Soil Sci.Soc.Amer .Proc., 30 ,156-162, (1966).

237. Tory, E.M., Church,B.H.,Tam,M.K.and Ratner,M.,Can.J.Chem.Eng., 51 ,484-493, (1973).

238. Van Bavel, C.H.M., Underwood, N. and Swanson, R.W.,Soil Sci., 82 , 29-41, (1956).

239. Versluys, J., Int.Mitt.fur.Bodenk , 7 ,117-140, (1917).

240. Visscher, W.M. and Bolsterli, M, Nature, 239 ,No.5374, (1972).

241. Von Engelhardt, W., Proc.4th. World Petr.Congr.Sect. I.C., (1955).

242. Washburn, E.W., Proc.Nat.Acad.Sci., 7 ,115, (1921).

243. Westman, A.E.R. and Hugill, H.R., J.Am.Cer.Soc., 13 ,767-778,(1930).

244. Wicksell, S.D., Biometrica, 17 ,84, (1925).

245. Wollny, E., Forisch.Geb.Agr.Phys., 7 ,269-308, (1884).

246. Wollny, E., Forisch.Geb.Agr.Phys., 8 ,206-220,(1885).

247. Woodrow, J.,Chilton, H. and Hawes, R.I., J.Neucl.Energy, Part B, Reactor Technology, 1 ,229, (1961).

248. Wyllie, M.R.J. and Spangler, M.B., Bull.Amer.Ass.Petrol.Geol., 36 ,359, (1952).

249. Youngs, E.G., Soil Sci., 86 ,117-125, (1958).

250. Youngs, E.G., Soil Sci., 86 , 202-220, (1958).

251. Youngs, E.G., Int.Congr.Soil Sci.Trans.,7th, 1 , 107-113, (1960).

ERRATA

Page II. Line no.1 add 'Satisfactory' to read 'Satisfactory prediction of rise and drain moisture'

Page 10. Line no. 10. Delete line no. 10 and replace by 'at different layers!

Page 14. Line no. 6 & 7. Delete 'If the porous body.....,then over' and replace by 'over' to read 'over a horizontal cross section...'.

Page 44. Line no. 22 ' used photomicrography and ... '

Page 47. Line nos. 12& 13 'Bernal(20,24) and Scott(208) independently studied packings of spherical particles and measured the co-ordinates of the centres of each '

Page 48. Line No.9 'Although void fractions larger than 0.40 have been observed'

Page 49. Line No.24 'Two methods of subdivision of packings have been..'

Page 61. Line No.9 'Several values of F^* are possible to dislocate a tetrahedral unit Tl depending'

Page 61. Equation (4.11)

$$\zeta = \left[\int_{F^*}^{F^*_{max}} f(F^*)dF^* \right] / \left[\int_{0}^{F^*_{max}} f(F^*)dF^*\right]$$

Page 61. Equation (4.12)

$$\zeta = \left[\int_{F^*}^{F^*_{max}} f(F^*)dF^*\right] / \left[\int_{F^*_{min}}^{F^*_{max}} f(F^*)dF^*\right]$$

Page 62. Between the end of Sect.4.61 and the begining of Sect.4.6.2 insert:

' where $\eta^*_A = F^*_A/F^*_{max}$, $\eta_B = F^*_B / F^*_{max}$ and $\eta_C = F^*_C / F^*_{max}$

Page 80. Line No.25 Delete 'If' to read ' It is assumed that..'

Page 110. Line No.9 'If a relationship of u(r) with r is assumed as: '

Page 111. Line No. 3. 'as long as there are wet regions in a given region of a packed bed'

Page 112. Line No.16 'be sorrounded by moisture in the upper layer can be expressed as: $\Psi_h . I_h + \Delta h$

Page 115. Line No.23 'seperation between a rubber lining and the adjacent perspex ring was clearly observed. Similar lines were'

Page 128. Line No.28 'liquid interfaces thus preventing draining of moisture in the pores. The existence of a single meniscus in '

Page 129. Equation nos.(4.10(a)) & (4.10(b)) to be replaced by (6.10(a)) & (6.10(b)) respectively.

Page 135. Line No. 2 $(pd/2\sigma')$ and the corresponding values of $(\overline{X}-\overline{X}_i)/(1-\overline{X}_i)$ where p is the capillary pressure,d is the average capillary diameter of'

Page 139. Line No. 17 'The resulting bed can be regarded to be similar to that of a uniform sphere packing, provided'

Page 146 Line No.1 'Upto present day,no satisfactory theory for the prediction of'

Page 174. Line No.2 'Solution of Equations (6.3) & (6.11)

Page 99. Between the last statement of Sect 5.1.2.1 & the title of Sect 5.1.2.2 insert: 'The behaviour of capillary pressure curves described by equations (5.11) and (5.12) can be seen to be similar to the behaviour of capillary pressure curves of porous bodies.'